UNIVERSITY OF LONDON THESIS

Degree PhD Year 2007 Name of Author RANCZ, Ede Attila

DENDRITIC SPIKES CONTROL SYNAPTIC PLASTICITY AND SOMATIC OUTPUT IN CEREBELLAR PURKINJE CELLS

Thesis submitted for the degree of
Doctor of Philosophy of University of London

Ede Attila Rancz

Department of Physiology

University College London
2007

ProQuest LLC
789 East Eisenhower Parkway
P.O. Box 1346
Ann Arbor, MI 48106-1346

Declaration

I hereby declare that this thesis, all data, analysis and conclusions are my own work.

London, 3rd July, 2007.

Abstract

Neurons receive the vast majority of their input onto their dendrites. Dendrites express a plethora of voltage-gated channels. Regenerative, local events in dendrites and their role in the information transformation in single neurons are, however, poorly understood. This thesis investigates the basic properties and functional roles of dendritic spikes in cerebellar Purkinje cells using whole-cell patch clamp recordings from the dendrites and soma of rat Purkinje cells in brain slices.

I show that parallel fibre (PF) evoked dendritic spikes are mediated by calcium channels, depend on membrane potential and stimulus intensity and are highly localized to the spiny branches receiving the synaptic input. A determining factor in the localization and spread of dendritic calcium spikes is the activation of large-conductance, calcium dependent potassium (BK) channels.

I provide a strong link between dendritic spikes and the endocannabinoid dependent short-term synaptic plasticity, depolarization-induced suppression of excitation (DSE). Gating the dendritic spikes using stimulus intensity or membrane potential, I show that the threshold of DSE is identical to that of the dendritic spikes and the extent of DSE depends on the number of dendritic spikes. Blocking BK channels increases the spatial spread of dendritic spikes and enables current injection or climbing fibre (CF) evoked dendritic spikes to suppress PF inputs via DSE.

By monitoring dendritic spikes during strong PF stimulation-induced long-term depression (LTD), I also provide a link between long-term synaptic plasticity and dendritic excitability. By showing that blocking CB1 cannabinoid receptors reduces the intensity requirement for LTD, I provide a connection between the short- and long-term changes in PF strength triggered by dendritic spikes

I also investigate the effect dendritic spikes have on somatic action potential output. Contrary to pyramidal cells, where dendritic spikes boost the output of

the neuron, the average Purkinje cell output becomes independent from the output strength for inputs triggering dendritic spikes. However, the temporal pattern of the output is strongly affected by dendritic spikes. I show that this phenomenon depends on BK channel activation resulting in a pause in somatic firing following dendritic spikes.

In summary, I present a description of PF evoked local dendritic spikes and demonstrate their functional role in controlling the synaptic input and action potential output of cerebellar Purkinje cells.

Acknowledgements

I would like to thank first and foremost my parents, who always supported me to do what I wanted. I have learnt the most important lessons from you. Köszönöm!

Géza Zboray directed me towards neuroscience. You made me choose the more challenging and I believe more satisfying path.
Tamás Freund and Norbert Hájos guarded my baby-steps in science, I have learnt a lot from you.
Michael Häusser, my supervisor deserves thanks for both his patience and support. By populating the lab with people both brilliant in science and personality, you established a very stimulating environment.

Arnd Roth, Kamilla Angelo, Troy Margrie, Beverley Clark, Mickey London, Jenny Davie, Wolfgang Mittmann, Ian Duguid, Paul Chadderton, Benjamin Judkewitz, Matteo Rizzi, Séverine Mahon, Taro Ishikawa, Jesper Sjöström, Alanna Watt, Herman Cuntz, Julian Jack, Bartlett Mel, Pablo Monsivais and Kazuo Kitamura all deserve thanks for discussions, directions, support and friendship.

Latha Ramakrishnan and Kate Powel provided outstanding technical assistance. Thanks to Kamilla Angelo, Alex Arenz, Talia Atkin, Paul Chadderton, Izumi Fukunaga, Mickey London, Wolfgang Mittmann, Daniella Muallem and Arnd Roth for making sure I knew what I was talking about. All remaining errors are mine.

The Department of Physiology and the Wolfson Institute for Biomedical Research were a second home. I thank the financial support of the Wellcome Trust, the Gatsby Foundation and the British government.

Finally, tremendous thanks goes again to my secret muse, you were always there when I was ready to give up, if only for those moments.

Thank you.

Table of Contents

1. Introduction

Extracting relevant features of the surrounding environment, detecting temporal order, building internal models of physical laws, planning and supervising motor movements or other tasks are only a few of the multitude of brain functions which require fast and efficient computation. Some of these computations are carried out at the network level and some in single neurons, but share many similarities. A single neuron itself is a highly sophisticated network of several subcellular compartments. This compartmentalization, let it be electrical or chemical, is thought to increase the information processing capacity of a neuron by allowing several independent computational units to work in parallel.

In this thesis, I will first review the theoretical and experimental background of single cell and dendritic computation. Second, I will compare experimental findings from different cell types regarding the basic properties and functional roles of dendritic spikes. Third, I will review the biophysical and neurophysiological literature on Purkinje cells before stating the questions addressed in this thesis. After the presentation of the results, I will put them into a systemic context by discussing the role of Purkinje cells in the cerebellar circuitry.

1.1 Theoretical background

1.1.1 The cable equation

The morphological diversity of neurons, especially their complex dendritic arborisation was already well known more than 100 years ago from the pioneering work of Cajal and Golgi (Ramón y Cajal, 1911; Figure 1.1). However, whether out of oversimplification or oversight, few neuroscientists considered dendrites as important features of neurons.

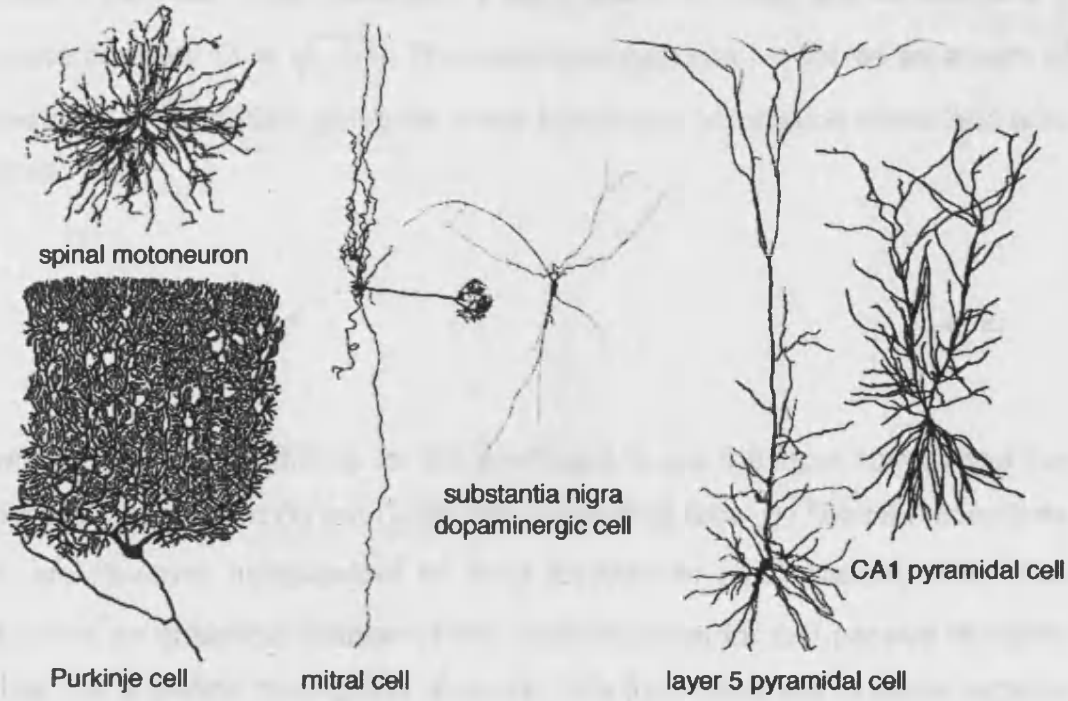

Figure 1.1 Dendritic trees have various shapes Modified from Mel (1994)

In the early 1950's, interpretation of sharp electrode recordings from spinal cord motoneuron somata (and occasionally dendrites) raised the first questions regarding electrical signal propagation in dendrites. Wilfrid Rall was

the first to realize the advantages of analytical modelling to tackle this experimentally impossible problem at the time. Starting from the simplest possible abstraction, an isopotential, passive soma, the first step was to solve the problem of membrane potential spread in a passive cylinder. With all electrical parameters constant, the current flow in a cable can be described mathematically by the cable equation (Rall, 1959):

$$\left(\frac{r_m}{r_i}\right)\frac{\partial^2 V(x,t)}{\partial x^2} - r_m c_m \frac{\partial V(x,t)}{\partial t} - V(x,t) = 0 \qquad \text{Eq. 1.}$$

where any current flowing in the cylinder can either flow along the cylinder through r_i (axial resistance, Ω/cm) or through the wall of the cylinder (the membrane) charging c_m (membrane capacitance, F/cm) and crossing the membrane resistance (r_m, Ω·cm). Two biologically relevant constants can be derived from Eq. 1: the membrane time constant ($\tau = r_m c_m$) and the membrane space constant ($\lambda = \sqrt{r_m / r_i}$). The cable equation can be solved as a sum of decaying exponentials giving the exact membrane potential in space and time (Rall, 1969):

$$V(x,t) = \sum_{i=0}^{\infty} C_i e^{-t/\tau_i} \qquad \text{Eq. 2.}$$

where the initial conditions for the coefficient C_i are the input current and the point of observation (x) but C_i are independent of time (t). The time constants τ_i are however independent of input location or input current. After Rall showed an analytical solution of the cable equation for any passive dendritic tree, the analytical description of current flow from dendrites to soma became possible both in abstract and anatomically reconstructed dendritic trees, leading to insights about bidirectional voltage and charge attenuation as well as integration of multiple inputs in passive dendrites (Segev et al., 1995).

However, Rall realized early on that dendrites are active structures and the cable equation is analytically intractable to describe non-linear interactions of

strong transient conductance changes (synaptic input) or voltage-dependent membrane-conductances. He thus divided the dendrites into a finite number of compartments (as RC elements, Figure 1.2) and solved the non-linear cable equation numerically (Rall, 1964). With sufficiently small compartments, the compartmental model converges to the corresponding cable model (Segev and Burke, 1998).

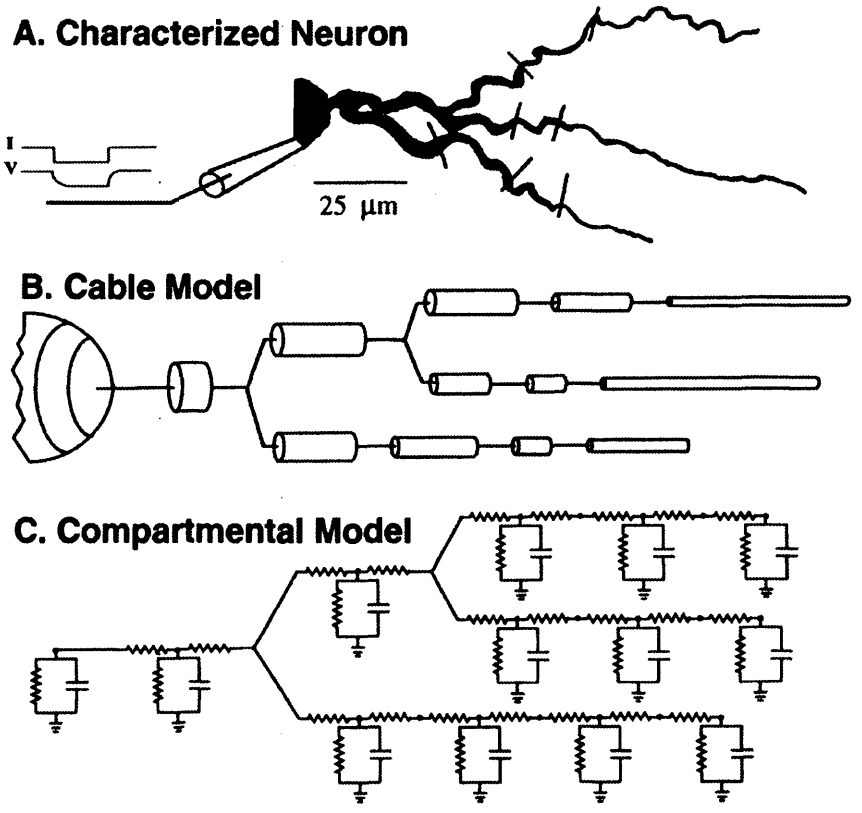

Figure 1.2 A real neuron, the equivalent cable structure and a multi-compartmental model Modified from Segev and London (1999).

The cable equation and compartmental modelling were implemented in user-friendly computational environments (GENESIS – Bower and Beeman, 1994 and NEURON - Hines and Carnevale, 1997), providing a powerful tool for both experimental and theoretical neuroscientists. The advent of dendritic patch-clamp recording (Stuart et al., 1993; Davie et al., 2006), 2-photon microscopy (Denk et al., 1990) and compartmental modelling revived the interest in dendritic physiology, opening up formerly inaccessible realms for research and furthering our understanding of the brain.

1.1.2 Single cell computation

Most of the synaptic input to a neuron arrives to its dendrites, and thus both the passive and active electrical properties of the dendrites are critical in determining the effect of any given input on the spike output. These properties also play a key role in influencing synaptic plasticity, as they define the electrical and chemical signals experienced by each synapse, and determine the interplay between synapses. As both the passive and active properties of the dendritic tree can be modulated, this offers a rich palette of mechanisms for regulating both neuronal output and plasticity (Frick and Johnston, 2005; Magee and Johnston, 2005).

Both the passive and active properties of neurons can vary widely, giving rise to a plethora of different possible input-output (i-o) functions. A classical way of characterizing the i-o function of a neuron is to record the frequency of somatic action potentials (AP, the output) in response to injected current (or conductance) input. The result is called a frequency-current (f/I) curve. Typical f/I curves obtained with current injection in the form of square pulses, steps or ramps show a threshold below which no APs are generated, and a linear or sublinear increase in AP frequency above that threshold. The exact shape of the f/I curve, e.g. whether it is continuous (type I) or discontinuous (type II) at threshold, depends on the intrinsic properties of a given cell type (Connors and Gutnick, 1990; Tateno et al., 2004; Figure 1.3). The interactions between different intrinsic mechanisms shaping the f/I curve can be complex. For example, intrinsic currents providing slow negative feedback can both linearize an originally highly nonlinear f/I curve (Ermentrout, 1998), and transform an originally linear f/I curve into a nonlinear, logarithmic one (Engel et al., 1999). The f/I curve can also be modulated by background synaptic activity. Changes in the statistics of noisy synaptic inputs and changes in the ratio of excitation to inhibition can change the slope of the f/I curve and thus the gain of the neuron (Chance et al., 2002; Mitchell and Silver, 2003; Prescott and De Koninck, 2003). The i-o functions have boundaries as well,

such as the limits of AP initiation and propagation (Raastad and Shepherd, 2003; Clark et al., 2005; Khaliq and Raman, 2005; Monsivais et al., 2005). Recently, Kerr et al. (2005) measured the i-o functions of single neurons in the functioning cortical network *in vivo*, with input statistics generated by the network itself, and found a threshold-linear relationship similar to those obtained using current injection and widely used in current network models.

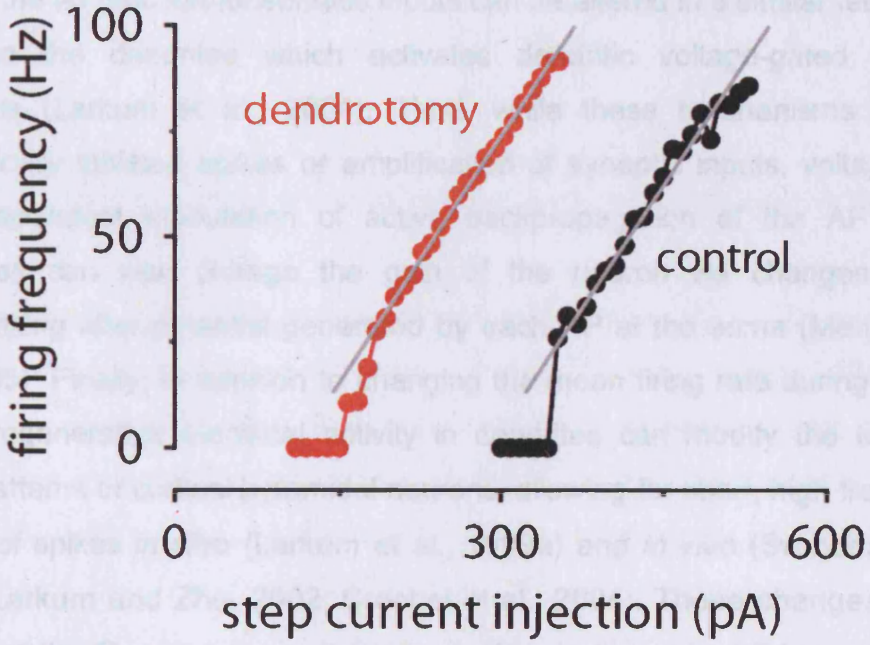

Figure 1.3 Example of a neuronal i-o function
Experimentally determined firing frequency vs. current injection relationship from a cerebellar Purkinje cell. Black circles illustrate the control condition. Note the discontinuity at threshold (type II f/I curve). Red circles are from the same cell after the dendrites were reversibly disconnected from the soma by physically obstructing them. Note the leftward shift compared to control without any change in gain (grey line, linear fit). Adapted from Bekkers and Häusser (2007).

Dendritic excitability plays a crucial role in determining both the processing and storage capacities of single neurons. Both the time-course and spatial spread of synaptic input is determined by the passive cable properties of the dendrite (Jaffe and Carnevale, 1999) together with the distribution (Migliore and Shepherd, 2002) and functional state of voltage-gated channels. Thus i-o functions are influenced by the morphology of the cell and the dendritic distribution and functional state of voltage and calcium-dependent

conductances in several ways. First, the dendrites constitute a large passive load which raises action potential threshold and effectively shifts the f/I curve to the right, as larger input currents are required to generate a given output frequency (Figure 1.3, Bekkers and Häusser, 2007). Second, dendritic inputs can be boosted by voltage-dependent sodium and calcium channels (Schwindt and Crill, 1995; Christensen, 2002) leading to increased somatic firing frequency (Archie and Mel, 2000; Oviedo and Reyes, 2002, 2005). The gain of the i-o function for somatic inputs can be altered in a similar fashion by input to the dendrites which activates dendritic voltage-gated calcium channels (Larkum et al., 2004). Third, while these mechanisms rely on dendritically initiated spikes or amplification of synaptic inputs, voltage- and state-dependent modulation of active backpropagation of the AP to the dendrites can also change the gain of the neuron via changes in the depolarizing after-potential generated by each AP at the soma (Mehaffey et al., 2005). Finally, in addition to changing the mean firing rate during regular firing, regenerative electrical activity in dendrites can modify the temporal firing patterns of cortical pyramidal neurons, allowing for short, high frequency bursts of spikes *in vitro* (Larkum et al., 1999a) and *in vivo* (Svoboda et al., 1999; Larkum and Zhu, 2002; Crochet et al., 2004). These changes of the shape of the f/I curve, as well as the switch in the output firing pattern of pyramidal neurons in response to appropriately timed proximal and distal synaptic input (Larkum et al., 1999a), can be viewed as results of the computations performed by the neuron. In fact, shifts of the f/I curve can be interpreted as additions or subtractions, changes of its slope constitute multiplications or divisions, and changes in the firing pattern in response to coincident distal and proximal inputs can be viewed as a logical 'AND' operation. Taking this view to the level of single dendritic branches, Bartlett Mel proposed a two-layer 'neural network' model for the i-o function of pyramidal neurons (Poirazi et al., 2003). In the first layer of this model, independent subunits represented by individual dendritic branches sum their synaptic inputs before applying a nonlinear operation, which could be implemented by a local dendritic spiking mechanism. The outputs of the first layer are in turn summed approximately linearly before the i-o function of

the second layer is applied at the soma (Mel, 1993; Häusser and Mel, 2003).

In some extreme cases, the intrinsic excitability of dendrites may even be more important in determining output spike patterns than the synaptic input (Heckman et al., 2003). Thus, together with synaptic properties and connectivity, the i-o functions of subcellular compartments and individual neurons determine which computations can be performed by a given network.

1.1.3 Functional compartmentalization and dendritic computation

The complex tree-like architecture of the dendrites can provide the anatomical substrate for multiple interconnected signal processing units. Defining the functional morphology of a neuron by discrete compartments with different biochemical and electrical dynamics as done by compartmental modelling is thus a good approximation to study information processing. One has to take into account, however, that different levels of compartmentalization exist and the boundaries between compartments are not discrete. So what are the functional compartments of a neuron? The first requirement for the generation of multiple functional compartments within a single dendritic tree is sufficient electrical segregation, which is mostly determined by the passive electrotonic properties of the dendritic tree. Examples of this segregation include the 100-fold attenuation of synaptic signals to distal dendrites recorded from the soma of pyramidal neurons (Stuart and Spruston, 1998; Nevian et al., 2007). Second, mechanisms for non-linear interactions at the level of synapses, branclets or branches are required, which are provided by voltage-dependent conductances. An early example is the first description of local dendritic spikes in Purkinje cells by Llinás and Nicholson (1968). A third prerequisite is a means for efficient and modifiable communication and interaction between different compartments, like forward and backpropagation of spikes. However, this third requirement is only essential if the compartments don't have their own, separate output, like dendritic transmitter release (Ludwig and Pittman, 2003).

To conclude, single neurons are complex signal transducers, which can be approximated by multiple compartments. The level of compartmentalization however is a question of viewpoint: every spine or calcium micro-domain can be considered as a compartment in its own right (Yuste and Denk, 1995; Goldberg et al., 2003b; Goldberg and Yuste, 2005), and so are dendritic branchlets (Losonczy and Magee, 2006), subtrees or even entire neurons. Although this thesis is written from a cellular point of view and focuses on the scale of dendritic branchlets, subtrees and single cells, I have to acknowledge that a valid systemic viewpoint exists as well. When thinking of the output of the brain, i.e. the behaviour of the animal, neuronal networks and even whole brain regions can be approximated as compartments.

1.2 Dendritic spikes

The toolbox for dendritic computation is vast and diverse (London and Häusser, 2005). This thesis focuses on a small segment, dendritic spikes in cerebellar Purkinje cells. As is generally the case in biological systems, the divergent and convergent paths of evolution led to similar functions being served by different mechanisms and the same mechanisms serving different functions, making it difficult to generalize between different brain regions. On the mechanistical level however many parallels are available, thus I continue with a general overview of dendritic spikes in different neuronal cell types.

1.2.1 Biophysics of dendritic spikes

Many different ion channels in the dendritic membrane open upon depolarization and cause more depolarization providing a positive-feedback mechanism to decrease the membrane potential in a regenerating fashion. Provided sufficient depolarization, the result may be a dendritic spike, and a nonlinear input-output relationship of the dendritic region supporting it (Figure 1.4). Dendritic spikes were first observed in cerebellar Purkinje cells (Llinás et al., 1968; Llinás and Nicholson, 1971; Llinás and Sugimori, 1980a) and in hippocampal pyramidal cells (Wong et al., 1979). Studies describing dendritic spikes in many other cell types followed, such as in neocortical pyramidal cells (Larkum et al., 1999a; Waters et al., 2003), in olfactory bulb mitral cells (Chen et al., 1997) and cortical interneurons (Martina et al., 2000; Goldberg et al., 2003a). In Purkinje cells, whose dendrites lack voltage-gated sodium channels (Stuart and Häusser, 1994), solely voltage-gated calcium channels generate dendritic spikes (Llinás and Sugimori, 1980a). In hippocampal pyramidal cells, dendritic spikes are produced by sodium (Golding and Spruston, 1998) and calcium (Golding et al., 1999) conductances in concert. In neocortical pyramidal cells there seems to be a location-dependence in the

conductances underlying dendritic spikes. Proximal dendrites are more prone to sodium channel-mediated dendritic spikes (Nevian et al., 2007; Figure 1.4C; Stuart et al., 1997), while voltage-gated calcium channels contribute relatively more to distal dendritic spikes (Schiller et al., 1997; Larkum et al., 1999b; Larkum et al., 1999a). A special case is the ligand- and voltage-gated NMDA receptor, which in addition to being a key candidate for the spine coincidence detector (Yuste and Denk, 1995) in spike-timing dependent synaptic plasticity (STDP), can also produce local dendritic spikes in the basal dendrites of pyramidal cells (Nevian et al., 2007; Figure 1.4B; Schiller et al., 2000) or in multi-tufted accessory olfactory bulb mitral cells (Urban and Castro, 2005).

The threshold of dendritic spikes is set by the passive properties of the dendrite acting in concert with the activation properties of the ion channels and general excitability of the dendrite (Gasparini and Magee, 2002). Branch-specific, local modulation of excitability (Frick et al., 2004) may thus make some parts of the dendritic tree more prone to dendritic spikes. This could lead to unbalanced dendritic trees (Goldberg et al., 2002), but could also allow the mapping of temporarily contiguous memory traces onto dendritic branches (Mehta, 2004).

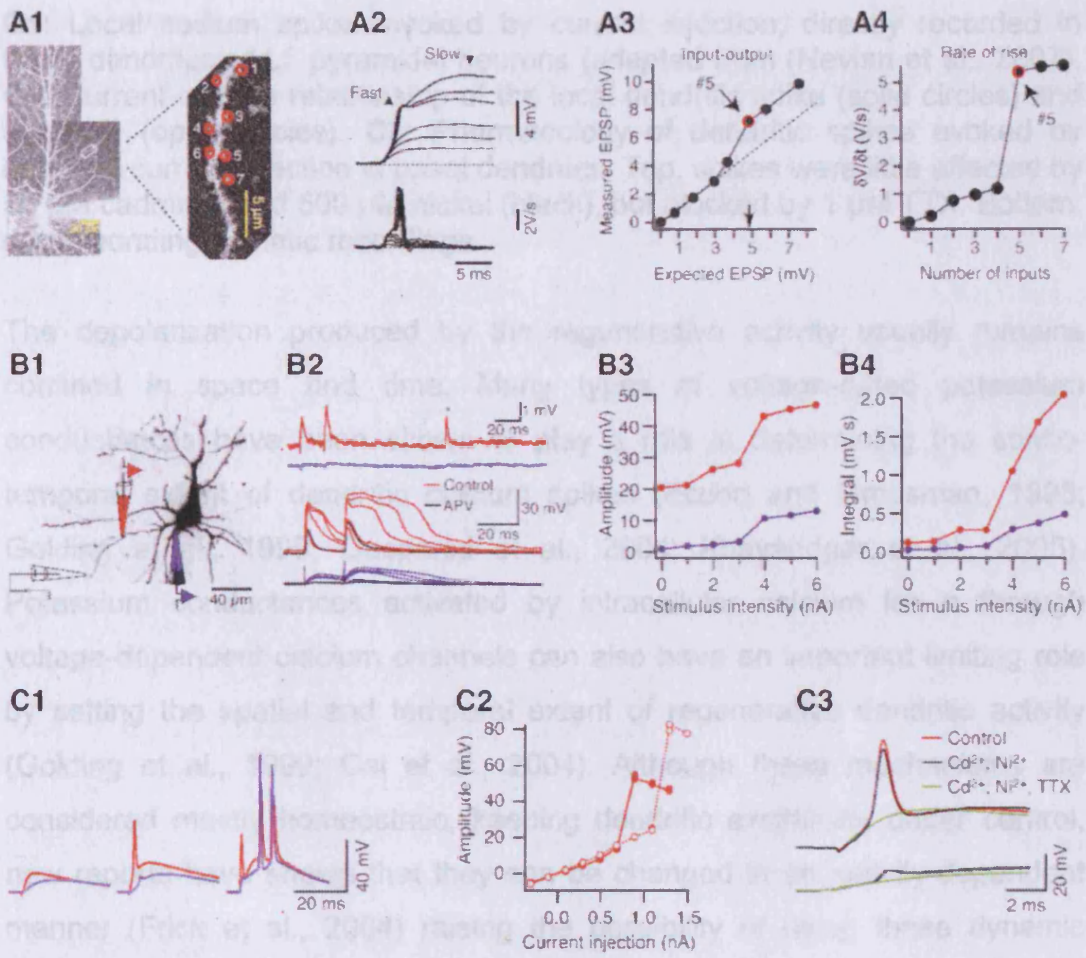

Fig. 1.4 Examples of dendritic spikes

A: Local spikes in radial oblique dendrites of CA1 pyramidal neurons evoked by multi-site two-photon uncaging of glutamate (adapted from (Losonczy and Magee, 2006). **A1**: Two-photon image of a CA1 pyramidal neuron (left) and single scan image showing seven spines selected for two-photon uncaging of glutamate. **A2**: Somatic excitatory postsynaptic potentials (EPSP) evoked by glutamate uncaging on another oblique branch (top), and time derivatives of the same traces (bottom). **A3**: Measured somatic EPSP amplitudes during simultaneous uncaging at multiple spines vs. the arithmetic sum of somatic EPSPs measured when the same spines are activated separately. **A4**: Maximum time derivative of the somatic EPSP versus the number of spines stimulated.

B: NMDA spikes evoked by synaptic stimulation, directly recorded in basal dendrites of L5 pyramidal neurons (adapted from (Nevian et al., 2007). **B1**: Two-photon image of the basal dendrites of a L5 pyramidal neuron. Blue, somatic patch pipette; red, dendritic pipette; white, extracellular stimulation electrode. **B2**: Top traces, two pulses separated by 20 ms were delivered to the stimulation electrode. Dendritic responses (red) show similarity to spontaneously occurring EPSP (asterisk). Bottom traces, increasing the stimulus intensity leads to a NMDA spike. **B3**: Amplitude of the dendritic (red) and somatic (blue) response as a function of stimulus intensity. **B4**: Time integral of the dendritic (red) and somatic (blue) response as a function of stimulus intensity. Note the discontinuity at threshold for the dendritic spike.

C1: Local sodium spikes evoked by current injection, directly recorded in basal dendrites of L5 pyramidal neurons (adapted from (Nevian et al., 2007). **C2**: Current-voltage relationship of the local dendritic spike (solid circles) and the bAP (open circles). **C3**: Pharmacology of dendritic spikes evoked by dendritic current injection in basal dendrites. Top, spikes were little affected by 50 µM cadmium and 500 µM nickel (black), but blocked by 1 µM TTX. Bottom, corresponding somatic recordings.

The depolarization produced by the regenerative activity usually remains confined in space and time. Many types of voltage-gated potassium conductances have been shown to play a role in determining the spatio-temporal extent of dendritic calcium spikes (Etzion and Grossman, 1998; Golding et al., 1999; Gasparini et al., 2004; Khavandgar et al., 2005). Potassium conductances activated by intracellular calcium let in through voltage-dependent calcium channels can also have an important limiting role by setting the spatial and temporal extent of regenerative dendritic activity (Golding et al., 1999; Cai et al., 2004). Although these mechanisms are considered mostly homeostatic, keeping dendritic excitability under control, new reports have shown that they can be changed in an activity-dependent manner (Frick et al., 2004) raising the possibility of using these dynamic parameters for the storage of memories through learning processes.

1.2.2 Functional roles of dendritic spikes *in vitro* and *in vivo*

A key issue in understanding the role of dendritic spikes is to determine under what conditions they are triggered *in vivo* (Kamondi et al., 1998; Waters et al., 2003; Crochet et al., 2004). Strong synaptic input, artificially activated with electrical stimulation, is known to produce dendritic spikes in cerebellar Purkinje cells, both *in vitro* (Llinás and Sugimori, 1980a) and *in vivo* (Llinás et al., 1968; Llinás and Nicholson, 1971), as well as in neocortical (Schiller et al., 1997) and hippocampal pyramidal cells (Golding and Spruston, 1998; Golding et al., 1999). The spatial distribution of the input is clearly an important factor because of the distance-dependent attenuation of synaptic depolarization (Gasparini et al., 2004; Gasparini and Magee, 2006). On the other hand, a substantial patch of membrane needs to be depolarized to engage enough voltage-gated channels, thus some spatial spread of the input is required. A

similarly important factor is temporal clustering (Gasparini and Magee, 2006; Losonczy and Magee, 2006). Under physiological conditions the closer the inputs are in time and space, the lower the threshold is to trigger a dendritic spike, so dendritic spikes can be considered as spatio-temporal coincidence detectors. A nice demonstration of this phenomenon is that coincident backpropagating action potentials (bAP) and excitatory postsynaptic potentials (EPSP) (Larkum et al., 1999a; Stuart and Häusser, 2001) or separate EPSPs (Williams and Stuart, 2002) can only evoke regenerative dendritic events if they coincide in a narrow time-window. Another determining factor in dendritic spike generation is synaptic inhibition, which can block voltage-gated calcium channel mediated supralinearity of high frequency bAPs (Larkum et al., 1999b) and suppress local regenerative events in an approximately 10-millisecond-long time window (Williams and Stuart, 2003). This is similar to the coincidence detection time window of regenerative dendritic spikes (Larkum et al., 1999a; Stuart and Häusser, 2001) and to the time window of spike timing-dependent plasticity (Abbott and Nelson, 2000; Dan and Poo, 2004, 2006). A recent study by Jarsky et al. (2005) shows a heterosynaptic regulation of dendritic spike propagation in hippocampal CA1 pyramidal cells. Dendritic spikes evoked in distal apical dendrites by synaptic stimulation generally fail to propagate to the soma. However, when synapses that are more proximal are also activated, the depolarization enables forward propagation towards the soma. This is especially interesting as the two locations are innervated by functionally different inputs: a direct input from the entorhinal cortex to the distal apical dendrites and the Schaffer collateral input to the more proximal apical regions (Yeckel and Berger, 1990). Gasparini and Magee (2006) further elucidate this picture by showing that network activity in different functional states (theta activity versus sharp waves) determines the mode of dendritic integration, thus enabling or disabling the propagation of dendritic spikes to the soma. Dendritic spikes thus start as local regenerative events, which depending on neuronal morphology, distribution of ion channels and the functional state of the neuron can propagate further and may even reach the soma. The interaction between local spikes and backpropagating action potentials can also extend the effect dendritic spikes have on somatic output (Larkum et al., 1999a) or increase the local effect of dendritic spikes.

Naturally, in dendritic compartments electrotonically very distant from the soma, backpropagation has little or no impact (Golding et al., 2002).

Functionally, dendritic spikes can fulfil various roles. They detect synchronous activity by providing a non-linear response. Depending on cell type and functional state of the neuron, the effect of dendritic spikes can become global and enhance somatic spike precision (Golding and Spruston, 1998; Ariav et al., 2003; Crochet et al., 2004) and may enable otherwise undetectable distal events to have their voice heard (Larkum et al., 1999a; Williams, 2004; Gasparini and Magee, 2006). Even if they fail to propagate and contribute to axonal output, they can trigger synaptic plasticity (Hartell, 1996; Golding et al., 2002; Holthoff et al., 2004) or retrograde neurotransmission (Murphy et al., 2005) by engaging voltage-gated calcium channels.

Overall, the existence of dendritic spikes makes a neuron a more powerful computational unit, not only providing several functional compartments, but—by the functional state-dependent determination of propagation—the number and function of these compartments can be regulated dynamically. In neuronal dendrites favouring backpropagation of the axo-somatic action potential, the relationship of local and global neuronal activity is more complex. Cerebellar Purkinje cells do not support active backpropagation of somatic spikes into the dendrites (Stuart and Häusser, 1994), thus are ideal candidates to study the functional effect of dendritic spikes in relative isolation.

1.3 Cellular overview

Purkinje cells form the sole output of the cerebellar cortex (Palay and Chan-Palay, 1974). They are GABAergic, thus their synapses, which impinge on deep cerebellar nuclei neurons (the output nuclei of the cerebellum) inhibit their targets.

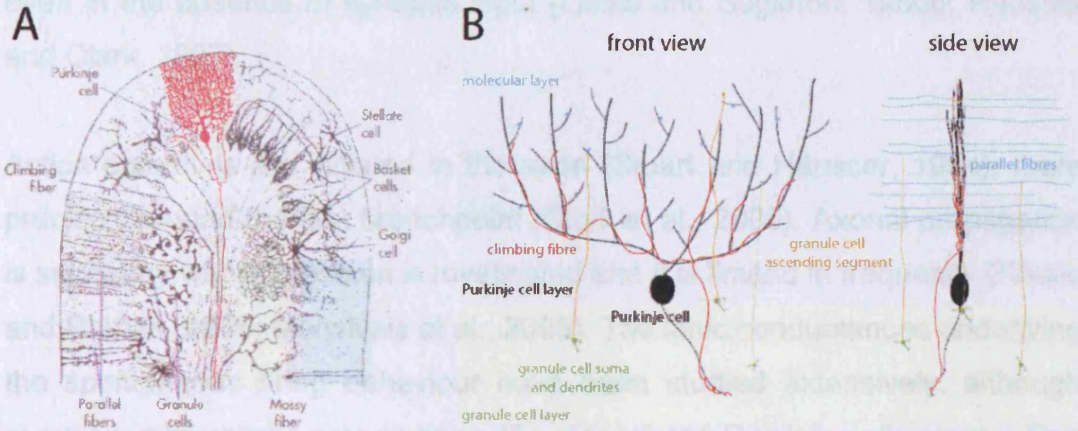

Figure 1.5 The cerebellar cortex and the Purkinje cell
A Composite drawing of Golgi stained sagittal sections of the cerebellar cortex. Modified from (Ramón y Cajal, 1911), adapted from (Nolte, 1999). **B** Schematic of a Purkinje cell and its excitatory inputs.

Sensory and motor input reaches the cerebellar cortex through mossy and climbing fibres. Glutamatergic climbing fibres innervate Purkinje, basket and stellate cells. Mossy fibres excite Golgi cells and granule cells, whose axon, the ascending segment and the parallel fibres synapse on Purkinje-, Golgi-, basket- and stellate cells. The first of the two granule cell layer inhibitory neurons, Golgi cells inhibit granule cells, while Lugaro cells innervate Golgi cells and are driven by serotoninergic inputs (Dieudonne, 2001). The molecular layer has two types of inhibitory interneurons, basket and stellate cells, which inhibit the somatic and dendritic region of Purkinje cells, respectively. The vestibulo-cerebellum also contains unipolar brush cells

(Mugnaini et al., 1997), which relay mossy fibre input to granule cells forming intrinsic mossy fibres.

1.3.1 The output of Purkinje cells

Purkinje cells generally fire continuously *in vivo* over a wide range of frequencies (10-250 Hz) with little variability in their interspike-intervals (Nitz and Tononi, 2002) but can also display bistable behaviour alternating between firing and non-firing states (Nitz and Tononi, 2002; Loewenstein et al., 2005b). In acute slices Purkinje cells fire spontaneously in the gamma range (~40 Hz) even in the absence of synaptic input (Llinás and Sugimori, 1980b; Häusser and Clark, 1997).

Action potentials are initiated in the axon (Stuart and Häusser, 1994), more precisely around the first branchpoint (Clark et al., 2005). Axonal propagation is salutatory where the axon is myelinated and it is limited in frequency (Khaliq and Raman, 2005; Monsivais et al., 2005). The ionic conductances underlying the spontaneous firing behaviour have been studied extensively, although mostly in minimalistic preparations, like dissociated Purkinje cell somata. This approach also helps isolate the axo-somatic firing mechanism from dendritic influences (Bekkers and Häusser, 2007). A TTX-sensitive resurgent sodium current activated during the downstroke and between action potentials was shown to be partly responsible for driving the spontaneous firing (Raman and Bean, 1997, 1999). Calcium currents flowing through the membrane during action potential firing have a mostly indirect effect by activating calcium-dependent potassium conductances, which contribute to the after-hyperpolarization of the neuron (Raman and Bean, 1999; Cingolani et al., 2002; Womack and Khodakhah, 2003). High firing rates are enabled by fast activating and deactivating potassium currents that repolarize both the soma (Raman and Bean, 1999) and the dendrites (Martina et al., 2003) quickly. Another voltage-dependent conductance, the HCN channel underlying the hyperpolarization activated non-selective cation current, I_h, was shown to play a major role in bistability of Purkinje cell firing (Williams et al., 2002; Loewenstein et al., 2005b) as well as keeping the dendrites slightly more

depolarized compared to the soma (E. Rancz and M. London; unpublished observation). The effect of I_h on the axo-somatic action-potential generation mechanism however is negligible (Raman and Bean, 1999) but they contribute to driving the spontaneous firing (Williams et al., 2002; Loewenstein et al., 2005b).

Most, if not all of these conductances are substrates to neuromodulation. Serotonin can for example inhibit I_h (Li et al., 1993) and facilitate bistable firing behaviour in Purkinje cells (Williams et al., 2002) in acute slices. Nitric oxide (NO) donors have also been shown to increase Purkinje cell firing rates through a cyclic guanosine monophosphate (cGMP)-dependent mechanism, possibly acting through BK channel or sodium channel phosphorylation by protein kinase G (PKG; Smith and Otis, 2003).

1.3.2 The input of Purkinje cells

Purkinje cells receive excitation from two, vastly different sources. First, the axons of granule cells form synapses mainly on spines in a one-parallel-fibre one-synapse ratio. These synapses on average show small quantal amplitude (~10 pA), low release probability and high amounts of short-term facilitation (Dittman et al., 2000; Isope and Barbour, 2002). The granule cell axons, transversing the molecular layer to bifurcate and form the parallel fibres (Figure 1.5B) also make synaptic connections with Purkinje cells located above them through the so-called ascending segment. These segments of the granule cell axons innervate the most distal parts of Purkinje cell dendrites (Gundappa-Sulur et al., 1999) and show higher release probability and quantal size than parallel fibre synapses (Sims and Hartell, 2005). Interestingly, ascending segment synapses are less susceptible to modification by classic synaptic plasticity induction protocols (Sims and Hartell, 2006). Some early extracellular recordings from Purkinje cells strongly suggests, that these ascending fibres play a crucial role in determining the spatio-temporal activity of Purkinje cells following sensory stimulation (Bower and Woolston, 1983). The issue of vertical vs. horizontal organization of granule cell input to Purkinje cells will be revisited in the general discussion

(Chapter 7.1). The second excitatory input to Purkinje cells is the axon of inferior olivary neurons, the climbing fibre, which derives its name from anatomy, as it is climbing along Purkinje cell axons and dendrites. In contrast to parallel fibres, only a single climbing fibre innervates a Purkinje cell, but through several hundred release sites, forming one of the most powerful synapse in the mammalian brain. Climbing fibre synapses release glutamate with high probability and in saturating concentrations, resulting in short-term depression when activated repeatedly (Zucker and Regehr, 2002).

The glutamate released from these 3 different types of synapses binds to postsynaptic glutamate receptors (as well presynaptic receptors not discussed in this thesis, but see e.g. Delaney and Jahr, 2002; Duguid and Sjöström, 2006; Satake et al., 2006). Of the ionotropic variety underlying excitatory postsynaptic currents (EPSC), mature Purkinje cells express AMPA type receptors with low calcium permeability and kainate receptors only but lack functional NMDA receptors (Häusser and Roth, 1997). Several metabotropic receptors are also expressed in Purkinje cells (Knöpfel and Grandes, 2002). The most prominent is the metabotropic glutamate receptor type 1 (mGluR1), which is located perisynaptically (Baude et al., 1993). Due to their location, the activation of mGluR1s depends on spatio-temporal pooling of glutamate (Tempia et al., 2001; Marcaggi and Attwell, 2005), stimulus intensity (Batchelor and Garthwaite, 1997; Reichelt and Knöpfel, 2002) and the density and activity of glutamate transporters (Otis et al., 1997; Auger and Attwell, 2000; Brasnjo and Otis, 2004; Wadiche and Jahr, 2005). The stimulation of mGluR1 activates phospholipase C (PLC) leading to inositol triphosphate (IP_3) and diacylglycerol (DAG) production. IP_3 in turn can trigger calcium release from internal stores and DAG activates protein kinase C (PKC) leading to various intracellular actions on ion channels, neurotransmitter receptors and signalling molecules (some prominent examples are elaborated in part 1.3.4).

Purkinje cells also receive inhibitory input. The predominantly axo-somatic inhibition comes from basket cells while dendritic inhibition is provided by stellate cell axons synapsing mostly on dendritic shafts. Both cell types have somas and dendrites located in the molecular layer. They are driven by

parallel fibre and climbing fibre excitation and fire continuously *in vivo* albeit at lower firing rates compared to Purkinje cells (7-28 Hz, Vos et al., 1999).

Having introduced the input and output of Purkinje cells I will move on to the main topic of my thesis: what is the transformation of the input made by Purkinje cells to generate an output? This apparently simple question embodies one of the conundrums of neuroscience and only by having good approximate algorithms to describe single cell computation can we start to understand the brain. Of course, knowing the algorithm is useless without the context of inputs and the outputs and after presenting the results of my research, I will elaborate on this by putting the Purkinje cell in the context of the cerebellar network and ultimately in the behaving animal in Chapter 7.

1.3.3 The Purkinje cell as a neuronal machine

Despite the importance of the question, relatively few direct studies of the i-o function of Purkinje cells exist. The pioneering work of Llinás and Sugimori (1980a, b) used sharp electrodes to penetrate the soma (Llinás and Sugimori, 1980b) and dendrites (Llinás and Sugimori, 1980a) of Purkinje cells in acute cerebellar slices. The choice of preparation made it possible to isolate different conductances by changing the ionic composition of the extracellular medium or applying ion-channel blockers. They found the somatic input resistance of Purkinje cells to be ~15MΩ, a remarkably good approximation given the uncontrollable leak associated with sharp electrode impalement (the range observed in my recordings and that of Roth and Häusser (2001) is 20-100 MΩ in P18-26 rat Purkinje cells). Llinás and Sugimori (1980b) described a firing vs. injected current (f/I) relationship which was non-continuous at threshold (type II, see Figure 1.3) and linear above that. With strong current injection to the soma, the regular firing epoch was usually terminated by a burst of diminishing fast action potentials (due to a progressive decrease in sodium channel availability) riding on a slower, lower amplitude spike. This slower spike was followed by a prominent after-hyperpolarization, which deinactivated the sodium channels and made fast, regular spiking possible

once more. Some recent reports considered this so-called "trimodal firing pattern", to be a 'physiological' state of Purkinje cells in acute slices (Womack and Khodakhah, 2002a; Womack and Khodakhah, 2004). This 'runaway' behaviour is the consequence of over-excitation, either by disruption of internal calcium buffering (e.g. by BAPTA) or various membrane conductances (e.g. blocking voltage-gated calcium or potassium channels) as well as temperatures above 42 °C or excessive positive current injection often results in this behaviour (Llinás and Sugimori, 1980b).

The slow spike persisted in TTX, was mediated by calcium channels and was initiated in the dendrites (Llinás and Sugimori, 1980a). Neurons however are rarely driven by steady-state current injection. A more recent study by Walter and Khodakhah examined Purkinje cell output following distributed activation of granule cells or granule cell axons using focal glutamate uncaging or electrical stimulation (Walter and Khodakhah, 2006). Regardless of whether beams of parallel fibres or clusters of granule cells were activated, the Purkinje cell output followed linearly the input intensity in the tested range.

When take into account the brevity of individual synaptic input, one may argue that these i-o functions are oversimplified. Several ways exist to describe the effect single synaptic inputs have on ongoing firing activity. One can quantify the shift in the integrated post-stimulus time histogram to compare the effect different synaptic inputs have on firing (Fetz and Gustafsson, 1983; Mittmann et al., 2005; Mittmann and Häusser, 2007). Alternatively, a temporal dimension can be added to the i-o function of a neuron by using the phase-resetting curve (for review, see Izhikevich, 2007), which characterizes the response of the neuron to transient inputs (Gutkin et al., 2005). However, no characterization of Purkinje cell responses using the phase-resetting curve is available to date.

Purkinje cells thus can respond to synaptic input in a linear fashion. This linearity is possibly maintained by a mixture of somato-dendritic conductances, thus can be modified by the modulation of Purkinje cell intrinsic

properties. Similarly, the input can be modified as well on different timescales through synaptic plasticity.

1.3.4 Intrinsic and synaptic plasticity

Little is know about plastic changes in Purkinje cell excitability compared to e.g. cortical pyramidal neurons (Schulz et al., 2006). The only study looking directly for this found no evidence of changes in intrinsic properties of Purkinje cells following a fear conditioning paradigm (Zhu et al., 2006) which leads to long lasting potentiation of parallel fibre synaptic input (Sacchetti et al., 2004). There are however well known changes in excitability during the maturation of Purkinje cells (Guan et al., 2006) or following the inactivation of the olive, thus removing climbing fibre input *in vivo* (Cerminara and Rawson, 2004). Also, holding Purkinje cells in a silent state by negative intracellular current injection triggers unknown mechanisms which push the membrane potential closer to the firing threshold, resulting in an increase in the required holding current over several minutes (Mittmann W and Rancz E; unpublished observations). It is however possible, that Purkinje cells maintain relatively stable local and global excitability throughout their lifetime, in striking contrast to cortical pyramidal cells (Frick and Johnston, 2005). This issue is thus wide open for further research.

In contrast to intrinsic plasticity, which is generally believed to serve mostly homeostatic functions (but see Frick et al., 2004), the case of synaptic plasticity could not be any more different (but see Marder et al., 1996). Since Hebb's famous postulate (Hebb, 1949) was substantiated by experimental demonstration of activity-dependent changes in synaptic strength (Bliss and Lømo, 1970), legions of neuroscientist have used mind-boggling varieties of induction protocols to trigger long-lasting changes in synaptic strength. Following the first theoretical framework about how the cerebellum may work (Marr, 1969; Albus, 1971) the first reports of the predicted long-term depression (LTD) of the parallel fibre synaptic transmission following the conjunctive activation of parallel and climbing fibres started to flow (Ito and Kano, 1982).

The best candidate for the detection of coincident PF and CF input is the level of intracellular calcium ions (Wang et al., 2000). The powerful and widespread CF input recruits P/Q-type calcium channels leading to dendritic calcium spikes and calcium entry through the cell membrane (Miyakawa et al., 1992; Watanabe et al., 1998). The more localized and modest PF input, when sufficient spatio-temporal pooling of glutamate is achieved (Batchelor and Garthwaite, 1997; Tempia et al., 2001; Marcaggi and Attwell, 2005), can activate mGluR1 receptors. The activation of these G-protein coupled receptors lead to the production of IP_3 which releases calcium from internal stores. The other product of the mGluR1 activated PLC, DAG, leads to PKC activation (Oancea and Meyer, 1998) and the consequent phosphorylation of serine residues of AMPA receptors (Leitges et al., 2004). Ultimately this phosphorylation leads to the clathrin-mediated endocytosis of phosphorylated AMPA receptors (Matsuda et al., 2000; Wang and Linden, 2000). The phosphorylation state of AMPA receptors is controlled by protein phosphatases (PP) 1 and 2A (Launey et al., 2004). Blockade of the molecular machinery responsible for the inhibition of PP occludes LTD (Boxall et al., 1996). The activation of neuronal nitric oxide synthase (nNOS) located in parallel fibre terminals and molecular layer interneurons and glia cells (Southam et al., 1992) is the first step in the pathway leading to PP inhibition. The membrane permeable NO then diffuses into Purkinje cells where it activates the soluble guanyl-cyclase causing elevation of cGMP levels (Garthwaite et al., 1988; Boxall and Garthwaite, 1996) which in turn activates G-substrate, a powerful PP inhibitor (Endo et al., 1999). The interplay of the mGluR/PKC and NO/PKG pathway remains to be elucidated. Most of the mechanisms and pathways described above have been shown to be relevant to synaptic plasticity and/or learning *in vivo* and *in vitro* (Boyden and Raymond, 2003; Gao et al., 2003; Koekkoek et al., 2003; Hopper and Garthwaite, 2006; Kishimoto and Kano, 2006).

As unidirectional synaptic plasticity leads to saturation (Goldberg et al., 2002) and excludes the possibility of the reversal or extinction of learning (Medina et al., 2000; Boyden et al., 2004), long-term potentiation of the PF-PC synapse

is also required for the balanced operation of any neuronal network. A presynaptic form of PF-LTP has been known for decades (Sakurai, 1990). It can be induced by repetitive stimulation of PFs at 4-8 Hz, it requires PKA activity (Salin et al., 1996; Linden and Ahn, 1999) and leads to an increase in release probability (Jacoby et al., 2001). As this form of plasticity is expressed presynaptically, it is a poor candidate for the reversal of LTD. A recently described form of PF-LTP however may just fulfil these criteria (Lev-Ram et al., 2002). It is induced by repetitive 1 Hz PF stimulation and is NO-dependent (but is independent of PKA activity). Even more importantly, it has been shown to reverse PF-LTD (Lev-Ram et al., 2003; Coesmans et al., 2004). The lack of CF activity requirement led Coesmans et al (2004) to speculate about the existence of an inverse Bienenstock-Cooper-Monroe rule (Bienenstock et al., 1982) where low intracellular calcium concentrations would lead to LTD and high concentrations to LTP, a mirror image to the rules governing synaptic spike-timing dependent synaptic plasticity in the cerebral cortex (Sjöström et al., 2001, 2003). For a comprehensive review on the molecular machinery available for the up- and down-regulation of parallel fibre – Purkinje cell synaptic transmission, see the comprehensive review of Ito (2002).

A relatively novel form of synaptic plasticity mediated by endocannabinoids was discovered recently (for a comprehensive review, see Freund et al., 2003) and was shown to underlie short-term suppression of both excitatory and inhibitory synaptic input to Purkinje cells (Llano et al., 1991; Kreitzer and Regehr, 2001). Endocannabinoid production shares some of the features for LTD, namely dependence on intracellular calcium increase and facilitation by mGluR activation (Brown et al., 2003). The lipophilic nature of endocannabinoids makes them excellent retrograde signal candidates (parallel to NO) and indeed, CB1 receptors are located exclusively on inhibitory and excitatory terminals impinging on Purkinje cell but are exempt from the postsynaptic membrane (Ferenc Mátyás, István Katona and Tamás Freund, personal communication). The activation of CB1 receptors leads to a G-protein-dependent inhibition of presynaptic calcium currents thus a suppression of neurotransmitter release (Brown et al., 2004). Parallel to other brain regions (Chevaleyre and Castillo, 2004; Sjöström et al., 2004; Kreitzer

and Malenka, 2007) endocannabinoids have been implied in long-term plasticity as well. Conjunctive CF-PF activity induced PF-LTD was shown to be dependent on CB1 receptor activation (Safo and Regehr, 2005) in acute slices. A very convincing *in vivo* study also proved the requirement of endocannabinoid signalling in a cerebellum-dependent discrete motor learning task, eyeblink conditioning (Kishimoto and Kano, 2006).

1.4 The aims of this thesis

This thesis aims to describe the basic biophysical properties of parallel-fibre input triggered dendritic spikes in Purkinje cells (Chapter 3) and to examine the potential roles dendritic spikes play in synaptic plasticity (Chapters 4 and 5) as well as controlling the somatic action potential output (Chapter 6). The main experimental technique utilised to this end is dendritic and somatic voltage recording using the whole-cell patch clamp method (Davie et al., 2006) combined with calcium imaging. The methods used in this study are given in Chapter 2.

2. Materials and Methods

2.1 Introduction

The data presented in this thesis were recorded from Purkinje cells of the cerebellar vermis of young rats (P18-26) maintained in acute slices. Whole-cell patch-clamp (Hamill et al., 1981) recordings were made in the current-clamp mode to record the somatic and dendritic membrane potential. In some experiments, calcium imaging was also performed using an epifluorescence microscope. These are standard, well established experimental methods. For a detailed protocol of dendritic patch-clamp recording, please see (Davie et al., 2006).

2.2 Slice preparation

Acute slices were prepared from P18-26 Sprague – Dawley rats and used for up to 5 hours. All procedures were carried out in accordance with the Animal Scientific Procedures Act (1996). In brief, animals were deeply anaesthetised using Isoflurane (Baxter Healthcare Ltd, Thretford, UK) and decapitated. The head was immediately immersed in artificial cerebro-spinal fluid (ACSF) and the scalp was quickly removed. The whole slicing procedure was conducted in ice-cold, carbogenated ACSF for neuroprotection and setting the pH, respectively. The entire brain was removed from the skull and pinned down through the forebrain to a Sylgard-bottomed Petri-dish containing ice-cold ACSF. The dura mater and arachnoidea covering the vermis were removed using a pair of fine forceps (Dumont No. 5). The cerebellum and brainstem

were removed from the brain using a coronal cut. After removing the brainstem and the choroids plexus of the fourth ventricle, the vermis was separated from the cerebellar hemispheres using two rostro-caudal cuts. The block of vermal tissue was then glued to a metal platform using a cyanoacrylate glue and covered in ACSF. Sagittal slices of the vermis 200-300 µm in thickness were prepared using a vibrating blade microtome (Leica VT1000S, Nussloch, Germany). The slices were then incubated at 32 °C in ACSF for 30 minutes to aid the recovery of the tissue. This helps endogenous proteases to clean the cut surface and more importantly, helps to equilibrate intracellular ion concentrations, as most pump and exchangers are highly temperature sensitive. After this incubation period, the slices were transferred to room temperature and stored in continuously carbogenated ACSF until use.

2.3 Patch-clamp recording

Slices were transferred to a submerged-type recording chamber and clamped down using a U shaped, flattened platinum wire covered with 4-5 thin elastic fibres obtained from stockings or dental-floss to help maintain physical stability. All recordings were done at near-physiological temperatures (33-36 °C) in continuously carbogenated ACSF. The flow rate was set to 6-10 ml/min to ensure optimal oxygenation of the tissue (Hájos et al., 2004).

Glass micropipettes were pulled from filamented borosilicate capillaries (GC150F, Harvard Apparatus, Edenbridge, UK) using a two-stage, vertical puller (PC-10, Narashige, Japan). Electrodes had a tip resistance of 3-8 MΩ when filled with the internal solution.

Target structures were visualised using differential interference optics (DIC) on an Olympus BX51WI upright microscope equipped with a 60x, 0.9 NA objective. A Hamamtsu C2400-7 Vidicon tube type camera was used together with a 2x – 4x magnifier to display the DIC image on a video monitor. The microscope was fixed to an XY table to allow change in the field of view independently of the recording electrodes and recording chamber, which were

fixed to a pneumatic vibration-isolation table (Technical Manifacturing Corporation). Somatic and dendritic recordings (60 – 220 µm from the soma, measured along the dendrite) were made using Multiclamp 700A and 700B amplifiers (Molecular Devices). The recording headstages were mounted on remote-controlled, motorized micromanipulators (Luigs and Neumann LN SM1) to ensure smooth and fine pipette movement and stability, both critical for successful dendritic patch-clamp recording.

Seals between the neuronal membrane and the pipettes were established in voltage-clamp mode using gentle suction if necessary. The seal resistance was 3-10 GΩ before rupturing the membrane to establish the whole-cell configuration. The amplifier was then switched to current-clamp mode and Purkinje cells were prevented from firing spontaneously by the injection of -300-500 pA holding current. The electrode capacitance was compensated and the bridge was balanced. Initial bridge-balance values ranged from 8-14 MΩ for somatic and 8-20 MΩ for dendritic recordings. Recordings were terminated when bridge balance values exceeded 50 MΩ. The junction potential (~7 mV) was not corrected for.

2.4 Calcium imaging

Two fluorophores were used in the imaging experiments: Alexa 594 (1 µM), a biologically inert dye to image the structure of Purkinje cells and fluo-5F (200 µM, both from Invitrogen, Carlsbad CA) to determine relative changes in calcium concentration (K_d = 3.2 mM in a cuvette, ~ 0.8 mM in neurons (Yasuda et al., 2004). The excitation was produced by a monochromator (Polychrome IV) and the emitted light was detected using a Imago-QE cooled CCD camera (both from TILL Photonics, Gräfelfing, Germany). Alexa 594 was excited at 570 nm and the emitted light was filtered at 610 ± 10 nm. For calcium imaging, fluo-5F was excited at 492 nm and the emitted light was filtered at 510 + 10 nm. These excitation / emission wavelength combination were chosen empirically for best signal-to-noise ratios.

Purkinje cells were filled through the soma for 30 minutes with internal solution supplemented with the two dyes. The somatic electrode was removed and the dendrite was patched with the same internal, allowing 10 minutes for the dyes to equilibrate before conducting any measurements. Fluorophores were illuminated for 18-22 ms and the emission was measured for 25 ms, resulting in a 40 Hz sampling rate.

2.5 Electrical stimulation

To activate afferent axons, a patch pipette was filled with ACSF and connected to a stimulus isolator (Dagan BSI-950 and Digitimer DS3). Biphasic voltage pulses of 1-100 V in intensity and 50-200 µs in duration were used. Parallel fibres were activated by placing the stimulation electrode into the molecular layer, buried deep under the dendritic tree. By placing the stimulating electrode directly underneath the dendritic recording electrode, parallel fibres innervating dendrites in the close vicinity of the dendritic recording were activated. Climbing fibres were stimulated by placing the stimulating electrode in the granule cell layer and adjusting the position and stimulation intensity to isolate pure climbing fibre responses.

2.6 Maintaining life – solutions and drugs

2.6.1 External solution

Throughout all experiments, I was using the same composition of artificial cerebrospinal fluid (ACSF) as an external solution (Table 2.1). The osmolarity of this solution was ~ 305 mOsm. It was continuously bubbled with a mixture of 95% O_2 (for oxygenation) and 5% CO_2 (for setting the pH to ~7.35) during the experiments.

Compound	Composition (mM)
NaCl	125
$NaHCO_3$	26
Glucose	25
KCl	2.5
NaH_2PO_4	1.25
$CaCl_2$	2
$MgCl_2$	1

Table 2.1 Composition of ACSF

2.6.2 Internal solution

Compound	Concentration (mM)
K-methanesulphonate	130
KCl	7
HEPES	10
EGTA	0.05
Na_2-ATP	2
Mg-ATP	2
Na_2-GTP	0.5

Table 2.2 Composition of the internal solution

The internal solution was made with the ingredients in Table 2.2. The osmolarity was 285 mOsm, the pH was set to 7.3 using KOH. The solution was aliquoted and stored at -20 °C for up to 12 months before use.

For the imaging experiments, 1 µM Alexa 594 and 200 µM fluo-5F was added to the internal. Biocytin (0.4-1 w/w%) was routinely added to the internal.

Whole cell recordings allow for faithful, high signal-to-noise ratio recordings of membrane potential and membrane currents because of the very high seal resistance to access resistance ratio. The good access to the interior of the cell comes at a price, though. The intracellular ion concentrations will equilibrate quickly with the internal solution. Second messengers and other soluble intracellular systems, like calcium buffers, may be washed out. Purkinje cells have a very high endogenous calcium buffering capacity, which seems to be insoluble (Fierro and Llano, 1996) thus calcium buffering was less affected by whole cell recording. The relatively high concentration of ATP in the intracellular solution used in this thesis on the other hand could have led to partial blockage of soluble guanylate cyclase (Ruiz-Stewart et al., 2004) thus impairing NO signalling. The relatively low free magnesium ion concentration (~ 70 µM) could also have led to minute alterations in channel kinetics. To minimise washout of intracellular signalling molecules and to retain the original intracellular ion concentrations, one can perform perforated patch recordings (Akaike, 1996). This technique however requires several tens of minutes for the access to the cell to develop and leads to relatively high access resistances, making it impractical if not impossible to use for dendritic recordings. Dendritic recordings on the other hand require smaller electrode tips, leading to relatively slower washout. Nevertheless one has to keep in mind the limitations coming from disturbing the intracellular milieu when interpreting results obtained by whole-cell recordings. I want to stress, however, that the results presented in this thesis are in line with the general electrophysiological behaviour of Purkinje cells measured previously by intracellular sharp-electrode or whole-cell patch clamp recordings (Llinas and Sugimori, 1980a, b).

2.6.3 Drugs

Several pharmacological agents were used (Table 2.3). The selective $GABA_A$ antagonist SR95531 was used in every experiment described in this thesis to isolate excitatory fast synaptic transmission. The selective and highly potent BK channel antagonist, penitrem A (Knaus et al., 1994) was used instead of the classical iberiotoxin for two main reasons: penitrem A is not a peptide, thus it is much easier to handle and wash out from the perfusion system and second, it cost's substantially less than iberiotoxin.
The drugs were dissolved in distilled water or dimethyl sulfoxide (DMSO, an organic solvent) at stock concentration (10-100 mM) and added to the ACSF before every experiment in the required dilution.

Drug	Concentration (µM)	References
SR95531	10	(Ueno et al., 1997)
$CdCl_2$	200	(Llinas and Sugimori, 1980b)
penitrem A	0.1	(Knaus et al., 1994)
AM251	1-5	(Gatley et al., 1996)
CPCCOEt	100	(Litschig et al., 1999)
APV	50-100	(Watkins and Evans, 1981)

Table 2.3 Drugs and concentrations used

2.6.4 Chemicals and purveyors

NaCl	Sodium Chloride, Sigma
$MgCl_2$	Magnesium chloride, Sigma
$CaCl_2$	Calcium chloride, Sigma
Glucose	D-glucose, Sigma
$NaHCO_3$	Sodium bicarbonate, Sigma
NaH_2PO_4	Sodium dihydrogen phosphate, Sigma
KCL	King's College London, Sigma
Na_2-GTP	Disodium guanosine triphosphate, Sigma
Na_2-ATP	Disodium adenosine triphosphate, Sigma
Mg-ATP	Magnesium adenosine triphosphate, Sigma
HEPES	4-(2-Hydroxyethyl)piperazine-1-ethanesulphonic acid
EGTA	Ethylene glycol–bis(2–aminoethylether) -N,N,N',N' - tetraacetic acid
$CdCl_2$	Cadmium chloride, Sigma
SR95531	Sigma
AM251	Tocris
penitrem A	Alomone Labs
CPCCOEt	Tocris
APV	Tocris
biocytin	Sigma
Alexa 594	Invitrogen
fluo-5F	Invitrogen

2.7 Data acquisition and analysis

Data was acquired using an Apple Power Mac G4 computer (Apple, Cupertino, CA) running Axograph 4.8 or 4.9 (Molecular Devices) connected to an ITC18 DAC board (Instrutech, Port Washington, NY). Data from the amplifier was low-pass filtered at 6-10 kHz and sampled at 20-50 kHz.

Data analysis was performed in Igor Pro (Wavemetrics, Lake Oswego, OR) using NeuroMatic (http://www.neuromatic.thinkrandom.com) and custom-written macros.

Imaging data was acquired at 40 Hz on a Windows PC running TILL VisION (TILL Photonics, Gräfelfing, Germany). Imaging data was analysed in ImageJ (http://rsb.info.nih.gov/ij/) and Igor Pro using built-in and custom-written routines.

Data is presented as mean ± SEM, statistical significance was assessed using Student's t-test (two-tailed, paired when possible).

3. Local dendritic spikes in cerebellar Purkinje cells

3.1 Introduction

The complex branching architecture of most dendritic trees provides anatomical substrate for having multiple interconnected signal processing units in a single neuron. Generating functional compartments requires, first, segregation between different dendritic compartments, determined by the passive morpho-electrical properties of the dendritic tree; second, mechanisms for local interactions between synaptic conductances, such as is provided by non-linear dendritic conductances; and third, a means for efficient and modifiable communication between different compartments. The stage on which sub- and suprathreshold interactions between different functional compartments are played out is the dendritic morphology of the neuron, which determines their size, number and spatial arrangement. The dendrites of mammalian neurons have been shown to express a variety of voltage-gated ion channels (Migliore and Shepherd, 2002), as a consequence dendrites exhibit a range of excitable behaviour (Häusser et al., 2000). One of the most prominent forms of dendritic electrogenesis is the dendritic spike. Dendritic calcium spikes were originally described in cerebellar Purkinje cells both *in vivo* (Llinás et al., 1968) and *in vitro* (Llinás and Sugimori, 1980a). They have also been reported in hippocampal (Wong et al., 1979) and neocortical pyramidal cells (Amitai et al., 1993; Schiller et al., 1997), where they have been shown to be triggered by sensory stimulation (Helmchen et al., 1999; Larkum and Zhu, 2002; Waters et al., 2003).

There are many possible functional roles of such non-linear dendritic events: if they propagate to the soma, they can evoke time-locked action potentials (Ariav et al., 2003) or can change the firing mode of the neuron (Larkum et al., 1999a). Even if they do not always propagate faithfully to the soma (Llinás and Sugimori, 1980a; Schiller et al., 1997) and do not reliably trigger axonal APs (Schiller et al., 1997; Larkum et al., 2001), local forms of readout may exist. Many intracellular processes can be activated by the calcium entry triggered by dendritic spikes, leading to various forms of synaptic and intrinsic plasticity (Golding et al., 2002; Holthoff et al., 2004; Holthoff et al., 2006; Kampa et al., 2006).

In this chapter, I will investigate the basic properties of dendritic spikes triggered by parallel fibre input in Purkinje cells using dendritic patch-clamp recording and calcium imaging techniques.

3.2 Results

3.2.1 Detection of dendritic spikes

To characterize dendritic spikes in Purkinje cells, I have made double and triple dendritic and somatic voltage recordings using the whole-cell patch-clamp technique. Dendritic spikes were evoked using PF stimulation or by injecting an EPSC-like double-exponential waveform (τ_{rise} = 0.6 ms, τ_{decay} = 6 ms). When more then one current pulse was injected, the kinetics of the amplitudes followed that of the PF synapse described by Dittman and colleagues (Dittman et al., 2000).

To detect and measure the voltage threshold of dendritic spikes in a quantitative manner, the following approach was adopted. The inflection point of the voltage trace, where the voltage increase is subjected to an abrupt acceleration (reflecting the non-linear recruitment of voltage-gated channels) marks the beginning of the dendritic spike. The method of Gasparini and Magee (2004) was adapted, involving the localization of the first positive peak in the second derivative preceding the peak of the dendritic spike, where the first derivative is positive. I took the 20% point of this peak as the timepoint at which the voltage threshold was measured (Figure 3.1). This somewhat arbitrary value was chosen to provide a robust measure, as the noise of the voltage recording is increased by the derivation. Empirically, this measure provided a consistent measure of the initiation point as judged by eye. Since the voltage recording was done at an unknown location with respect to the site of dendritic spike initiation, and there are no straightforward experimental techniques to determine if the measured dendritic spike was active, or just a passive reflection of the spike at the recording location, I termed this threshold as the 'apparent voltage threshold'.

The apparent voltage threshold of dendritic spikes triggered by single PF EPSPs was –29 ± 2 mV (n = 14 cells) and the threshold amplitude of single dendritic EPSPs for triggering dendritic spikes was 19.1 ± 2.7 mV (n = 10 cells, EPSPs measured at the dendritic recording site at –70 mV).

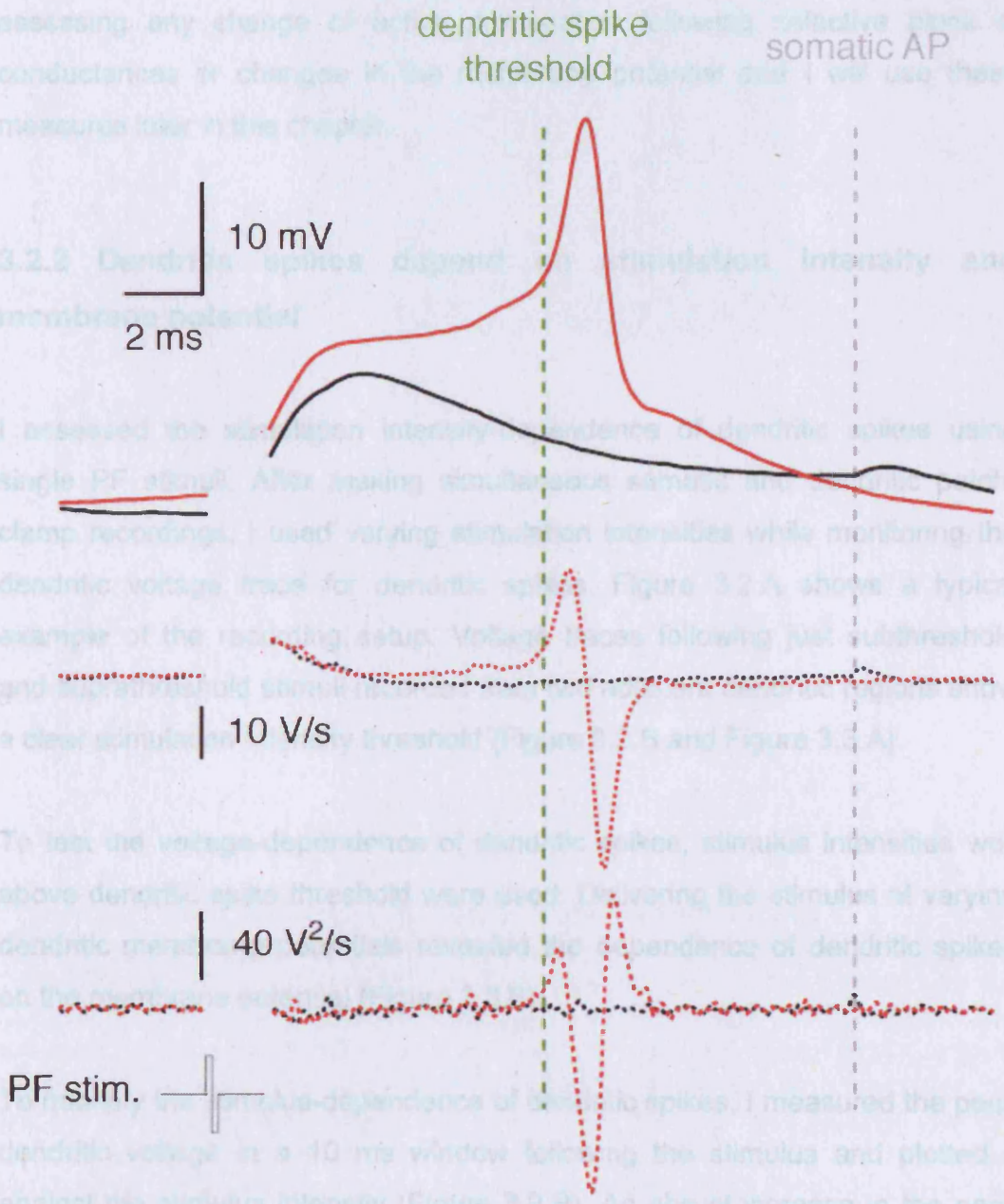

Figure 3.1 Determining the apparent voltage threshold of a dendritic spike
Dendritic voltage recording of a subthreshold EPSP (black) and a dendritic spike triggering EPSP (red). First and second derivatives were used to determine the apparent voltage threshold (green dashed line). Note the heavily attenuated backpropagation of somatic action potentials (grey dashed line).

Other measures can also be used to characterise spikes. The peak amplitude and half width of the spike can be used to assess the relative contribution of calcium and potassium channels. Similarly, the amplitude of after-hyperpolarization can convey information about the underlying channels. The amplitude and half-width measurements can be especially informative for assessing any change of active propagation following selective block of conductances or changes in the membrane potential and I will use these measures later in this chapter.

3.2.2 Dendritic spikes depend on stimulation intensity and membrane potential

I assessed the stimulation intensity-dependence of dendritic spikes using single PF stimuli. After making simultaneous somatic and dendritic patch-clamp recordings, I used varying stimulation intensities while monitoring the dendritic voltage trace for dendritic spikes. Figure 3.2.A shows a typical example of the recording setup. Voltage traces following just subthreshold and suprathreshold stimuli recorded from two adjacent dendritic regions show a clear stimulation intensity threshold (Figure 3.2.B and Figure 3.3.A).

To test the voltage-dependence of dendritic spikes, stimulus intensities well above dendritic spike threshold were used. Delivering the stimulus at varying dendritic membrane potentials revealed the dependence of dendritic spikes on the membrane potential (Figure 3.3.B).

To quantify the stimulus-dependence of dendritic spikes, I measured the peak dendritic voltage in a 10 ms window following the stimulus and plotted it against the stimulus intensity (Figure 3.2.B). An abrupt increase in the peak dendritic voltage when increasing the stimulus intensity from 30 V to 40 V signals the appearance of dendritic spikes (cf. Figure 1.4).

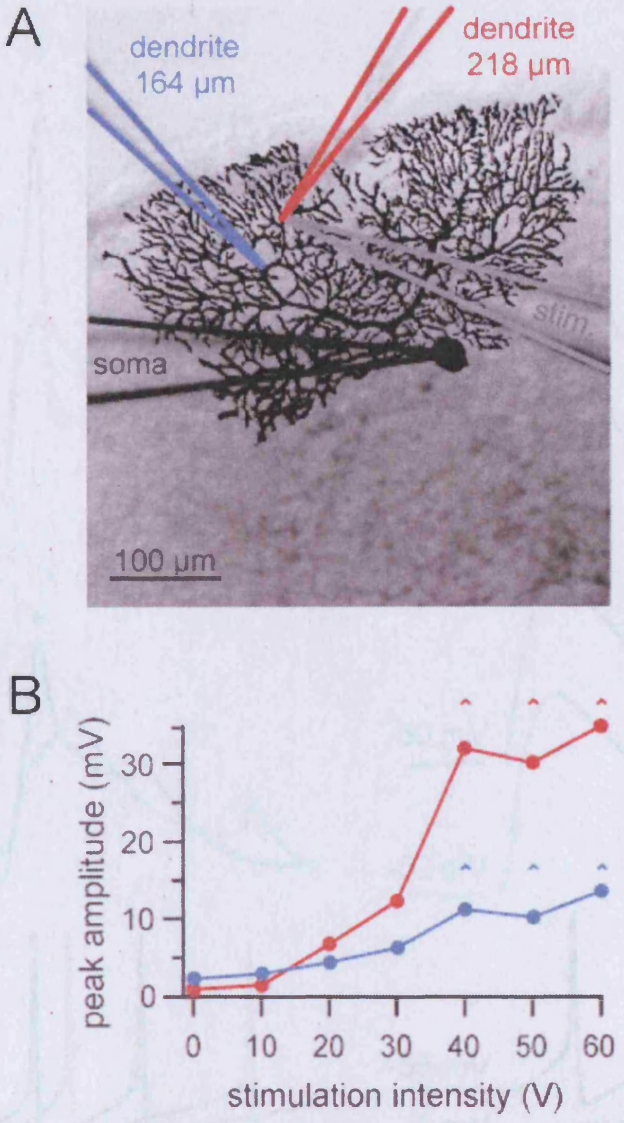

Figure 3.2 Dendritic spikes depend on stimulation intensity
A. Simultaneous triple whole-cell dendritic and somatic recordings were made from a Purkinje cell. An image of the biocytin-filled cell is superimposed on the DIC image of the slice taken at the end of the recording. The position of the recording electrodes is colour-coded: red for the distal dendrite (218 µm from the soma), blue for the more proximal dendrite (164 µm) and black for the soma. The stimulating electrode (grey) was buried in the slice directly underneath the distal recording electrode. **B.** Graph showing the non-linear relationship between stimulation intensity and peak depolarization evoked by the PF stimulation at the two dendritic locations (red: distal, blue: proximal). Note the step-like increase in peak depolarization at the distal recording site associated with initiation of the dendritic spike (^), and the strong attenuation of the dendritic spike at the more proximal recording site (54 µm away from the distal dendritic recording).

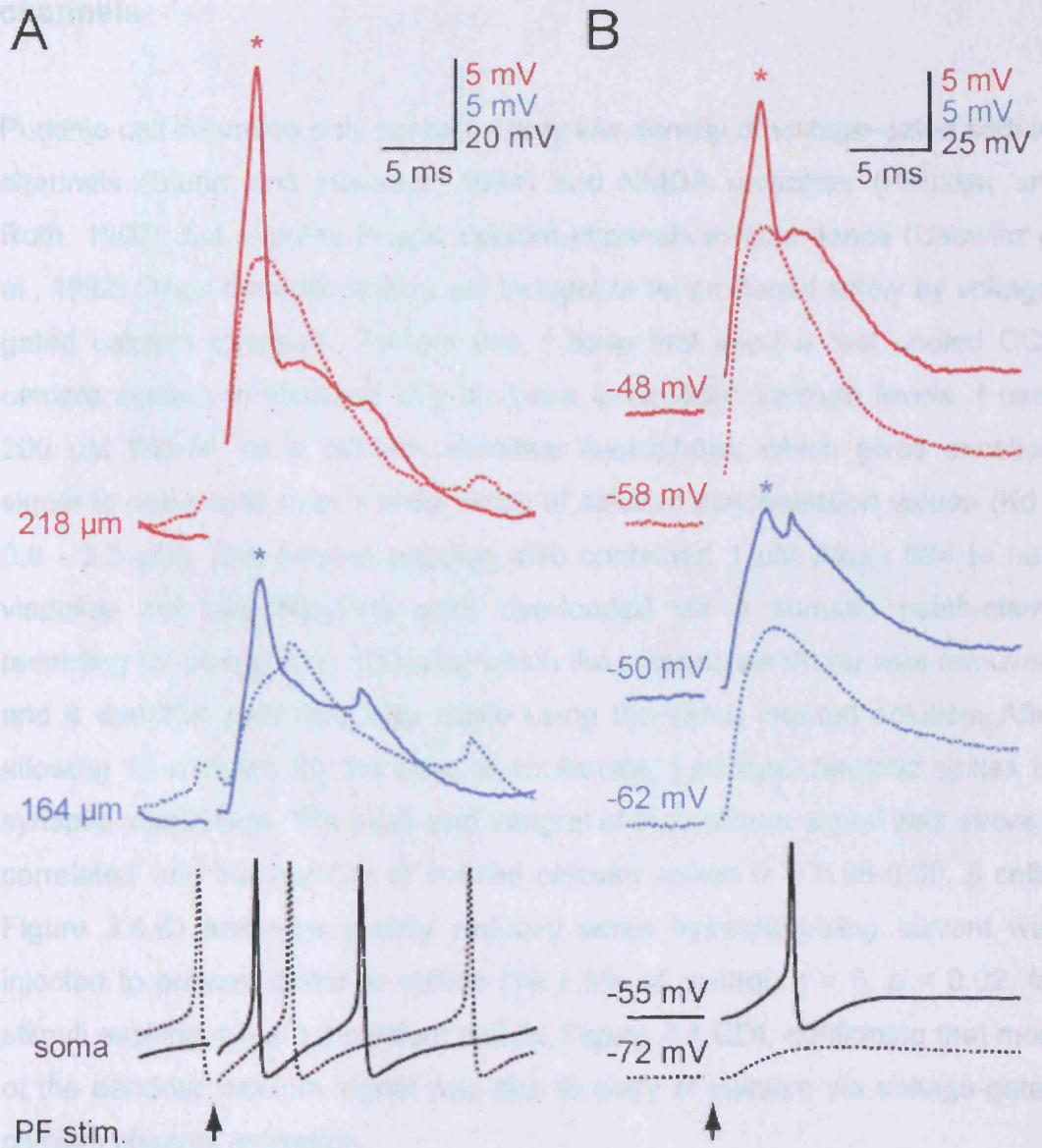

Figure 3.3 Dendritic spikes are gated by stimulus intensity and membrane potential

A. Traces from the recording shown in Figure 3.2; raising the PF stimulation intensity from 30 to 40 V (stimulus at the arrowhead) resulted in initiation of a dendritic spike (asterisk) near the distal dendritic recording site. Note the small amplitude of the passively backpropagating action potentials at the dendritic recording sites. **B.** Supra-threshold stimulation evokes dendritic spikes at rest (spontaneous firing with no holding current) that are blocked when the cell is hyperpolarized.

3.2.3 Dendritic spikes are mediated by voltage-gated calcium channels

Purkinje cell dendrites only contain a very low density of voltage-gated sodium channels (Stuart and Häusser, 1994) and NMDA receptors (Häusser and Roth, 1997), but express P-type calcium channels in abundance (Usowicz et al., 1992). Thus dendritic spikes are thought to be produced solely by voltage-gated calcium channels. To test this, I have first used a fast cooled CCD camera system to visualize any increase in dendritic calcium levels. I used 200 µM fluo-5F as a calcium sensitive fluorophore, which gives excellent signal to noise ratio over a wide range of calcium concentration values (Kd = 0.8 - 2.3 µM). The internal solution also contained 1 µM Alexa 594 to help visualize the cell. Neurons were dye-loaded via a somatic patch-clamp recording for 30 minutes, following which the somatic electrode was removed, and a dendritic recording was made using the same internal solution. After allowing 10 minutes for the dyes to equilibrate, I evoked dendritic spikes by synaptic stimulation. The peak and integral of the calcium signal was strongly correlated with the number of evoked calcium spikes ($r = 0.98$-0.99, 5 cells, Figure 3.4.B) and was greatly reduced when hyperpolarizing current was injected to prevent dendritic spikes ($19 \pm 5\%$ of control, $n = 5$, $p < 0.02$, for stimuli evoking 4.3 ± 1.2 calcium spikes, Figure 3.4.CD), confirming that most of the dendritic calcium signal was due to entry of calcium via voltage-gated calcium channel activation.

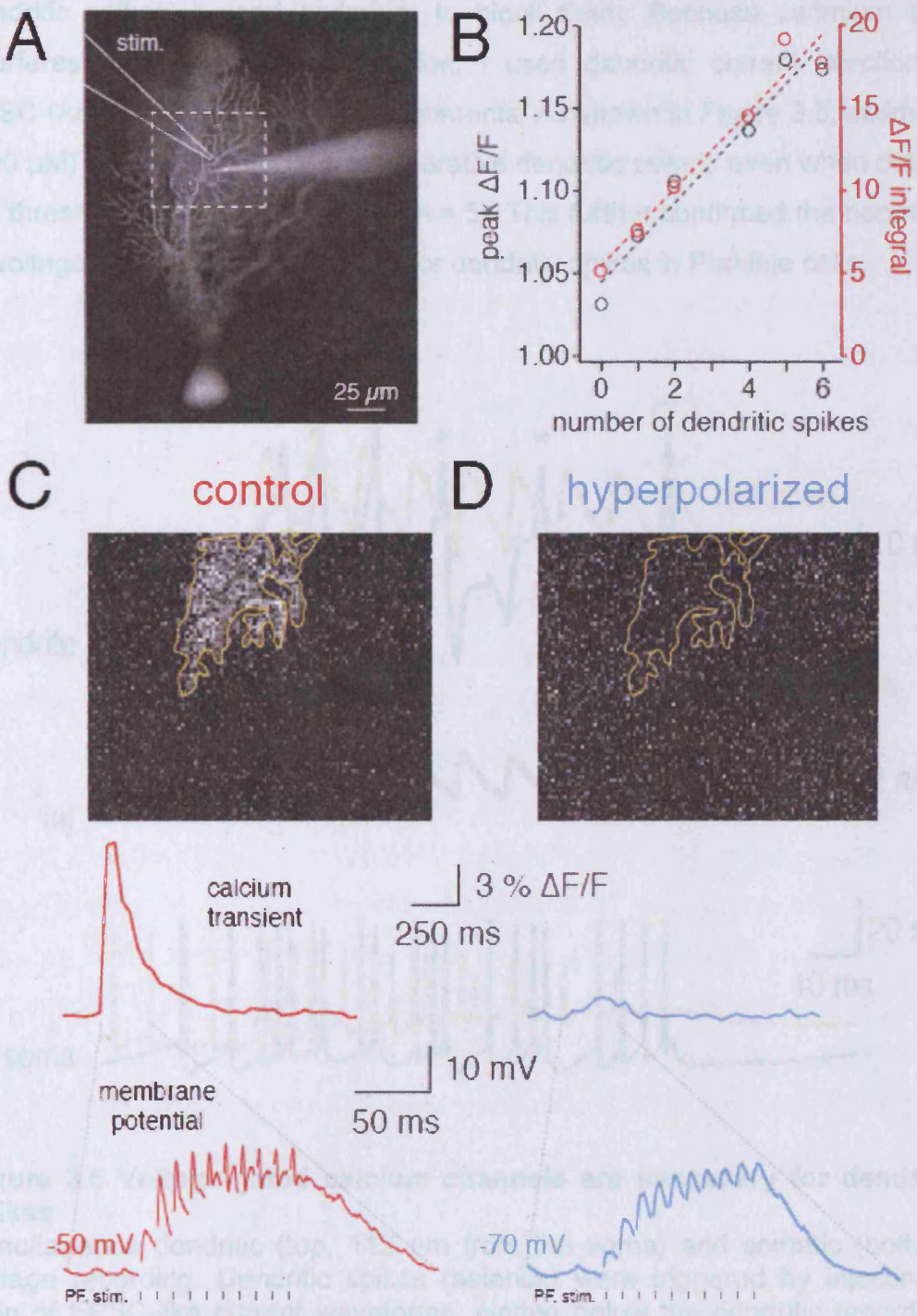

Figure 3.4 Dendritic spikes are the main source of dendritic calcium transients after PF stimulation

A. Purkinje cell filled with Alexa 594 and fluo-5F. **B.** Strong, linear correlation between the number of dendritic spikes and the peak (black) and integral (red) of the calcium signal. The dashed lines are linear fits to the data. **C.** Maximum intensity projection, calcium transient from the ROI (yellow) and dendritic membrane potential during parallel fibre stimulation from the same cell as A. **D.** Same as in C but the cell was hyperpolarized to prevent dendritic spikes.

To confirm that voltage-gated calcium channels are necessary to produce dendritic spikes, I used cadmium to block them. Because cadmium also interferes with synaptic transmission, I used dendritic current injection of EPSC-like waveforms in these experiments. As shown in Figure 3.5, cadmium (200 µM) completely blocked regenerative dendritic events even when double the threshold current was injected (n = 5). This further confirmed the necessity of voltage-gated calcium channels for dendritic spikes in Purkinje cells.

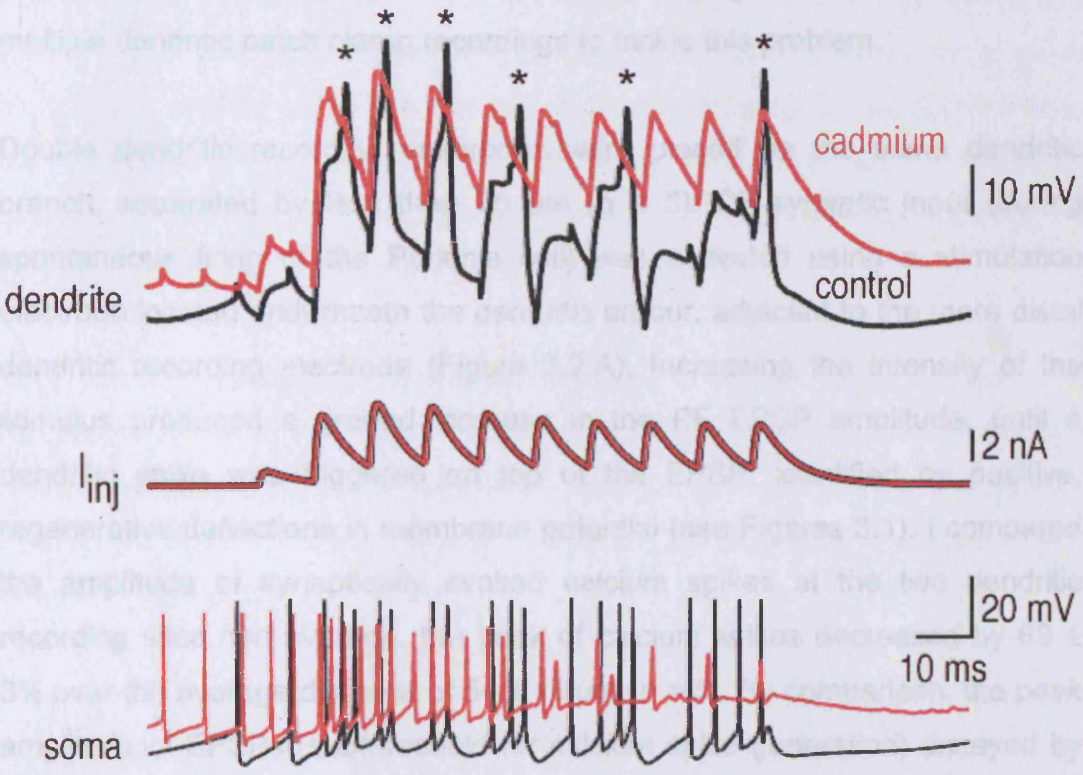

Figure 3.5 Voltage-gated calcium channels are necessary for dendritic spikes
Simultaneous dendritic (top, 112 µm from the soma) and somatic (bottom) voltage recording. Dendritic spikes (asterisk) were triggered by injecting a train of EPSC-like current waveforms, plotted below the dendritic recording. The amplitude of current injection was set at double the threshold required to elicit dendritic spikes. The addition of 200 µM $CdCl_2$ to the ACSF resulted in the disappearance of dendritic spikes for all tested current injections (red traces).

3.2.4 Parallel fibre stimulation evoked dendritic spikes are local

To understand the functional role of dendritic calcium spikes in Purkinje cells, it is essential to know their spatial extent. Previous imaging studies (Ross and Werman, 1987; Miyakawa et al., 1992; Hartell, 1996; Wang et al., 2000) have shown that synaptically evoked calcium transients are localized to their initiation site, but the regenerative nature of the calcium transient was never proven due to the low temporal resolution of imaging techniques. I thus used multiple dendritic patch clamp recordings to tackle this problem.

Double dendritic recording electrodes were placed on the same dendritic branch, separated by less than 75 µm (n = 5). PF synaptic input (during spontaneous firing of the Purkinje cell) was activated using a stimulation electrode located underneath the dendritic arbour, adjacent to the more distal dendritic recording electrode (Figure 3.2.A). Increasing the intensity of the stimulus produced a graded increase in the PF EPSP amplitude, until a dendritic spike was triggered on top of the EPSP, identified by positive, regenerative deflections in membrane potential (see Figures 3.1). I compared the amplitude of synaptically evoked calcium spikes at the two dendritic recording sites. On average, the peak of calcium spikes decreased by 69 ± 3% over the average distance of 54 ± 11 µm (n = 5). By comparison, the peak amplitude of EPSPs (subthreshold for calcium spike generation) decayed by only 41 ± 3%, significantly less than attenuation of the calcium spikes ($p < 0.005$) over the same distance. Figure 3.3.A and B shows traces from such an experiment.

Despite having high temporal resolution, thus allowing the detection of regenerative events, voltage recording has limited spatial resolution (basically the number of recording electrodes). To visualise the spatial spread of dendritic calcium spikes and to compare synaptically and current-injection evoked calcium spikes, I combined calcium imaging with dendritic recordings. Dendritic spikes triggered by synaptic activation (10 PF stimuli at 100 Hz) were associated with calcium transients which were highly localized to a few spiny branchlets close to the stimulation electrode (Figure 3.4 and Figure 3.6),

consistent with previous reports (Miyakawa et al., 1992; Hartell, 1996; Brown et al., 2003) and with my dendritic electrophysiological recordings (Figure 3.2.B). Approximately twice the number of calcium spikes triggered by current injection (10.1 ± 1.3 for current injection vs. 4.8 ± 0.2 for synaptic stimulation; n = 5) was required to evoke calcium transients of similar magnitude to synaptically triggered calcium spikes (peak amplitude 108 ± 22% of synaptically evoked transients). An intriguing segregation was detected when comparing the calcium transients triggered by synaptic stimulation and current injection, which revealed a spatial separation of calcium influx during the two different protocols. During current injection-evoked calcium spikes the peak at ROI_{SYN} was only 25 ± 4% (n = 8, $p < 0.001$) of the peak at ROI_{INJ}. Conversely, during synaptic stimulation, the calcium transient at the location of the peak calcium signal during dendritic current injection (ROI_{INJ}) reached only 21 ± 4% (n = 8, $p < 0.001$) of the peak at the ROI_{SYN} (Figure 3.6).

Thus dendritic calcium spikes evoked by PF stimulation are highly localized to the site of synaptic activation. In contrast, current injection evoked calcium spikes are triggered in neighbouring spiny branchlets having the lowest threshold determined by the electro-morphological properties of the dendrites (Vetter et al., 2001).

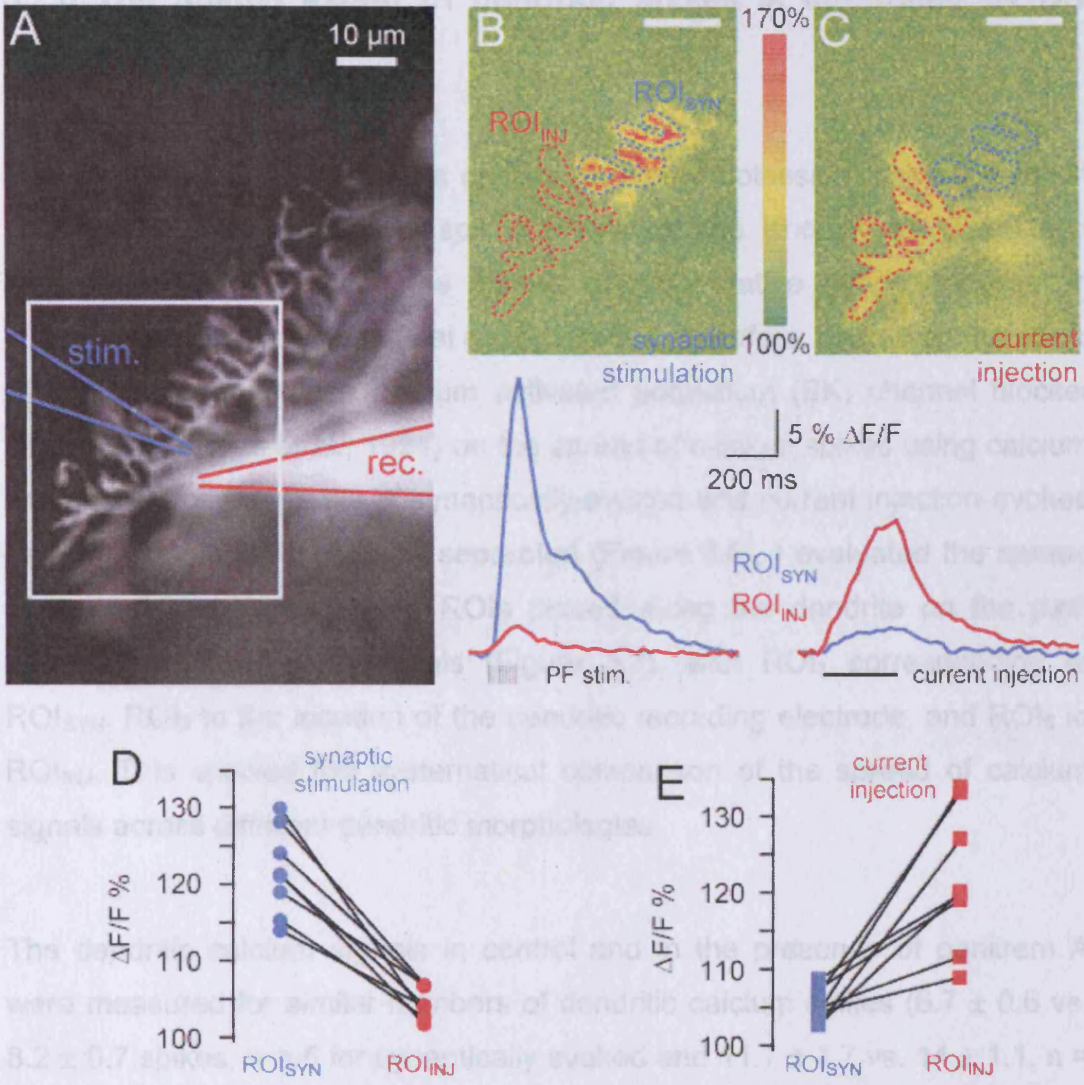

Figure 3.6 Different localization of synaptic stimulation and current injection triggered dendritic spikes

A. Purkinje cell filled with Alexa 594 and fluo-5F. The position of the PF stimulation electrode (blue) and the dendritic recording electrode (red; 90 µm from the soma) are indicated. **B**. The area of interest (white rectangle in A) was imaged for calcium signals during synaptic stimulation triggering dendritic spikes. The image is a maximum intensity projection of a stack of 41 consecutive images acquired at 40 Hz. **C**. Maximum intensity projection of a stack recorded during calcium spikes evoked by current injection. Two regions of interests (ROI) outlining the branchlets showing calcium signals during synaptic stimulation (ROI_{SYN}) or current injection (ROI_{INJ}) were selected. The timecourse of the fluorescent signal in the two ROIs is plotted below the images. The same number of calcium spikes was evoked by the synaptic stimulation and the current injection. Scale bars in B and C are 10 µm. **D.** Data from 8 cells showing the peak fluorescence change during synaptic stimulation evoked calcium spikes at the two ROIs selected in the same way as in B and C. **E.** Data from the same 8 cells showing fluorescence changes during current injection-evoked calcium spikes.

3.2.5 The spatial extent of dendritic spikes is controlled by BK channels

Purkinje cell dendrites express calcium-activated potassium channels which can be activated by calcium spikes (Womack and Khodakhah, 2004) and have been shown to limit the spread of regenerative dendritic events in cultured pyramidal neurons (Cai et al., 2004). I, therefore, examined the effect of the high conductance calcium activated potassium (BK) channel blocker penitrem A (Knaus et al., 1994) on the spread of calcium spikes using calcium imaging. Since the peaks of synaptically-evoked and current injection-evoked calcium signals were spatially separated (Figure 3.6), I evaluated the spread of the calcium signals using ROIs placed along the dendrite on the path between the two peak signals (Figure 3.7), with ROI_1 corresponding to ROI_{SYN}, ROI_3 to the location of the dendritic recording electrode, and ROI_5 to ROI_{INJ}. This allowed the systematical comparison of the spread of calcium signals across different dendritic morphologies.

The dendritic calcium signals in control and in the presence of penitrem A were measured for similar numbers of dendritic calcium spikes (6.7 ± 0.6 vs. 8.2 ± 0.7 spikes, n = 5 for synaptically evoked and 11.7 ± 1.7 vs. 14 ± 1.1, n = 3 for current injection-evoked calcium spikes, $p > 0.05$ for both cases). The calcium signal evoked by synaptic stimulation at the site of the active synapses (ROI_{SYN}) was significantly increased by penitrem A (161 ± 24% of control, n = 5, $p < 0.04$). The peak current injection-evoked calcium signal (ROI_{INJ}) also appeared to increase, although this was not statistically significant (135 ± 10% of control, n = 3, $p = 0.11$). Penitrem A enhanced the spread of calcium transients evoked by synaptic stimulation, as determined by the normalized peak calcium signals at successive ROI's from ROI_{SYN} (Figure 3.7). The calcium signal associated with dendritic spikes evoked by current injection spread even more effectively from the location of the peak in the presence of penitrem A (Figure 3.7EF). As a consequence, the peak calcium transient reached during current injection-evoked dendritic spikes at the site of

the activated synapses was dramatically enhanced (Figure 3.7G; 435 ± 32%; $n = 3$; $p < 0.01$).

These results suggest that blocking BK channels improves the propagation of calcium spikes evoked by dendritic current injection. To verify this directly, I examined the properties of calcium spikes reaching the dendritic recording site, which presumably represent propagated spikes since the maximal calcium signal was always located away from this site. Synaptically evoked calcium spikes showed small increases in amplitude (6.4 ± 1.1 mV vs. 5.1 ± 1.5mV in control, $n = 3$ cells, $p = 0.1$) and half-width (1.02 ± 0.1 ms vs. 0.89 ± 0.11 ms in control, $n = 3$ cells, $p = 0.1$) in the presence of penitrem A. However, calcium spikes evoked by dendritic current injection (Figure 3.7H) were dramatically enhanced both in amplitude (9.9 ± 3.8 mV vs. 2.4 ± 2.2 mV in control, $n = 3$ cells, $p < 0.04$) and half-width (0.71 ± 0.17 ms vs. 0.38 ± 0.22 ms in control, $n = 3$ cells, $p < 0.03$), consistent with the calcium imaging data.

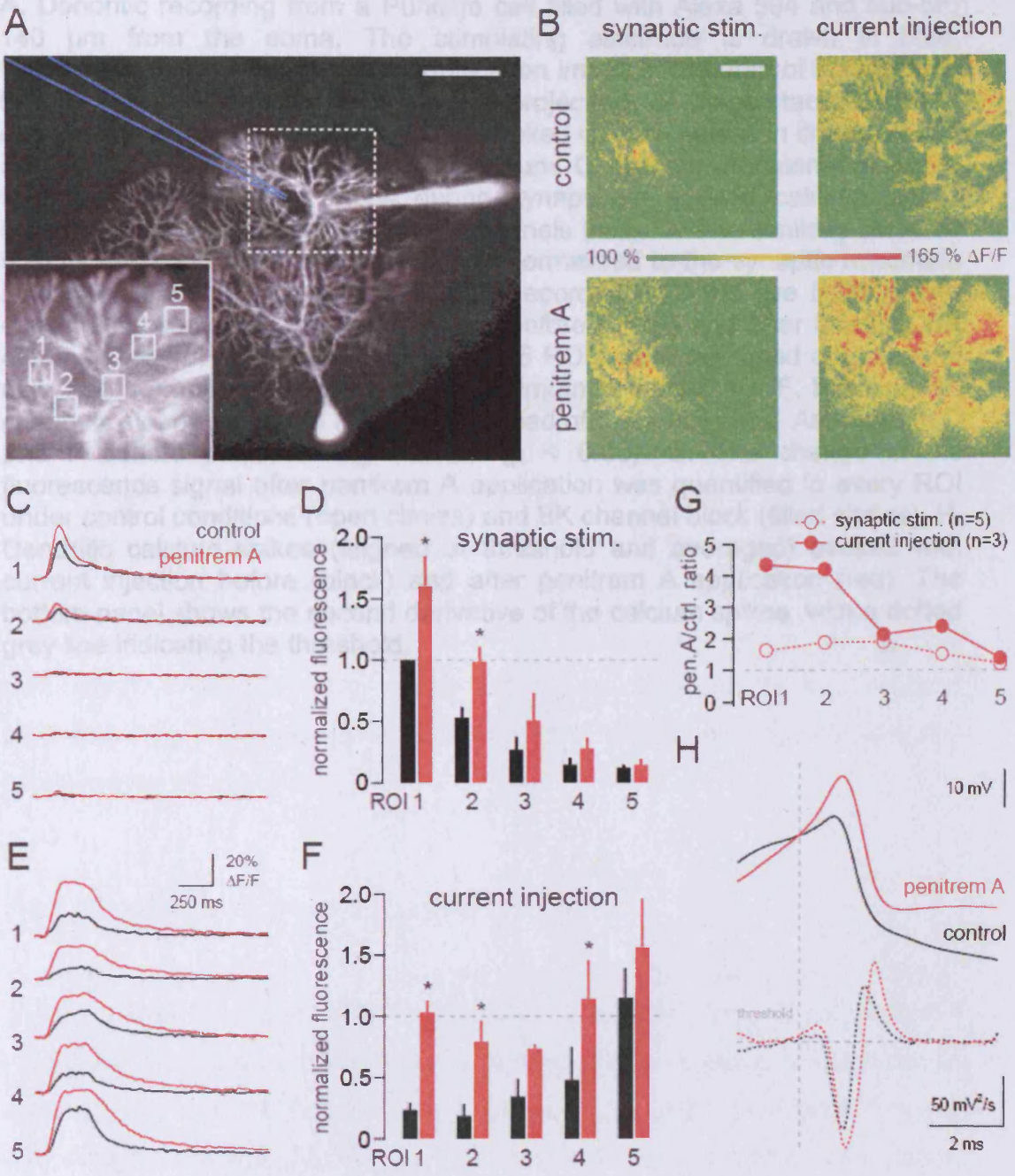

Figure 3.7 BK channels control dendritic calcium spike propagation
Legend on the next page.

Figure 3.7 BK channels control dendritic calcium spike propagation
A. Dendritic recording from a Purkinje cell filled with Alexa 594 and fluo-5F, 140 µm from the soma. The stimulating electrode is drawn in blue. Calibration: 50 µm. Inset: high magnification image of the area of interest with 5 ROIs indicated. **B.** Maximum intensity projections of image stacks acquired during synaptically or current injection-evoked calcium spikes in control ACSF and 100 nM penitrem A. Calibration: 20 µm. **C.** Calcium transients recorded from the five respective ROIs during synaptically evoked calcium spikes before (black) and after blocking BK channels (red). **D.** The similarly selected 5 ROIs were averaged over 3 cells and normalized to the synaptic maximum in control ACSF. **E.** Calcium transients recorded from the five ROIs during current injection-evoked calcium spikes before (black) and after blocking BK channels (red). **F.** The similarly selected 5 ROIs were averaged over several cells and normalized to the synaptic maximum in control ACSF. Blocking BK channels clearly improved the spatial spread of calcium spikes. Asterisks in D and F denote statistical significance ($p < 0.05$). **G.** The change in the fluorescence signal after penitrem A application was quantified in every ROI under control conditions (open circles) and BK channel block (filled circles). **H.** Dendritic calcium spikes (aligned at threshold and averaged) evoked with current injection before (black) and after penitrem A application (red). The bottom panel shows the second derivative of the calcium spikes, with a dotted grey line indicating the threshold.

3.3 Discussion

Using combined electrophysiological recording and calcium imaging, I have characterized dendritic spikes triggered by parallel fibre input in Purkinje cell dendrites. Dendritic spikes could be readily evoked by synaptic stimulation or current injection. I have shown that dendritic spikes are mediated by voltage-gated calcium channels and lead to significant increases in local dendritic calcium concentration. Synaptic stimulation, which directly depolarizes the spiny dendrites, the main initiation site, leads to larger and more localized calcium increases than injecting EPSC-like waveforms into the main dendrite. Also, current injection usually evoked calcium spikes in a discrete subpopulation of the many spiny branchlets adjacent to the injection electrode. The magnitude and spatial extent of the calcium influx was tightly controlled by BK channels.

3.3.1 Threshold of dendritic spikes

The average threshold EPSP amplitude (measured at -70mV dendritic membrane potential) required to evoke a dendritic spike with a single synaptic stimulus was ~20 mV. Assuming an average 10 pA EPSC peak amplitude (at a holding potential of -70 mV) for every parallel fibre synaptic contact (Isope and Barbour, 2002) and 50 MΩ dendritic input resistance (Roth and Häusser, 2001) leads to an estimated 400 synaptic contacts being required for a single-shock stimulus. This is a small fraction of the ~ 200.000 PF synapses found on single Purkinje cells. As dendritic spike initiation needs spatial and temporal coincidence of synaptic inputs, this number is only a vague estimate. Granule cells fire bursts of action potentials following sensory stimulation (Chadderton et al., 2004) and PF synapses exhibit profound paired-pulse facilitation (Dittman et al., 2000), thus the number of granule cells required to be activated by a sensory stimulus in order to trigger dendritic spikes is

probably much lower. Spatial coincidence could also occur easily if clusters of granule cells activated by mossy fibres send their parallel fibres to the same part of the molecular layer.

The apparent voltage threshold of dendritic calcium spikes was ~-30 mV. This is probably an underestimate, as the recordings were done distal to the calcium spike initiation site, which is usually in spiny dendrites, inaccessible by patch-clamp electrodes. This value is not far from the upstate membrane potential (Loewenstein et al., 2005b) or dendritic plateau potential (Llinás and Sugimori, 1980a). In addition, the powerful CF input profoundly depolarizes most of the dendritic tree well above this threshold, leading to widespread calcium spikes. PF synaptic input following CF activation could ride this depolarization and evoke extra local dendritic spikes in the spiny branchlets (Wang et al., 2000; Christensen, 2002).

3.3.2 Dendritic spikes are local and their spread is regulated by BK channels

Functional compartments have been shown before to exist in neuronal dendrites, especially regarding intracellular calcium levels (Yuste et al., 1994). I showed that calcium spikes are confined to a few spiny branchlets, localized to the activated synapses (Miyakawa et al., 1992; Hartell, 1996). As a consequence of injecting current into a main dendrite connected to many spiny branchlets (which provide a big electrical load), current injection evoked calcium spikes were more widespread. My results provide direct evidence for the regulation of dendritic calcium spikes by BK channels in Purkinje cells, supporting earlier findings that BK channels play an important role in modulating the excitability of these neurons (Edgerton and Reinhart, 2003; Sausbier et al., 2004; Womack and Khodakhah, 2004). My findings are consistent with the results of (Golding et al., 1999) in CA1 pyramidal cells, who showed that BK channels are responsible in part for determining the duration of dendritic calcium spikes. I also demonstrated that BK channels are critical for regulating the spatial spread of calcium spikes, in contrast with the situation in cultured hippocampal pyramidal neurons, where SK-type calcium-

activated potassium channels appear to play a dominant role (Cai et al., 2004). Interestingly, BK channels can be located presynaptically (Knaus et al., 1996), where they limit transmitter release from synaptic terminals (Raffaelli et al., 2004). Their postsynaptic localization in Purkinje cell dendrites could serve an analogous role, as endocannabinoids (Brown et al., 2003) and glutamate (Duguid and Smart, 2004) can be released from Purkinje cell dendrites. Interestingly, BK channels are activated by the endogenous cannabinoid anandamide (Sade et al., 2006) and several other intracellular messengers (PKC, protein phosphatases; (Widmer et al., 2003) or PLC; (Clarke et al., 2002) providing several mechanisms to physiologically modulate the spread of dendritic calcium spikes via neuromodulator systems (Schweighofer et al., 2004).

3.3.3 Functional role of dendritic spikes in Purkinje cells

What functional role could dendritic calcium spikes play? By triggering calcium entry into the dendrite, they can initiate a plethora of intracellular cascades ultimately leading to changes in the way dendrites process information by changing excitability or synaptic weights. Their localized nature provides a biophysical substrate for synapse- or branchlet-specificity of synaptic plasticity (Brown et al., 2003) and help define the large number of dendritic compartments, which can increase the information processing power of the neuron (Poirazi et al., 2003).

Further studies involving high-resolution calcium imaging and dendritic recording *in vivo* are required to establish under what circumstances local dendritic spikes occur in Purkinje cells. In the following parts of my thesis I will investigate in detail the role dendritic spikes potentially may have in regulating synaptic strength and the output firing of Purkinje cells.

4. Local dendritic spikes are tunable triggers of endocannabinoid mediated short-term plasticity

4.1 Introduction

Given that dendritic calcium spikes cause significant postsynaptic calcium influx (Chapter 3; Ross and Werman, 1987; Miyakawa et al., 1992; Yuste et al., 1994; Schiller et al., 1997), one attractive possibility is that dendritic calcium spikes could act as triggers for local synaptic plasticity, which is thought to require significant elevations in postsynaptic calcium. In pyramidal cells, initiation of calcium spikes by strong synaptic stimulation has been linked to the induction of non-Hebbian long-term potentiation (Golding et al., 2002) or depression (Holthoff et al., 2004). Recently, a novel form of short-term plasticity at excitatory synapses, termed depolarization-induced suppression of excitation (DSE), has been demonstrated at parallel fibre (PF) synapses in cerebellar Purkinje cells (Kreitzer and Regehr, 2001). DSE induction depends on dendritic cannabinoid release, which appears to require high postsynaptic calcium elevations (Brenowitz and Regehr, 2003), and can be triggered by bursts of PF inputs which are associated with large local calcium signals in Purkinje cell dendrites (Brown et al., 2003). This raises the possibility that physiological patterns of stimulation may cause DSE via the triggering of dendritic calcium spikes. I therefore made direct patch-clamp recordings from Purkinje cell dendrites in conjunction with calcium imaging to investigate the link between dendritic calcium spikes and synaptic efficacy at PF synapses.

4.2 Results

4.2.1 Stimulus-dependence of dendritic calcium spikes and DSE induction

Previous work has shown that a train of PF stimuli can produce DSE of PF inputs (Brown et al., 2003). I made simultaneous somatic and dendritic recordings from spontaneously firing Purkinje cells during DSE induction triggered by 10 PF stimuli delivered at 100 Hz (Brown et al., 2003). Figure 4.1 shows a sample experiment and the protocol with which DSE was measured. These experiments revealed that there was a stimulus-dependent threshold for the induction of DSE, which matched that observed for initiation of dendritic calcium spikes during the induction protocol. At low stimulation intensities, no dendritic calcium spikes were evoked, and no DSE was observed (Figure 4.2; n = 12 cells). However, when stimulation intensity was raised sufficiently to generate dendritic calcium spikes (Figure 4.2A), DSE was always observed (Figure 4.2B; n = 12).

To demonstrate the link between dendritic calcium spike initiation and DSE induction, I plotted the number of calcium spikes detected in the dendritic recordings during the induction period against the resulting DSE (measured as the minimum normalized EPSP amplitude after induction; Figure 4.2C). When no dendritic calcium spikes were evoked, no DSE was observed (EPSP amplitude 105 ± 3% of control). As more dendritic calcium spikes were recruited with increasing stimulus intensities, the degree of DSE was correlated with the number of calcium spikes evoked during induction in all cells (n = 12; Figure 4.2C, filled circles). This relationship could be described by a sigmoidal curve, with saturation of DSE being observed after 5 calcium spikes (no significant difference in the DSE value with larger numbers of calcium spikes, $p_{0\text{-}2,\ 2\text{-}3,\ 4\text{-}5} < 0.05$, $p_{3\text{-}4,\ 5\text{-}6,\ 6\text{-}7} > 0.2$). To assess the involvement

of cannabinoid release in DSE triggered by calcium spikes, I blocked CB1 receptors using AM251 (1 μM). Under these conditions, no change in EPSP amplitude was observed even when up to 5 dendritic calcium spikes were evoked by synaptic stimulation (EPSP amplitude 101 ± 2% of control, n = 6, p = 0.6, Figure 4.2C). This indicates that dendritic calcium spikes cause DSE by triggering endocannabinoid release.

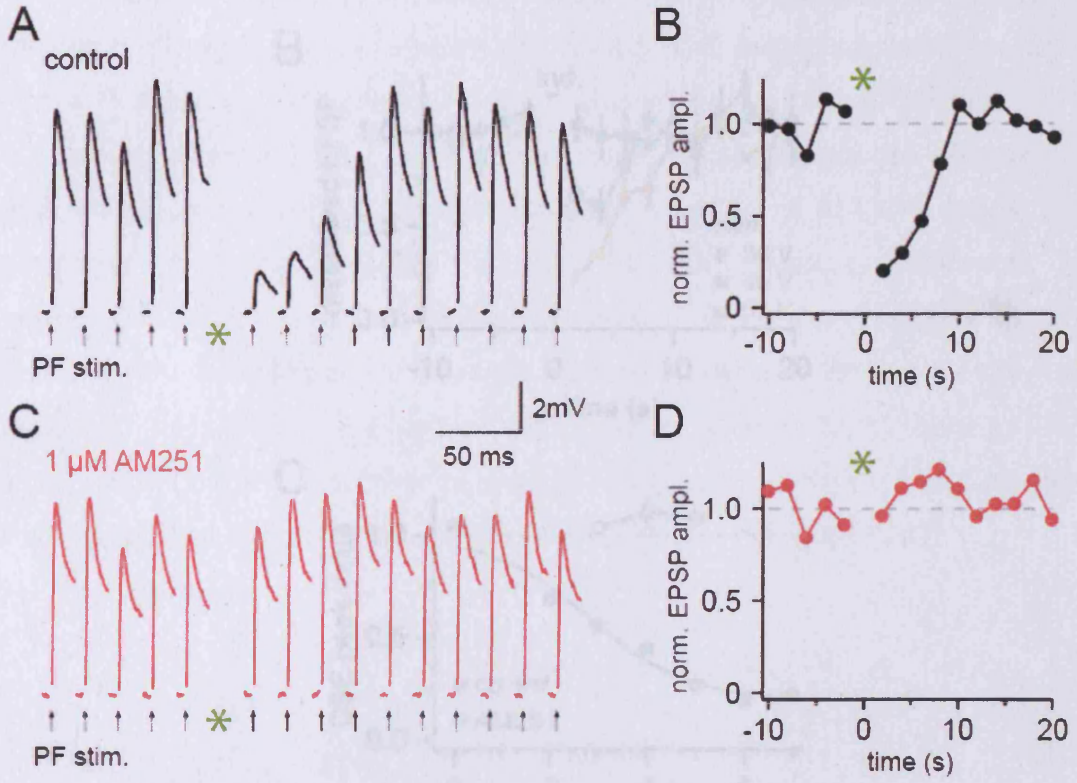

Figure 4.1. The measurement of DSE
A. Parallel fibres were stimulated every 2 seconds (arrows). The EPSPs were truncated (5 ms before and 15 ms after stimulation) and the stimulus artefacts were removed for clarity. The induction protocol (10 PF stimuli at 100 Hz) is marked by a green asterisk. **B.** The EPSP amplitudes were normalized to the average value of the first 5 EPSPs and plotted versus time. DSE was measured as the minimum normalized amplitude after the induction protocol. **C.** and **D.** Same as in A and B, but in the presence of AM251 (1 μM), a CB1 receptor antagonist.

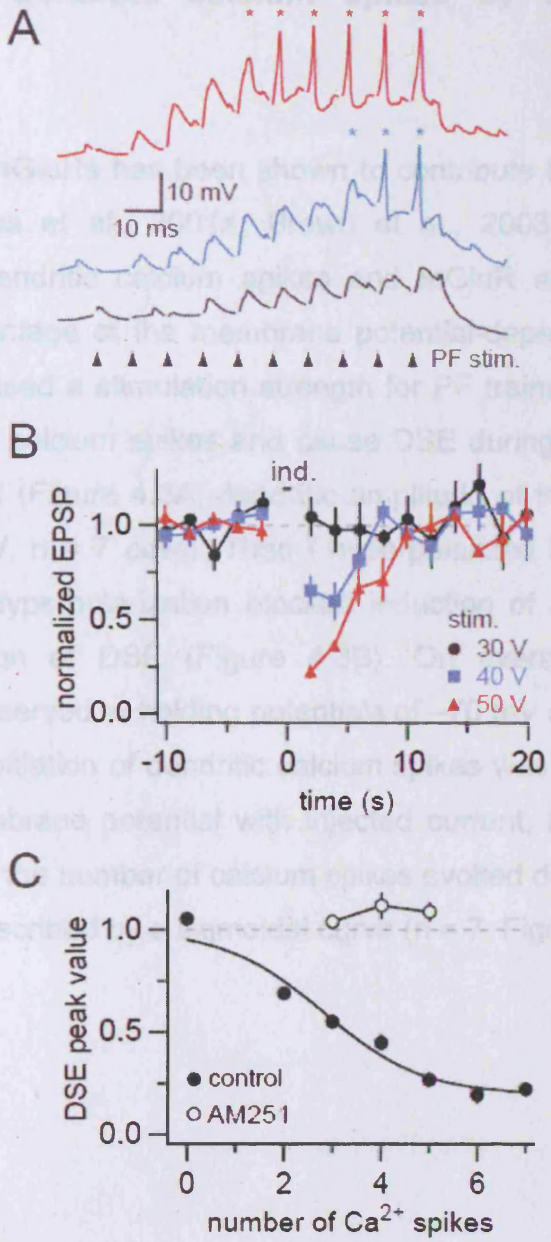

Figure 4.2. The amount of DSE depends on the number of dendritic calcium spikes

A. Dendritic recording 134 µm from the soma during DSE induction. Different stimulation intensities were used (black: 30 V; blue: 40 V; red: 50 V) during a train of 10 PF stimuli (arrowheads) at 100 Hz. Note the calcium spikes (asterisks) evoked at the higher stimulus intensities. **B.** Time-course of changes in normalized dendritic PF EPSP amplitude (black, n = 4 trials; blue, n = 5 trials; red, n = 3 trials). All data from the same cell as in A. **C.** Relationship between the number of dendritic calcium spikes during the train and the amount of DSE averaged across 12 cells. Open circles show block of DSE by the CB1 antagonist AM251 (1 µM; n = 4 cells). The control data points were fitted with a sigmoidal curve with baseline constrained to 1.

4.2.2 Blocking dendritic calcium spikes by hyperpolarization prevents DSE

The activation of mGluRs has been shown to contribute to DSE activated by PF trains (Maejima et al., 2001a; Brown et al., 2003). To separate the contributions of dendritic calcium spikes and mGluR activation during PF trains, I took advantage of the membrane potential-dependence of dendritic calcium spikes. I used a stimulation strength for PF trains that was sufficient to trigger dendritic calcium spikes and cause DSE during spontaneous firing of the Purkinje cell (Figure 4.3A; dendritic amplitude of the EPSP was 2.3 ± 0.2 mV at –70 mV, n = 7 cells). Then I hyperpolarized the cell with steady injected current. Hyperpolarization blocked induction of calcium spikes and prevented induction of DSE (Figure 4.3B). On average, there was no significant DSE observed at holding potentials of –70 mV and –90 mV (Figure 4.3B). When the initiation of dendritic calcium spikes was titrated by carefully adjusting the membrane potential with injected current, the amount of DSE was dependent on the number of calcium spikes evoked during induction, with the relationship described by a sigmoidal curve (n = 7; Figure 4.3C).

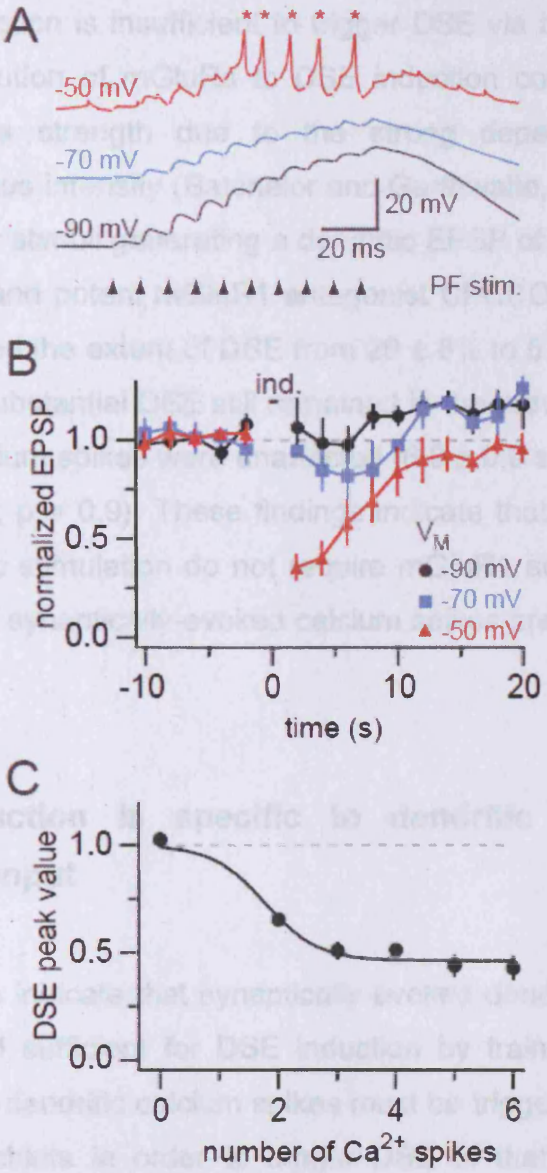

Figure 4.3 DSE and dendritic calcium spikes have a similar voltage threshold

A. Dendritic recording 108 µm from the soma. The same stimulation intensity was used to evoke 10 PF EPSPs at 100 Hz (arrowheads) when the dendrite was held at different membrane potentials (black: -90 mV, blue: -70mV, red: no holding current, ~ -50 mV). Note that calcium spikes (asterisks) were only observed at the most depolarized potentials. **B.** Time-course of changes in normalized dendritic PF EPSP amplitude (black, n = 3 trials; blue, n = 3 trials; red, n = 3 trials). All data from the same cell as in A. **C.** Relationship between the number of calcium spikes during the train and the amount of DSE averaged across 7 cells. The data points were fitted with a sigmoidal curve with baseline constrained to 1.

These findings indicate that the level of synaptic activation required for calcium spike induction is insufficient to trigger DSE via the mGluR pathway alone. The contribution of mGluRs to DSE induction could be revealed by increasing stimulus strength due to the strong dependence of mGluR activation on stimulus intensity (Batchelor and Garthwaite, 1997; Reichelt and Knöpfel, 2002). For stimuli generating a dendritic EPSP of 6.0 ± 0.9 mV at -70 mV, the selective and potent mGluR1 antagonist CPCCOEt (100 µM; Brown et al., 2003) reduced the extent of DSE from 29 ± 6% to 57 ± 13% ($p < 0.009$; $n = 8$). However, substantial DSE still remained in the presence of CPCCOEt, while dendritic calcium spikes were unaffected (6.9 ± 0.9 spikes in control, 6.9 ± 1.1 in CPCCOEt; $p = 0.9$). These findings indicate that the calcium spikes evoked by synaptic stimulation do not require mGluR1 activation to produce DSE, and thus that synaptically-evoked calcium spikes are sufficient to trigger DSE.

4.2.3 DSE induction is specific to dendritic calcium spikes triggered by PF input

These experiments indicate that synaptically evoked dendritic calcium spikes are necessary and sufficient for DSE induction by trains of PF inputs. To determine whether dendritic calcium spikes must be triggered by the PF input to the spiny branchlets in order to trigger DSE of that input, I examined whether calcium spikes activated by postsynaptic depolarization of the main dendrite alone could also trigger DSE. Dendritic calcium spikes were evoked in the absence of synaptic stimulation by injecting a train of EPSC waveforms via the dendritic pipette (Figure 4.4A) which was connected to the main dendrite close to the synaptically activated spiny branchlets. Activation of a large number of such current-evoked dendritic calcium spikes (5.3 ± 0.5 spikes) did not significantly change the amplitude of PF EPSPs activated by synaptic stimulation close to the dendritic recording site (98 ± 2% of control, $p = 0.4$, $n = 6$; Figure 4.4C). However, when the same synaptic input was used to activate dendritic calcium spikes (4.6 ± 0.4 spikes, Figure 4.4B), robust DSE was obtained (35 ± 9% of control, $p < 0.0005$, $n = 6$, Figure 4.4C). These results could be explained for example by different spatial localization of

calcium spikes evoked by PF input versus current injection to the main dendrite (Figure 3.6) or by a requirement of presynaptic activity for DSE.

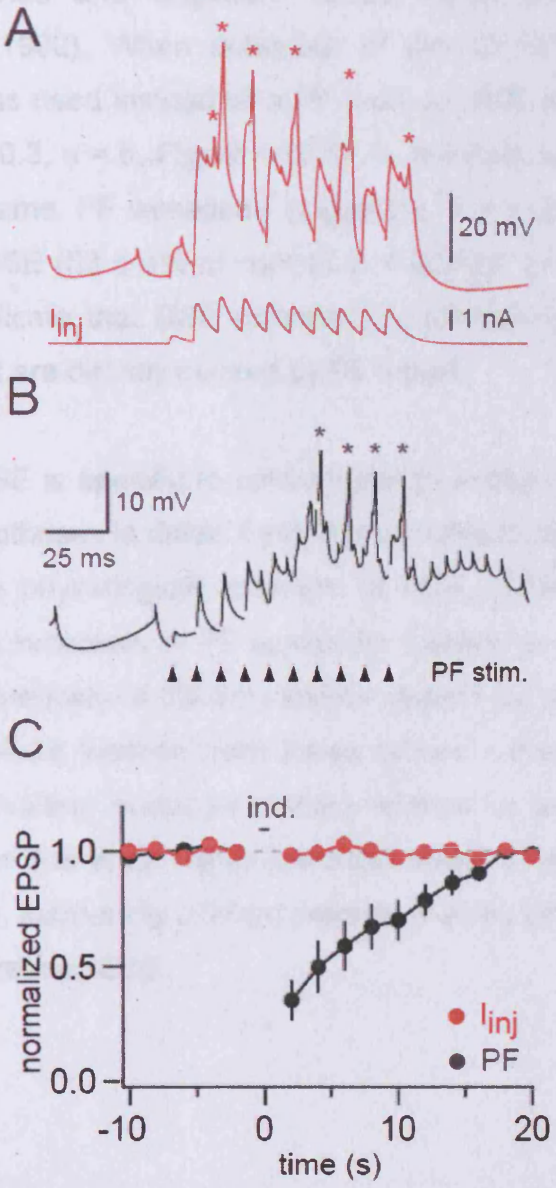

Figure 4.4 Dendritic spikes evoked by current injection input fail to trigger DSE

A. Dendritic recording 112 µm from the soma. Dendritic calcium spikes (asterisks) were evoked by injecting a train of EPSC-like waveforms (shown below the dendritic recording). **B.** Dendritic calcium spikes (asterisks) evoked in the same cell by stimulating PFs adjacent to the recording electrode. **C.** Comparison of the effect of calcium spikes evoked by current injection (red) or PF stimulation (black) on PF EPSP amplitudes averaged across 6 cells.

I also examined whether climbing fibre (CF) synaptic input is sufficient to induce DSE at PF synapses, since CF activation has been shown to trigger dendritic calcium spikes and widespread calcium entry in the Purkinje cell dendritic tree (Llinás and Sugimori, 1980a; Ross and Werman, 1987; Miyakawa et al., 1992). When activation of the CF (triggering 2.4 ± 0.2 calcium spikes) was used instead of a PF train, no DSE was observed (98 ± 6% of control, $p = 0.3$, $n = 6$, Figure 4.5AC). In contrast, activation of calcium spikes with the same PF synapses (triggering 3.2 ± 0.4 calcium spikes) produced robust DSE (53 ± 3% of control; $p < 0.0001$; $n = 6$, Figure 4.5BC). These findings indicate that DSE activated by calcium spikes is specific to calcium spikes that are directly evoked by PF inputs.

To explain why DSE is specific to calcium spikes evoked by PF synapses, I examined two hypotheses in detail. First, it is possible that presynaptic activity is required for the physiological induction of DSE (potentially mediated by presynaptic NMDA receptors at PF synapses: Casado et al., 2000; Sjöström et al., 2003). Alternatively, if calcium spikes evoked by current injection are triggered at a different location from those evoked synaptically, as seen in Chapter 3, the resulting endocannabinoid release is unable to reach the activated synapses due to its highly restricted range of action (Brown et al., 2003). In this case, increasing calcium spike spread by blocking BK channels (Figure 3.7) could rescue DSE.

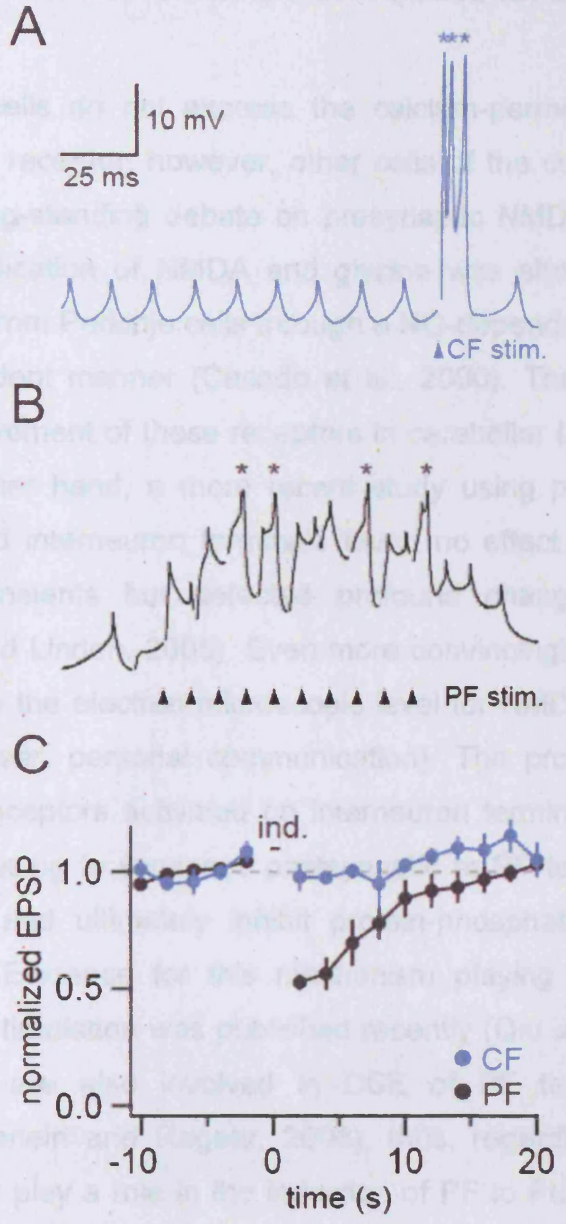

Figure 4.5. Dendritic spikes evoked by climbing fibre synaptic input fail to trigger DSE

A. Dendritic recording 114 µm from the soma. Stimulating CF input evoked a complex spike, which was associated with 3 dendritic calcium spikes (asterisks). **B.** Dendritic recording from the same cell showing a PF train which evoked 4 dendritic calcium spikes. **C.** Time-course of PF EPSP amplitude before and after the two different induction protocols (blue: CF stimulation; black: PF stimulation) averaged across 6 cells.

4.2.4 NMDA channel activation is not required for DSE

Mature Purkinje cells do not express the calcium-permeable and voltage-dependent NMDA receptor, however, other cells of the cerebellar cortex do, and there is a long-standing debate on presynaptic NMDA receptors on PF terminals. Co-application of NMDA and glycine was shown to depress PF EPSCs recorded from Purkinje cells through a NO-dependent mechanism in a PF activity-dependent manner (Casado et al., 2000). The same group also reported the involvement of these receptors in cerebellar LTD (Casado et al., 2002). On the other hand, a more recent study using presynaptic calcium imaging in PF and interneuron terminals found no effect of NMDA receptor block on PF transients but detected profound changes in interneuron terminals (Shin and Linden, 2005). Even more convincingly, no evidence has yet been found on the electron microscopic level for NMDA receptors on PF terminals (Z. Nusser, personal communication). The proposed model thus involves NMDA receptors activated on interneuron terminals and the locally produced NO diffusing to synapses postsynaptic to PF terminals to activate guanylyl cyclase and ultimately inhibit protein-phosphatases (Duguid and Sjöström, 2006). Evidence for this mechanism playing a part in PF-LTP induced by 4 Hz stimulation was published recently (Qiu and Knöpfel, 2007). NMDA receptors are also involved in DSE of PF terminals contacting interneurons (Beierlein and Regehr, 2006), thus, regardless of their exact location, they may play a role in the induction of PF to Purkinje cell DSE. To test if NMDA receptors are involved in the induction or expression of DSE, I used 50-100 µM APV (also known as D-AP5), a selective NMDA receptor antagonist.

I used 10 PF stimuli delivered at 100 Hz to induce DSE. Under control conditions, this induction resulted in strong DSE (21 ± 12% of control, n = 8). When NMDA receptors were blocked by 50-100µM APV, the same stimulus in the same cells resulted in statistically undistinguishable levels of DSE (22 ± 6% of control, n = 8, p = 0.8 compared to the control condition, Figure 4.6). These results thus argue against the involvement of NMDA receptors in

cerebellar PF DSE in Purkinje cells but do not rule out the involvement of other presynaptic mechanisms.

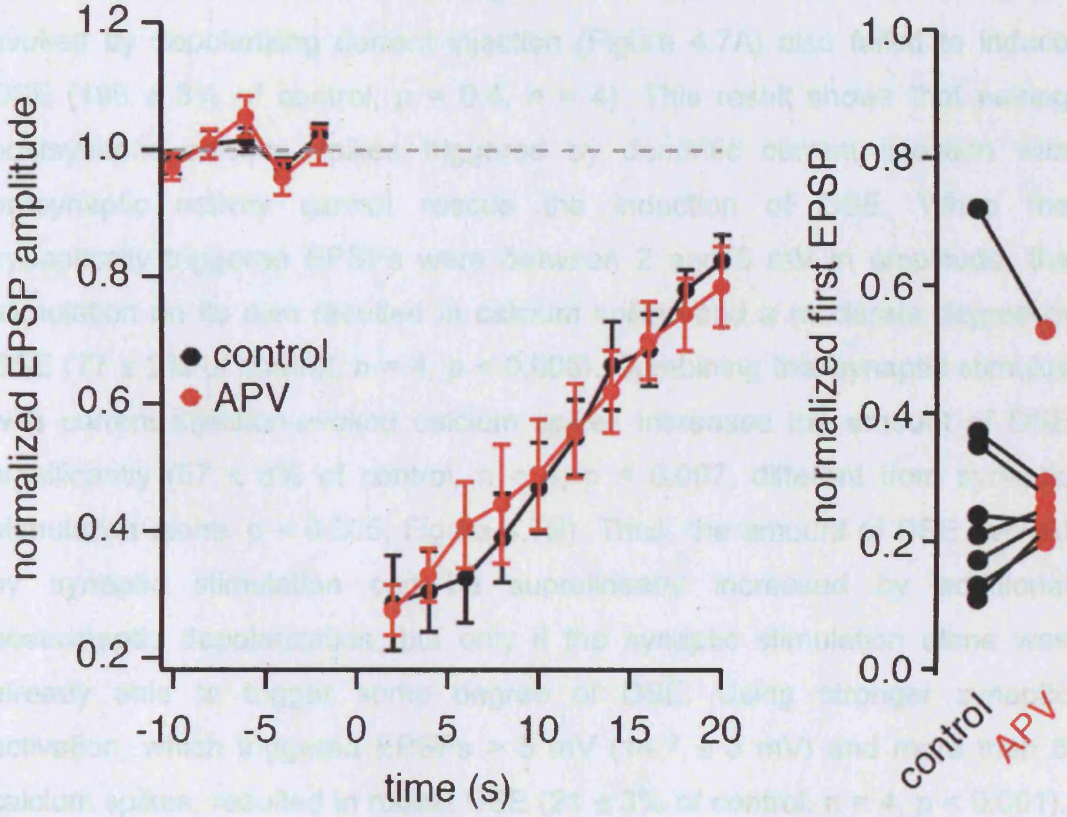

Figure 4.6 NMDA receptors are not involved in PF to Purkinje cell DSE
Timecourse of DSE recorded from Purkinje cells after the stimulation of PFs with a train of 10 stimuli at 100Hz. APV (50-100 µM), a specific NMDA receptor antagonist had no effect on DSE. Pooled data from 8 cells. Right: distribution of maximal DSE values in control and APV.

4.2.5 Calcium spikes evoked by current injection are insufficient to trigger DSE but can act synergistically with synaptic stimulation

To test if presynaptic activity is required during induction of DSE by dendritic calcium spikes, I paired calcium spikes evoked by dendritic current injection with different intensities of synaptic stimulation. The stimulus train during induction was always delivered with the same intensity as the stimuli testing for synaptic strength in order to activate the same pool of parallel fibres. Dendritic current injection capable of activating many calcium spikes, which did not induce DSE on its own (103 ± 4% of control, n = 4; p = 0.6; see

above), was paired with three different intensities of synaptic stimulation. When the evoked EPSPs were < 2 mV, they failed to trigger calcium spikes and evoke DSE (106 ± 7% of control, $p = 0.7$, $n = 4$) when delivered in a train of 10 stimuli at 100 Hz. Combining the stimulus train with calcium spikes evoked by depolarizing current injection (Figure 4.7A) also failed to induce DSE (105 ± 8% of control, $p = 0.4$, $n = 4$). This result shows that pairing postsynaptic calcium spikes triggered by dendritic current injection with presynaptic activity cannot rescue the induction of DSE. When the synaptically triggered EPSPs were between 2 and 5 mV in amplitude, the stimulation on its own resulted in calcium spikes and a moderate degree of DSE (77 ± 2% of control, $n = 4$, $p < 0.005$). Combining this synaptic stimulus with current injection-evoked calcium spikes increased the amount of DSE significantly (57 ± 8% of control, $n = 4$, $p < 0.007$; different from synaptic stimulation alone, $p < 0.005$, Figure 4.7B). Thus, the amount of DSE evoked by synaptic stimulation can be supralinearly increased by additional postsynaptic depolarization, but only if the synaptic stimulation alone was already able to trigger some degree of DSE. Using stronger synaptic activation, which triggered EPSPs > 5 mV (14.7 ± 3 mV) and more than 6 calcium spikes, resulted in robust DSE (21 ± 3% of control, $n = 4$, $p < 0.001$). Pairing this stimulation with current injection was unable to increase the amount of DSE triggered (23 ± 4% of control, $n = 4$, $p < 0.003$; compared with stimulation alone, $p = 0.7$, Figure 4.7C). Thus, DSE triggered by synaptically evoked calcium spikes can be saturated, such that additional depolarization fails to increase the amount of DSE.

These results demonstrate that calcium spikes triggered by postsynaptic depolarization can act in a synergistic manner to enhance DSE evoked by synaptic stimulation, but do not appear to change its threshold or maximal value. The inability of low intensity stimulation paired with calcium spikes evoked by current injection to evoked DSE can either indicate that presynaptic activity is not required for DSE induction, or that the current injection-evoked calcium spikes fail to propagate to the activated synapses. If this is the case, BK channels block should not only rescue DSE by current injection, but also enable CF evoked calcium spikes to evoke DSE.

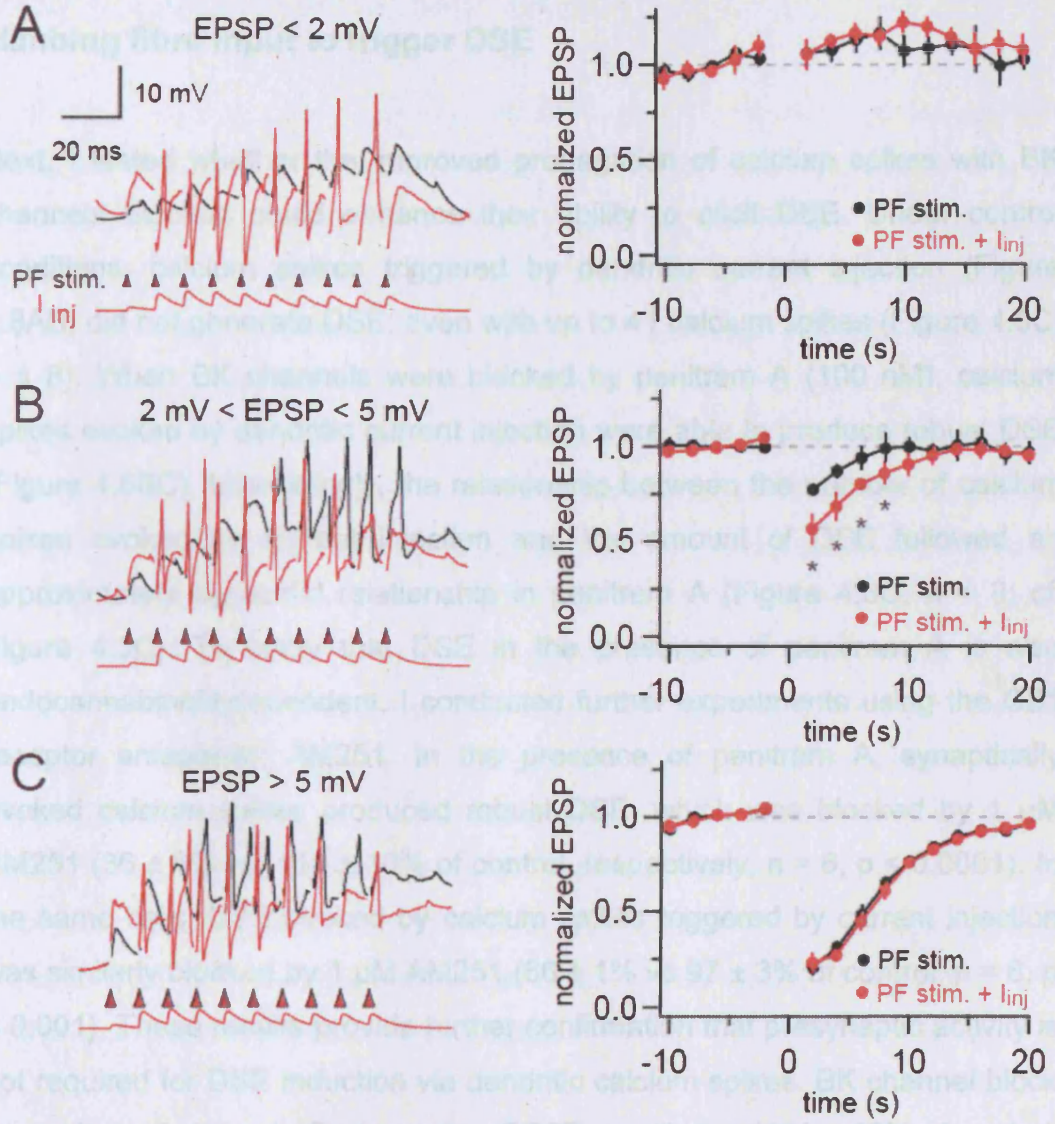

Figure 4.7 Presynaptic activity during calcium spikes evoked by current injection does not rescue DSE

A. Dendritically recorded calcium spikes (150 µm from the soma) during synaptic stimulation (black) and combined current injection and synaptic stimulation (red). The current injection was adjusted to evoke several calcium spikes. The time-course of normalized synaptic strength of 4 cells. Weak synaptic stimulation during current injection-evoked calcium spikes failed to depress the stimulated synapses. **B.** When the current injection (same as in A) was paired with stronger synaptic stimulation, which alone evoked calcium spikes and some degree of DSE, the amount of depression was increased (pooled data from 4 cells, asterisks denote $p < 0.05$ between the two conditions). **C.** When using synaptic stimuli evoking 6 or more calcium spikes, pairing with current injection (same as in A and B) failed to increase the degree of DSE (pooled data from 4 cells). EPSP amplitudes were measured at -70 mV.

4.2.6 BK channel block enables current-evoked calcium spikes and climbing fibre input to trigger DSE

Next, I tested whether the improved propagation of calcium spikes with BK channels blocked could enhance their ability to elicit DSE. Under control conditions, calcium spikes triggered by dendritic current injection (Figure 4.8AB) did not generate DSE, even with up to 41 calcium spikes (Figure 4.8C, n = 8). When BK channels were blocked by penitrem A (100 nM), calcium spikes evoked by dendritic current injection were able to produce robust DSE (Figure 4.8BC). Interestingly, the relationship between the number of calcium spikes evoked by current injection and the amount of DSE followed an approximately sigmoidal relationship in penitrem A (Figure 4.8C, n = 8; cf. Figure 4.3C). To verify that DSE in the presence of penitrem A is also endocannabinoid-dependent, I conducted further experiments using the CB1 receptor antagonist, AM251. In the presence of penitrem A, synaptically evoked calcium spikes produced robust DSE, which was blocked by 1 μM AM251 (36 ± 6% vs. 111 ± 10% of control, respectively, n = 6, $p < 0.0001$). In the same cells, DSE evoked by calcium spikes triggered by current injection was similarly blocked by 1 μM AM251 (66 ± 1% vs 97 ± 3% of control, n = 6, $p < 0.001$). These results provide further confirmation that presynaptic activity is not required for DSE induction via dendritic calcium spikes. BK channel block by penitrem A did not affect baseline EPSP amplitudes (101 ± 12% of control; n = 6, p = 0.4), paired-pulse facilitation (99 ± 2% of control; 10 ms interval; n = 6, p = 0.4) or input resistance (99 ± 4% of control; n = 6, p = 0.8), ruling out effects of BK channel block on baseline synaptic transmission or postsynaptic properties.

I also tested if BK channel block affected the ability of calcium spikes evoked by synaptic stimulation to evoke DSE. The relationship between the number of calcium spikes and the amount of DSE evoked during trains of PF stimuli was sigmoidal (see Figure 4.2C), which was unchanged when BK channels were blocked by penitrem A (n = 5, p = 0.8, Figure 4.8D). This suggests that the block of BK channels did not change the ability of calcium spikes to trigger DSE at their initiation site (i.e. there was no change in synaptically evoked

DSE), but instead may help calcium spikes evoked at other dendritic locations to spread to the test synapses and evoke DSE.

To further test this idea, I investigated activation of the climbing fibre, which produces widespread dendritic calcium entry in Purkinje cells (Miyakawa et al., 1992; Wang et al., 2000) but which is normally insufficient to trigger DSE of PF input (Figure 4.5; Brenowitz and Regehr, 2005). To test whether BK channel activation also limits the spread of the CF-triggered depolarization to PF synapses, I examined the effect of penitrem A on the ability of the CF to trigger DSE of PF inputs. Experiments were carried out in the presence of the mGluR1 antagonist CPCCOEt to block the effect of glutamate spillover from the CF terminals to mGluR1 receptors present on PF synapses (Maejima et al., 2001a; Brenowitz and Regehr, 2005). In control conditions, 20 CF stimuli (at 50 Hz) were required to produce significant DSE (80 ± 7% of control, $p < 0.025$, $n = 5$, Figure 4.8E). However, when BK channels were blocked by penitrem A (100 nM), as few as 3 CF stimuli triggered significant DSE (85 ± 7% of control, $p < 0.02$, $n = 5$). For all numbers of CF stimuli (except single CF stimuli), DSE produced in the presence of penitrem A was significantly greater than in the control condition ($p < 0.05$, $n = 5$, Figure 4.8F). This suggests that activation of BK channels limits the ability of CF input to modulate PF transmission via endocannabinoid release.

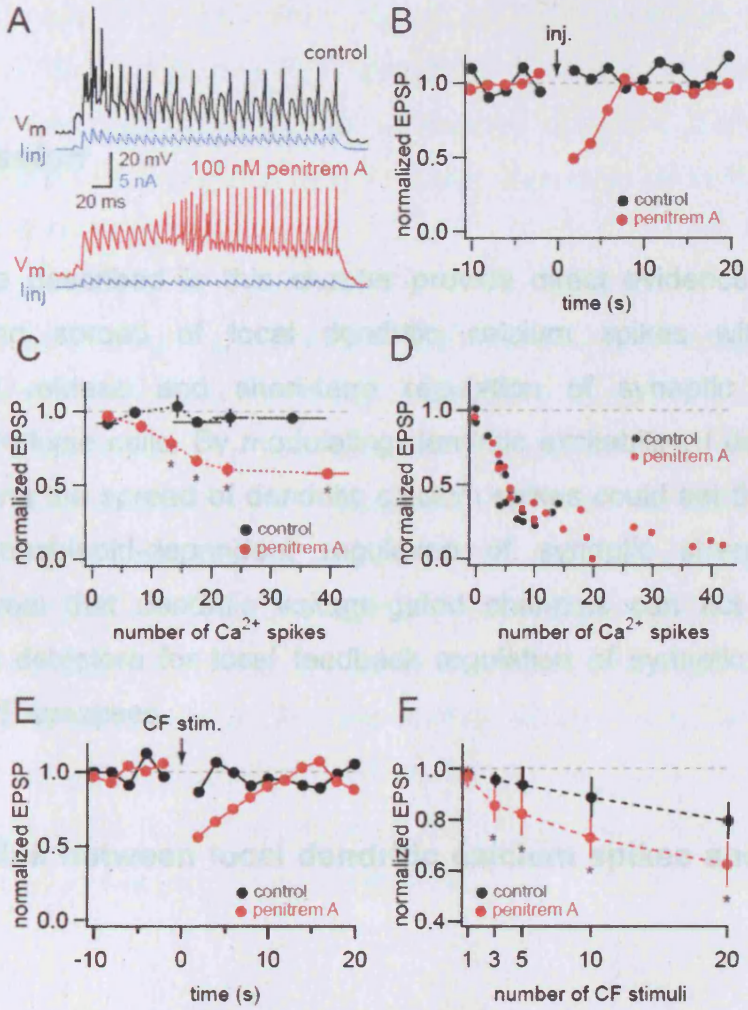

Figure 4.8. Blocking BK channels enables calcium spikes evoked by current injection or climbing fibre activation to trigger DSE
A. Dendritic calcium spikes evoked by dendritic current injection in control ACSF (black trace) and 100 nM penitrem A (red trace), recorded 130 µm from the soma. The amplitude of the injected dendritic current waveform (blue traces) was adjusted to evoke similar numbers of calcium spikes under the two conditions. **B.** Timecourse of PF synaptic strength before and after the calcium spikes evoked by current injection. The same number of calcium spikes, which were unable to trigger DSE in control ACSF, produced strong DSE when BK channels were blocked. **C.** The amount of DSE was plotted versus the number of calcium spikes evoked by current injection. An increasing amount of DSE was triggered with increasing number of calcium spikes, but only when BK channels were blocked by 100 nM penitrem A. Pooled data from 6 cells. **D.** The amount of DSE plotted against the number of synaptically evoked calcium spikes. Block of BK channels did not change the efficacy of synaptically evoked calcium spikes to evoke DSE. Pooled data from 4 cells. **E.** Timecourse of PF synaptic strength shows prominent DSE after 20 CF stimuli when BK channels were blocked, but not in control conditions. Single trials from the same cell. **F.** The amount of DSE was plotted versus the number of CF stimuli delivered during the induction. Pooled data from 5 cells. In C and F error bars show SEM and asterisks denote $p < 0.05$.

4.3 Discussion

The findings described in this chapter provide direct evidence linking the initiation and spread of local dendritic calcium spikes with dendritic cannabinoid release and short-term regulation of synaptic efficacy in cerebellar Purkinje cells. By modulating dendritic excitability, I demonstrated that regulating the spread of dendritic calcium spikes could set the threshold for endocannabinoid-dependent regulation of synaptic strength. These findings reveal that dendritic voltage-gated channels can act as tunable coincidence detectors for local feedback regulation of synaptic strength at cerebellar PF synapses.

4.3.1 The link between local dendritic calcium spikes and synaptic plasticity

I have used four different approaches to directly link the initiation of dendritic calcium spikes with plasticity at PF synapses. First, I showed that the stimulus threshold for induction of dendritic calcium spikes is identical to that for induction of DSE: whenever dendritic calcium spikes were initiated by PF stimulation, DSE also followed; when no calcium spikes were triggered, DSE induction also failed. This link is exemplified by the sigmoidal relationship between the number of calcium spikes and the degree of DSE, which revealed that significant DSE was observed with only 2 dendritic calcium spikes, with DSE saturating above 5 dendritic calcium spikes. Second, I showed that DSE induction and dendritic calcium spike initiation both have a similar voltage threshold, such that hyperpolarization blocks both dendritic calcium spikes and DSE induction. When the number of dendritic calcium spikes was titrated by adjusting membrane potential, the degree of resulting DSE tracked the number of calcium spikes elicited. Third, I demonstrated that DSE can be triggered by synaptically evoked calcium spikes in the presence

of an mGluR1 antagonist, indicating that calcium spikes alone are sufficient to trigger DSE even in the absence of mGluR1 activation. Finally, I demonstrated that enhancing the spread of dendritic calcium spikes by blocking BK-type calcium-activated potassium channels also gates the induction of DSE by dendritic calcium spikes triggered by dendritic current injection or CF stimulation.

Together these findings suggest that dendritic calcium spikes are both necessary and sufficient for triggering DSE with a train of PF stimuli under physiological conditions. My results thus provide some of the strongest evidence to date linking dendritic calcium spikes with induction of synaptic plasticity. Previous work has correlated initiation of calcium spikes by strong synaptic stimulation with non-Hebbian long-term potentiation (Golding et al., 2002) or depression (Holthoff et al., 2004) in pyramidal neurons, but relied on relatively indirect evidence, as in these studies dendritic recordings were not performed during the induction of plasticity. In contrast, I directly manipulated dendritic spike initiation and propagation via dendritic recordings, providing a strong quantitative link with synaptic plasticity.

4.3.2 Implications for the regulation of plasticity

The tight link between dendritic calcium spikes and DSE induction has several implications for our understanding of this form of short-term synaptic plasticity. First, these results provide a biophysical basis for the specificity of DSE induction by PF input. I demonstrated that dendritic calcium spikes evoked by current injection in the absence of PF stimulation and calcium spikes activated by CF input were both insufficient to trigger DSE at the PF synapses tested. This indicates that physiological activation of DSE is restricted to calcium spikes triggered by the PF synapses undergoing DSE. Such specificity is important, since otherwise continuous CF activity *in vivo*, occurring at mean rates of ~1 Hz (Lang et al., 1999), would tonically suppress the approximately 200,000 PF synapses. The specificity is due to the fact that the calcium spike must be sufficiently large at the site of the active synapses in order to deliver sufficient calcium influx to exceed the high calcium threshold for cannabinoid

release (Brenowitz and Regehr, 2003). As suggested by the calcium imaging data in Chapter 3, calcium spikes activated by current injection or via CF activation (Wang et al., 2000) do not reach this threshold. I also ruled out the requirement of coincident presynaptic activity for DSE activated by PF input under physiological conditions. This is consistent with previous evidence that prolonged postsynaptic depolarization to 0 mV when postsynaptic potassium channels have been blocked with internal caesium, which presumably produces calcium influx far in excess of that generated via dendritic calcium spikes, can trigger DSE in the absence of presynaptic activity (Kreitzer and Regehr, 2001; Maejima et al., 2001a; Brenowitz and Regehr, 2003).

Second, my results provide a deeper understanding of the cooperativity requirements for DSE induction by PF input (Brown et al., 2003; Marcaggi and Attwell, 2005). I demonstrated that both the activation of dendritic calcium spikes by PF input and the induction of DSE require a threshold level of synchronous PF activity. Thus, calcium spikes and DSE induction read out the level of spatial and temporal synchrony in the PF population. This is presumably due to the highly non-linear recruitment of voltage-gated calcium channels during the initiation of dendritic calcium spikes by synaptic input.

As for initiation of dendritic calcium spikes, activation of mGluR receptors also requires both temporal and spatial clustering of PF input (Batchelor and Garthwaite, 1997; Reichelt and Knöpfel, 2002). The fact that DSE was prevented when calcium spikes were blocked by hyperpolarization indicates that the threshold for DSE induction via calcium spikes is lower than for via mGluR activation. However, although mGluR activation is not required for DSE induction, there may exist some additional cooperativity between postsynaptic mGluR activation and calcium entering via the dendritic calcium spike to cause supralinear calcium signals (Wang et al., 2000; Ohno-Shosaku et al., 2002), or acting synergistically via a Ca-independent mGluR pathway (Maejima et al., 2001b). The involvement of phospholipase Cβ, which can integrate calcium and G_q-coupled receptor signals leading to DSI in the hippocampus (Hashimotodani et al., 2005), may contribute to the supralinear effect on DSE induction of combining synaptic stimulation and dendritic spikes

evoked by current injection, as well as the cooperativity between PF and CF input (Brenowitz and Regehr, 2005). Although our understanding of endocannabinoid production and release is still limited (Freund et al., 2003; Piomelli, 2003), the local nature of both dendritic calcium spikes and mGluR activation, potentially acting in concert, may help to ensure the synapse-specificity of the resulting synaptic plasticity.

4.3.3 Modulation of dendritic spikes influences plasticity

I demonstrate that the modulation of dendritic calcium spikes by block of BK channels can in turn influence endocannabinoid release and thus the induction of plasticity by dendritic calcium spikes. This provides the first direct evidence that modulation of dendritic excitability can in turn regulate the threshold for induction of synaptic plasticity. Since BK channel block extends the spatial range of action of dendritic calcium spikes evoked by dendritic current injection or climbing fibre activation, the modulation of BK channels may also influence the spatial specificity of DSE evoked by synaptic stimuli. Recent work has demonstrated that the induction of synaptic plasticity can also alter dendritic excitability in pyramidal neurons (Frick et al., 2004; Li et al., 2004). My results thus "close the loop" and show that dendritic excitability may in turn regulate the induction of plasticity and be a substrate for metaplasticity (Frick and Johnston, 2005; Sjöström et al., In press).

What are the physiological regulators of BK channels and thus DSE induction? BK channels are activated by the endogenous cannabinoid anandamide (Sade et al., 2006), providing a negative feedback loop for self-regulation of dendritic calcium spikes and subsequent endocannabinoid release. BK channels are also subject to modulation by numerous second messenger pathways via PKC, protein phosphatases (Widmer et al., 2003) or PLC (Clarke et al., 2002). These pathways, activated by noradrenaline and serotonin (Schweighofer et al., 2004), could thus also influence DSE. P-type calcium channels, underlying dendritic spikes are also subject to modulation by endocannabinoids (Fisyunov et al., 2006) raising the possibility of profound intrinsic excitability changes triggered alongside DSE. Interestingly, the

induction of long-term depression is also accompanied by activation of PKC and protein phosphatase pathways (Daniel et al., 1998). Since dendritic calcium spikes may also be involved in the induction of long-term depression (Wang et al., 2000), this might provide a form of metaplasticity whereby LTD in turn regulates the link between calcium spikes and DSE, setting the threshold at which subsequent patterns of activity are converted into long-term changes in synaptic strength. I will investigate some of these hypotheses in detail in the next chapter.

5. Local dendritic spikes trigger long-term depression of PF input

5.1 Introduction

There is a growing awareness of the important role dendritic excitability plays in synaptic plasticity and vice versa (Frick and Johnston, 2005; Magee and Johnston, 2005; Sjöström et al., In press). Dendritic spikes, one of the hallmarks of excitable dendrites, have been linked with different forms of long-term plasticity. Distal, perforant-path inputs to hippocampal CA1 pyramidal cells were shown to undergo LTP only under conditions favouring dendritic spikes with no requirement for somatic firing (Golding et al., 2002). Furthermore, brief local calcium transients evoked by relatively strong synaptic stimulation in cortical pyramidal cells were shown to produce long-term depression (Holthoff et al., 2004). In the cerebellum, PF stimulation producing local dendritic calcium transients were shown to be associated with LTD (Hartell, 1996). These studies, however, fall short of providing a direct link between dendritic spikes and synaptic plasticity. In the previous chapter, I have provided a strong link between dendritic spikes and DSE. Here I will apply the same technique of dendritic patch-clamp recordings, not only to record the two phenomena simultaneously, but also control dendritic spikes as well. This approach provides a tool to test if there is a causal relationship between dendritic spikes and long-term synaptic plasticity.

Ito and Kano (1982) showed that conjunctive activation of PF and CF input results in long term depression (LTD) of the PF input activated. This discovery strongly supported the theory of cerebellar function envisaged by Marr (1969). He proposed that an error or teaching signal from the powerful CF input should decrease the efficacy of the PF input, which led to the erroneous movement signal. One necessary trigger for PF-LTD is an elevation of intracellular calcium, as shown by block of LTD by intracellular calcium chelators (Sakurai, 1990; Konnerth et al., 1992). Calcium signals in the neuronal cytosol can have two main origins: internal stores, like the endoplasmatic reticulum, and the extracellular space through voltage- or ligand-gated calcium-permeable channels. The release from internal stores is IP3 receptor-dependent (Ross et al., 2005), and IP3 is produced in abundance upon mGluR1 receptor activation. As these receptors surround the synaptic sites (Baude et al., 1993), to achieve significant pooling of glutamate to activate them, spatial and temporal coincidence of PF activity is required (Batchelor and Garthwaite, 1997; Tempia et al., 2001; Reichelt and Knöpfel, 2002; Marcaggi and Attwell, 2005), similar to the conditions leading to local dendritic spikes (Chapter 3).

The archetypal cerebellar LTD induction protocol uses coincident CF and PF activation, producing supralinear calcium increases in spines and spiny branchlets (Wang et al., 2000). Hartell (1996) described a new form of PF-LTD, which did not require the conjunctive activation of the CF, but a dense activation of PFs. Using imaging techniques he showed that above-threshold strong PF stimuli triggered calcium entry restricted to spiny branchlets near the stimulation site. From escape currents seen in the somatic voltage clamp recording of these EPSCs, Hartell concluded that local calcium spikes were mediating the LTD he described. However, the low temporal resolution of the imaging technique and the lack of direct electrical recording from the dendrites prevented Hartell from testing this hypothesis. The regenerative and local nature of dendritic calcium spikes in Purkinje cells described in Chapter 3 makes them a well-suited target to induce localized, coincidence-dependent synaptic plasticity, just as demonstrated in Chapter 4.

There are other requirements for LTD as well, possibly unrelated to an increase in intracellular calcium. For example, activation of PKC is necessary (Linden and Connor, 1991), which occurs via through mGluR1 type metabotropic glutamate receptors *in vivo* (Gao et al., 2003). A long line of evidence points to the necessity of NO as well (Lev-Ram et al., 1995; Lev-Ram et al., 1997b; Lev-Ram et al., 1997a), which may be released following presynaptic NMDA receptor activation (Casado et al., 2002; Shin and Linden, 2005; Duguid and Sjöström, 2006). Thus an increase in intracellular calcium is necessary but not sufficient to evoked PF-LTD. However, using synaptic input to trigger dendritic spikes, which let in ample amounts of calcium, may be enough to recruit the other necessary mechanisms.

My goal in this chapter is to determine the link between local dendritic calcium spikes and long-term depression of PF input. Purkinje cells represent an excellent model for this study because they do not have actively backpropagating action potentials or NMDA channels that would complicate the interpretation of dendritic excitability. Recording the electrical activity at both the soma and the dendrite during the different induction protocols with and without dendritic spikes in the same cell will clarify the role of dendritic spikes in modifying the synaptic strength of parallel fibre synapses.

5.2 Results

5.2.1 Parallel fibre evoked dendritic spikes trigger LTD

To test if local dendritic calcium spikes are able to modify long-term synaptic strength, as well as transiently (Chapter 4), I used dual somato-dendritic patch-clamp recordings to monitor dendritic spikes during different induction protocols leading to changes in synaptic strength. Parallel fibres were stimulated every 5 seconds by an ACSF-filled patch electrode buried deep into the slice under the dendritic recording electrode. EPSP amplitude was monitored using a single synaptic stimulus. The amplitude of the synaptic potential was monitored for at least 10 minutes before the induction to test the stability of the evoked synaptic response. The measured EPSP amplitudes were averaged for two consecutive 5-minute periods before the induction protocol. If the two averages differed by more than 10 %, the recording was excluded from the analysis to avoid contamination of the results by sloping changes in the baseline synaptic transmission. I also monitored the somatic input resistance using a -100 pA, 400 msec current pulse delivered after each stimulus. Experiments where the input resistance of the cell changed by more than 20 % were also excluded from the analysis. These measures are crucially important when monitoring long-term changes in synaptic strength to ensure that the measured changes are real reflections of changes in synaptic transmission.

To evoke dendritic calcium spikes during the induction protocol, the negative holding current was removed and the synaptic stimulation strength was increased gradually until dendritic spikes could be detected in the dendritic recording (Figure 5.1.A). This stimulus was repeated 50 times every 5 seconds, resulting in 47 ± 4 calcium spikes (range: 35 – 60). After the

induction protocol, stimulation intensity was returned to the pre-induction value to monitor any changes in synaptic strength for at least 20 minutes. The amplitude of the EPSP decreased to 61 ± 7 % of the baseline ($P < 0.01$, $n = 7$, Figure 5.1.D) immediately after the induction protocol and remained so during the rest of the recording (Figure 5.1.C).

To test if there is a threshold number of dendritic spikes in the induction of LTD, I have conducted additional experiments with the induction protocol consisting of only 20 repetitions of calcium spike-triggering PF stimulation resulting in 21 ± 3 calcium spikes (range 16 – 27). After the induction protocol, the EPSP amplitude was depressed to 67 ± 7 % of the baseline ($P < 0.05$, $n = 3$, Figure 5.1D). The amount of the LTD was similar to that produced by the 50 calcium spike triggering PF stimuli ($P = 0.55$). These results show that 20 - 50 repetitions of a dendritic calcium spike triggering PF stimulation are capable of producing robust, immediate long-term depression.

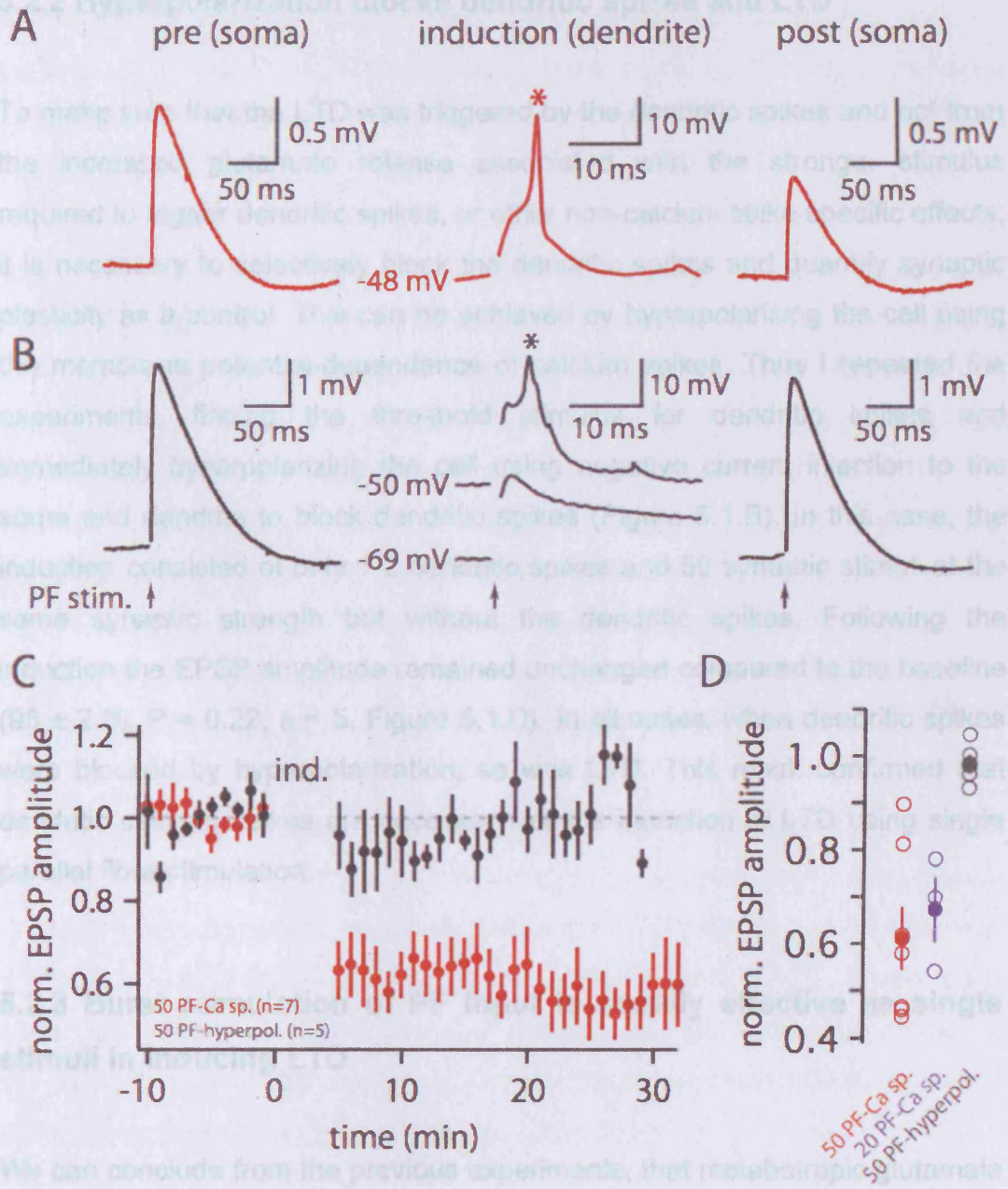

Figure 5.1.A PF triggered dendritic spikes induce LTD
A. Example experiment. PF evoked EPSPs recorded from the soma before and after the induction protocol. The induction consisted of 50 repetitions of strong PF stimulation, which triggered dendritic spikes (asterisk). **B.** Same as in panel A, except the induction protocol. Stimulus strength was increased to reach dendritic spike threshold (asterisk), after which the cell was hyperpolarized to prevent dendritic spikes. **C.** Pooled timecourse of normalized EPSP amplitude during experiments described in A and B. **D.** Distribution of LTD values recorded from individual cells using 50 (red) or 20 (blue) repetitions of dendritic spikes triggering PF stimulation or 50 suprathreshold stimuli when dendritic spikes were blocked by hyperpolarization (black).

5.2.2 Hyperpolarization blocks dendritic spikes and LTD

To make sure that the LTD was triggered by the dendritic spikes and not from the increased glutamate release associated with the stronger stimulus required to trigger dendritic spikes, or other non-calcium spike specific effects, it is necessary to selectively block the dendritic spikes and quantify synaptic plasticity as a control. This can be achieved by hyperpolarizing the cell using the membrane potential-dependence of calcium spikes. Thus I repeated the experiments, finding the threshold stimulus for dendritic spikes and immediately hyperpolarizing the cell using negative current injection to the soma and dendrite to block dendritic spikes (Figure 5.1.B). In this case, the induction consisted of only 1-2 dendritic spikes and 50 synaptic stimuli at the same synaptic strength but without the dendritic spikes. Following the induction the EPSP amplitude remained unchanged compared to the baseline (98 ± 2 %, P = 0.22, n = 5, Figure 5.1.D). In all cases, when dendritic spikes were blocked by hyperpolarization, so was LTD. This result confirmed that dendritic calcium spikes are necessary for the induction of LTD using single parallel fibre stimulation.

5.2.3 Burst stimulation of PF input is equally effective as single stimuli in inducing LTD

We can conclude from the previous experiments, that metabotropic glutamate receptors situated around the PF synapses are not sufficiently activated by the glutamate released by strong PF stimulation to induce LTD. This could be because mGluR activation alone is not sufficient to induce LTD (similarly to DSE in Chapter 3). Alternatively, the extent of mGluR activation was insufficient, as it depends on spatial and temporal pooling of glutamate. The spatial pooling is provided by the focal stimulation, producing a "beam" of activated PFs. To achieve temporal pooling of glutamate, I used an induction protocol consisting of 3 PF stimuli delivered at 100 Hz (Figure 5.2.A), which is similar to GC firing patterns *in vivo* (Chadderton et al., 2004) and has been shown to produce mGluR mediated slow EPSPs in Purkinje cells (Batchelor

and Garthwaite, 1997). This induction protocol also requires a smaller number of synchronously active parallel fibres because dendritic spike threshold will be reached by weaker stimulation owing to the strong paired-pulse facilitation of parallel fibre synapses. It thus represents a physiologically more plausible activation pattern of granule cell axons.

The induction protocol was repeated 20 times, evoking 29 ± 3 dendritic spikes (range 18 – 42). The EPSP amplitude was significantly reduced immediately after resuming the baseline synaptic stimulation intensity (63 ± 3% of baseline, n = 7, P < 0.002, Figure 5.2.D). This depression lasted for at least 20 minutes in all cells tested (Figure 5.2.C). As the monitoring of PF EPSPs was also done using trains of 3 stimuli at 100 Hz, these experiments presented an opportunity to measure the paired-pulse ratio before and after the induction protocol. Consistently with a postsynaptic expression of cerebellar PF – Purkinje cell LTD (Ito, 2002), the paired-pulse ratio was unaffected by the induction protocol (98 ± 3 % of baseline, n = 7, p > 0.05).

To test if dendritic spikes were necessary or not using a train of stimuli to induce LTD, I blocked dendritic spike initiation using hyperpolarization (Figure 5.2.B). Hyperpolarization efficiently prevented LTD (101 ± 3 % of baseline, n = 5, P = 0.81, Figure 5.2.C) in all cells tested (Figure 5.2.D). These result show that using parallel fibre stimuli similar to *in vivo* GC firing patterns results in LTD only if dendritic calcium spikes are triggered; thus mGluR activation alone is not sufficient to induce synaptic plasticity.

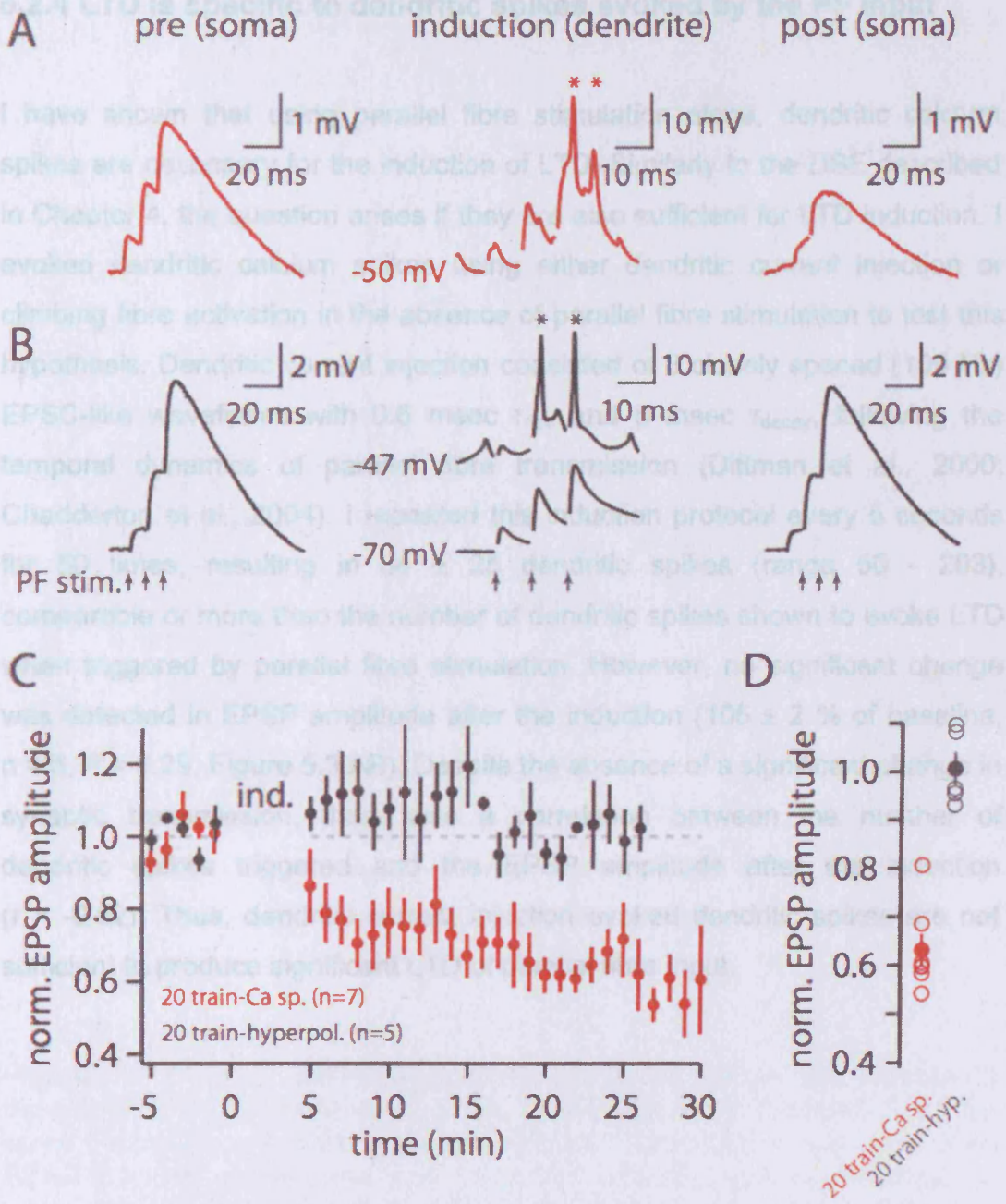

Figure 5.2 Dendritic spikes triggered by PF trains induce LTD.
A. Sample experiment. Parallel fibres were stimulated with a train of 3 stimuli at 100Hz. EPSPs were measured in the soma before and after the induction. During the induction protocol, PF stimulus intensity was raised to trigger dendritic spikes (asterisks). Stimulation artefacts were removed for clarity. **B.** Similar to panel A, except dendritic spikes were blocked by hyperpolarization during the induction protocol. Note that in this case no LTD was detected. **C.** Pooled data from several cells showing the timecourse of EPSP amplitude. **D.** Amount of LTD in individual experiments. Note, that when dendritic spikes were triggered, LTD always followed. Conversely, when dendritic spikes were blocked by hyperpolarization, no LTD was detected.

5.2.4 LTD is specific to dendritic spikes evoked by the PF input

I have shown that using parallel fibre stimulation alone, dendritic calcium spikes are necessary for the induction of LTD. Similarly to the DSE described in Chapter 4, the question arises if they are also sufficient for LTD induction. I evoked dendritic calcium spikes using either dendritic current injection or climbing fibre activation in the absence of parallel fibre stimulation to test this hypothesis. Dendritic current injection consisted of 3 closely spaced (100 Hz) EPSC-like waveforms with 0.6 msec τ_{rise} and 6 msec τ_{decay}, following the temporal dynamics of parallel fibre transmission (Dittman et al., 2000; Chadderton et al., 2004). I repeated this induction protocol every 5 seconds for 50 times, resulting in 84 ± 25 dendritic spikes (range 50 - 203), comparable or more than the number of dendritic spikes shown to evoke LTD when triggered by parallel fibre stimulation. However, no significant change was detected in EPSP amplitude after the induction (105 ± 2 % of baseline, n = 6, P = 0.29, Figure 5.3.AB). Despite the absence of a significant change in synaptic transmission, there was a correlation between the number of dendritic spikes triggered and the EPSP amplitude after the induction (r = -0.62). Thus, dendritic current injection evoked dendritic spikes are not sufficient to produce significant LTD of parallel fibre input.

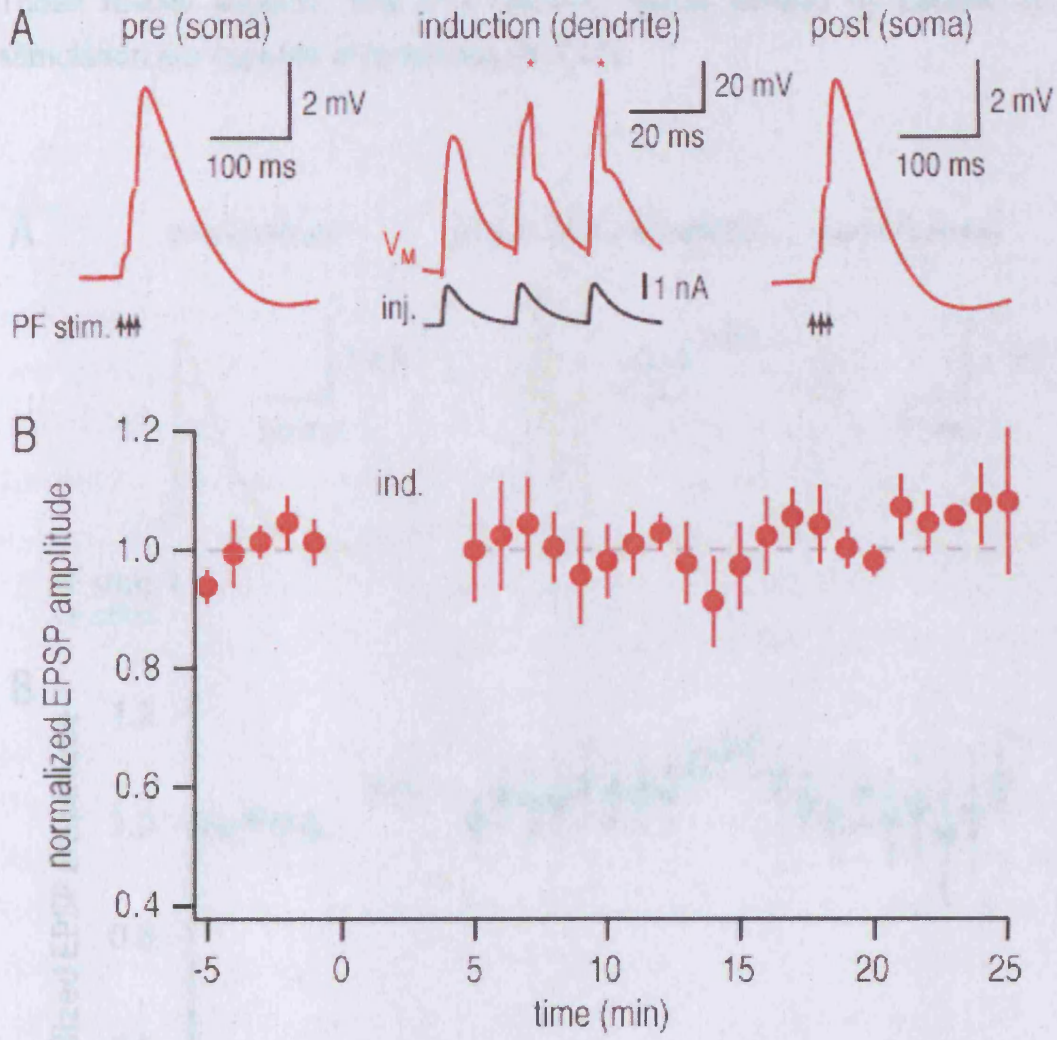

Figure 5.3 Current injection-triggered dendritic spikes are unable to induce LTD A. Example experiment. PF-EPSPs were recorded from the soma before and after the induction protocol. The induction consisted of an EPSC-train-like current injection triggering dendritic spikes, repeated 50 times. No significant changes in EPSP amplitude were detected after the induction. **B.** Pooled data from 6 cells showing the timecourse of the EPSP amplitude.

Next, I tested the efficacy of a more global dendritic spike, produced by the powerful climbing fibre input, which, in contrast to parallel fibre input, forms many hundreds of synaptic contacts along the main dendrites. The induction protocol consisted of 50 repetitions of single climbing fibre stimuli every 5 seconds, typically producing 2-3 dendritic spikes per stimulus. Similarly to current injection evoked dendritic spikes, CF activation alone failed to depress

parallel fibre EPSPs (104 ± 6 % of baseline, n = 6, p = 0.65, Figure 5.4). These results suggest, that only dendritic spikes evoked by parallel fibre stimulation are capable of producing PF-LTD.

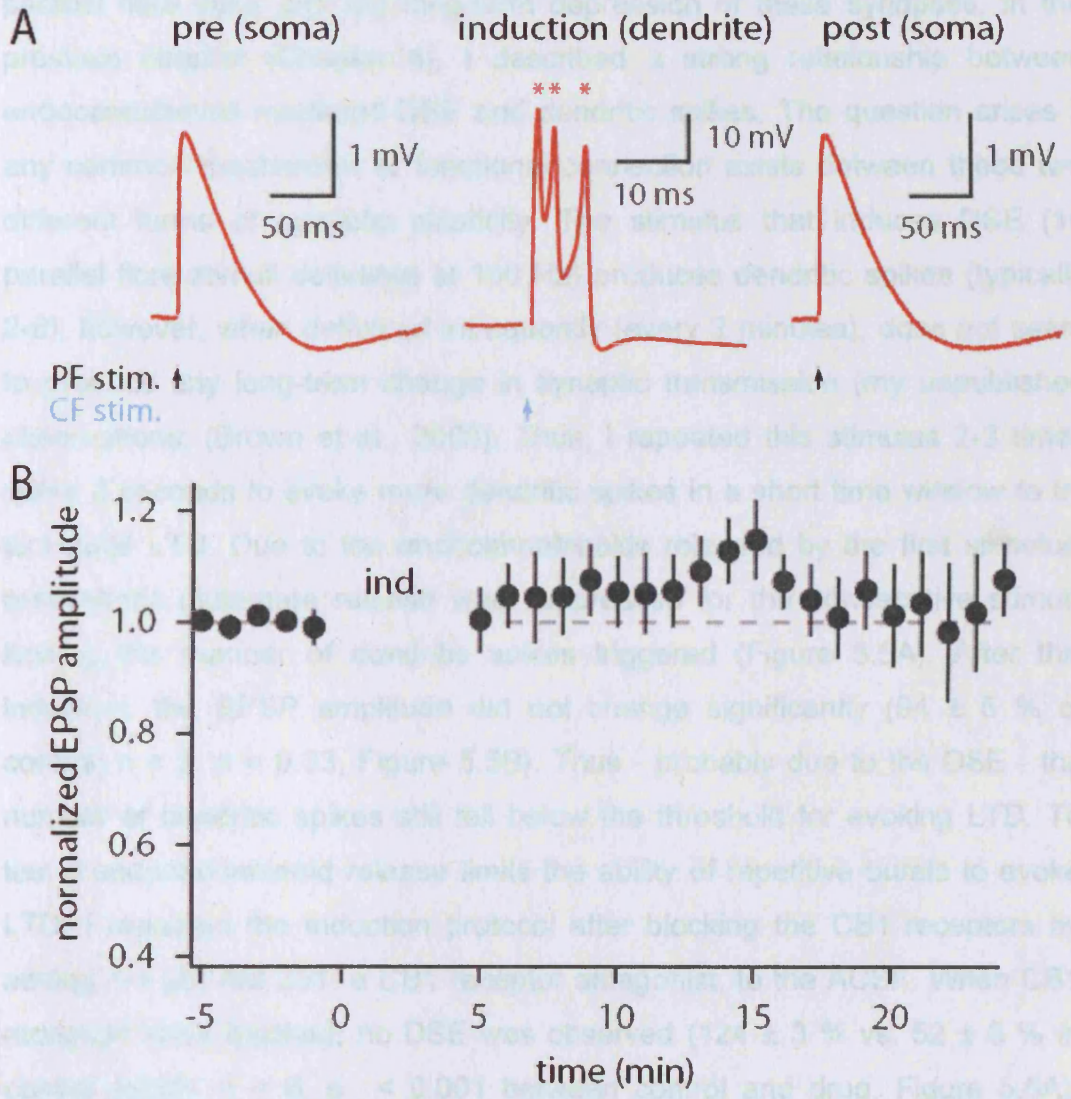

Figure 5.4 Climbing fibre triggered dendritic spikes fail to induce LTD
A. Example experiment. PF-EPSP amplitudes were recorded from the soma before and after the induction protocol. The induction consisted of 50 repetitions of CF stimulation at 0.2 Hz in the absence of PF stimulation. Stimulus artefacts were removed for clarity. **B.** Pooled timecourse of EPSP amplitudes from 6 cells.

5.2.5 Is there a link between DSE and LTD?

In this chapter, I have established a link between dendritic spikes triggered by parallel fibre input and the long-term depression of these synapses. In the previous chapter (Chapter 4), I described a strong relationship between endocannabinoid mediated DSE and dendritic spikes. The question arises if any common mechanism or functional connection exists between these two different forms of synaptic plasticity. The stimulus that induces DSE (10 parallel fibre stimuli delivered at 100 Hz) produces dendritic spikes (typically 2-8), however, when delivered infrequently (every 2 minutes), does not seem to produce any long-term change in synaptic transmission (my unpublished observations; (Brown et al., 2003). Thus, I repeated this stimulus 2-3 times every 2 seconds to evoke more dendritic spikes in a short time window to try to induce LTD. Due to the endocannabinoids released by the first stimulus, presynaptic glutamate release was suppressed for the consecutive stimuli, limiting the number of dendritic spikes triggered (Figure 5.5A). After this induction, the EPSP amplitude did not change significantly (94 ± 5 % of control, $n = 7$, $p = 0.33$, Figure 5.5B). Thus - probably due to the DSE - the number of dendritic spikes still fell below the threshold for evoking LTD. To test if endocannabinoid release limits the ability of repetitive bursts to evoke LTD, I repeated the induction protocol after blocking the CB1 receptors by adding 1-5 µM AM 251, a CB1 receptor antagonist, to the ACSF. When CB1 receptors were blocked, no DSE was observed (124 ± 3 % vs. 52 ± 6 % in control ACSF, $n = 6$, $p < 0.001$ between control and drug, Figure 5.6A). Consequently all burst stimulation during the induction protocol evoked numerous dendritic spikes in the dendrite (Figure 5.5A). This second induction protocol resulted in a significant, long-term reduction in synaptic strength (77 ± 5 % of control, $n = 6$, $p < 0.05$, Figure 5.5B and Figure 5.6B). Plotting the amount of LTD vs. the number of dendritic spikes during induction in the individual cells, a positive correlation became evident ($r = 0.63$, Fig 5.6C), suggesting that the increased number of dendritic spikes is responsible for the larger amount of depression when CB1 receptors are blocked.

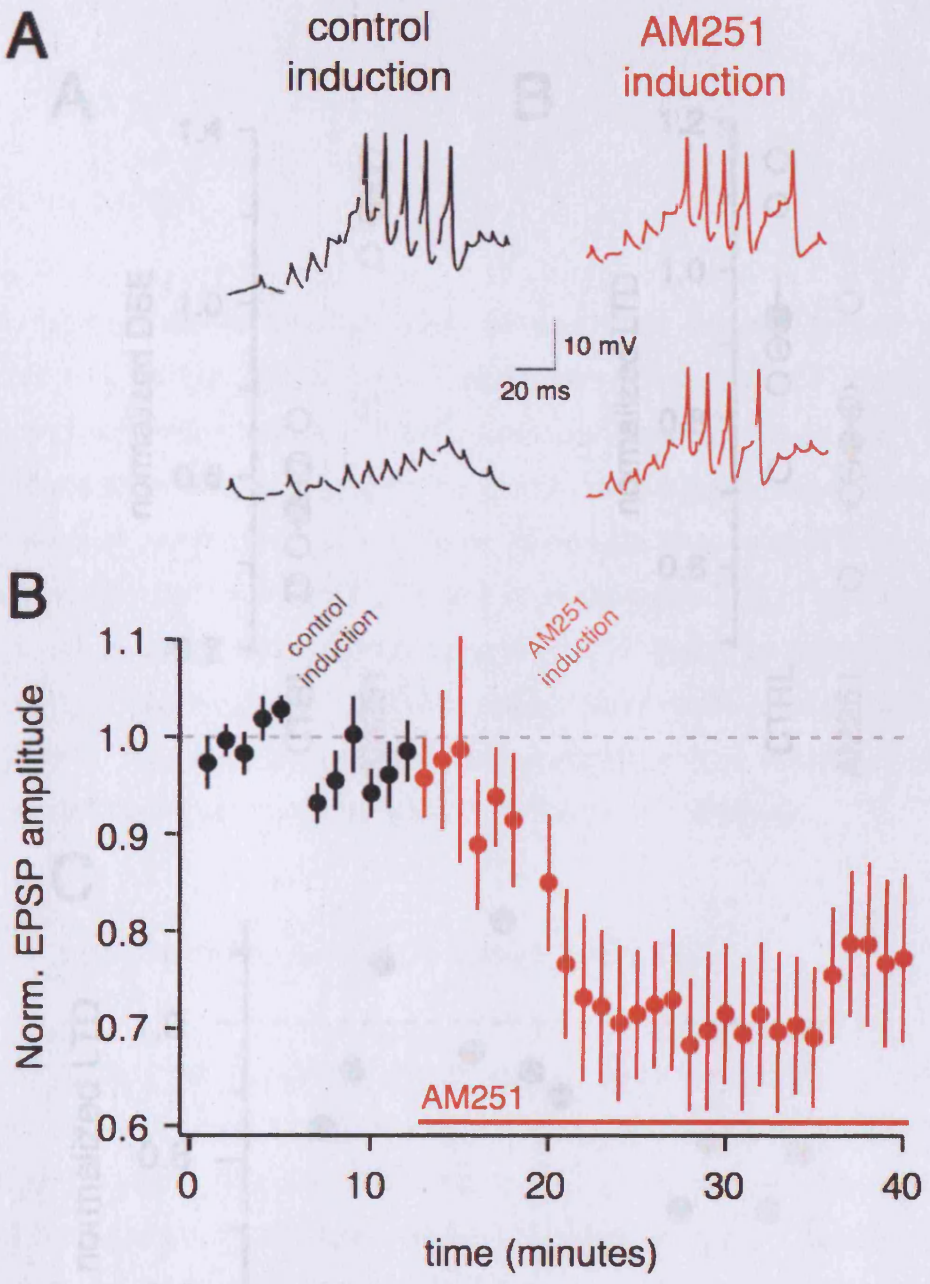

Figure 5.5 Block of CB1 receptors facilitates LTD induction
A. Parallel fibres were stimulated with a train of 10 stimuli delivered at 100 Hz repeated 2-3 times every 2 seconds. With endocannabinoid signalling intact (black traces) only the first stimulus triggered dendritic spikes. When CB1 receptors were blocked (red), all repetitions were producing comparable number of dendritic spikes. **B.** Effect of CB1 receptor block on the ability of repeated trains to induce LTD. Normalized average EPSP amplitudes from 7 (control) and 6 (AM251) cells.

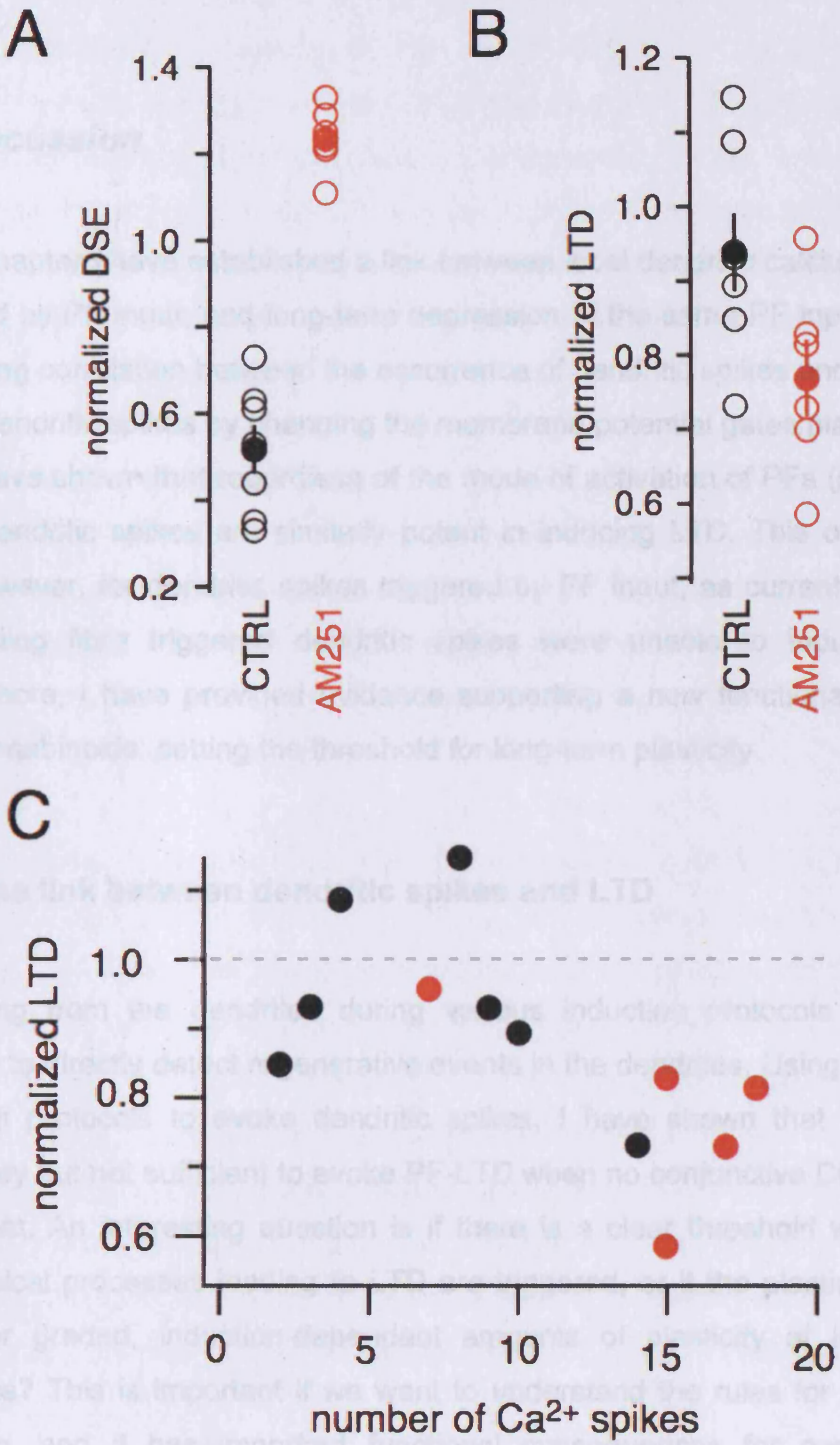

Figure 5.6 CB1 receptors mediate DSE and decrease the probability of dendritic spikes

A. DSE obtained in individual cells in the absence and presence of AM251, a CB1 antagonist. **B.** LTD obtained by 2-3 repetitions (0.5 Hz) of 10 PF stimuli at 100 Hz in the absence and presence of AM251. **C.** Relationship between the number of dendritic spikes triggered during induction and the amount of synaptic plasticity. Black – control. Red – AM251.

5.3 Discussion

In this chapter I have established a link between local dendritic calcium spikes triggered by PF input, and long-term depression of the same PF input. There is a strong correlation between the occurrence of dendritic spikes and LTD, as gating dendritic spikes by changing the membrane potential gates plasticity as well. I have shown that regardless of the mode of activation of PFs (single vs. train), dendritic spikes are similarly potent in inducing LTD. This only holds true, however, for dendritic spikes triggered by PF input, as current injection or climbing fibre triggered dendritic spikes were unable to induce LTD. Furthermore, I have provided evidence supporting a new functional role for endocannabinoids: setting the threshold for long-term plasticity.

5.3.1 The link between dendritic spikes and LTD

Recording from the dendrites during various induction protocols made it possible to directly detect regenerative events in the dendrites. Using different induction protocols to evoke dendritic spikes, I have shown that they are necessary but not sufficient to evoke PF-LTD when no conjunctive CF activity is present. An interesting question is if there is a clear threshold when the biochemical processes leading to LTD are triggered, or it the plasticity rules allow for graded, induction-dependent amounts of plasticity at individual synapses? This is important if we want to understand the rules for plasticity induction, and it has important functional consequences for cerebellum-dependent learning. The different induction protocols triggered not only different kinds of dendritic spikes, but also different numbers of spikes as well. Thus, by plotting the amount of LTD achieved versus the number of dendritic spikes triggered during the induction, one can obtain a better picture of the plasticity rules at this synapse. In Figure 5.7, I separated the different protocols depending on the mode the dendritic spikes were triggered. For

dendritic spikes triggered by PF synaptic stimulation, the amount of LTD appears to be independent of the temporal dynamics of the synaptic input. Induction protocols consisting of the same number of dendritic spikes triggered by repetitive single stimuli or by trains of 3 or 10 PF stimuli at 100 Hz are similarly potent and induce comparable amounts of LTD. This indicates that, across the different protocols, it is the number of dendritic spikes that is critical for setting the degree of plasticity. However, when dendritic spikes were triggered by dendritic current injection, regardless of the number of dendritic spikes triggered, LTD was never observed.

Based on this relationship, there is a narrow window between ~15 – 25 dendritic spikes where the amount if LTD is highly sensitive to the number of dendritic spikes. Below this threshold, no LTD is observed. Above this threshold the extra dendritic spikes are much less effective in increasing the amount of synaptic plasticity, as there appears to be saturation in the amount of synaptic depression achievable.

In the absence of coincident CF input, PF triggered dendritic spikes are thus necessary to evoke LTD (Figure 5.8). The source of depolarization is crucially important, however. Dendritic spikes triggered by dendritic current injection (Figure 5.3) or climbing fibre activation (Figure 5.4) fail to induce LTD. One reason for this could be the lack of spatial overlap between the tested synapses and the calcium entry similarly to the case of DSE (see Chapters 3 and 4). Complementary to this scenario, dendritic spikes alone may not be sufficient to induce LTD. A supralinear calcium increase following mGluR1 activation (Wang et al., 2000) or the involvement of other neurotransmitters may require glutamate release paired with dendritic calcium increase.

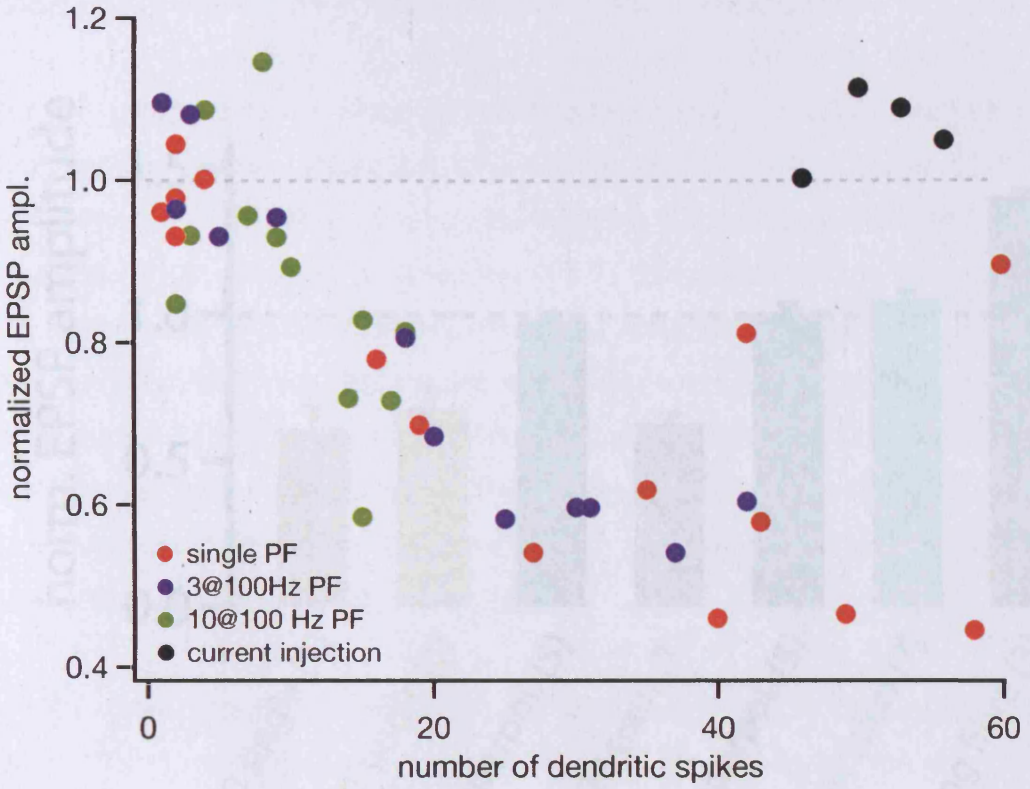

Figure 5.7 Relationship between the number of dendritic spikes and LTD
The number of dendritic spikes recorded during different induction protocols is plotted against the normalized EPSP amplitude measured at the end of the experiment (minimum 20 minutes after induction). Red circles represent dendritic spikes triggered by single PF stimulation. Blue and green circles represent dendritic spikes triggered by a train of 3 or 10 PF stimuli delivered at 100 Hz, respectively. Black circles represent dendritic spikes triggered by dendritic current injection.

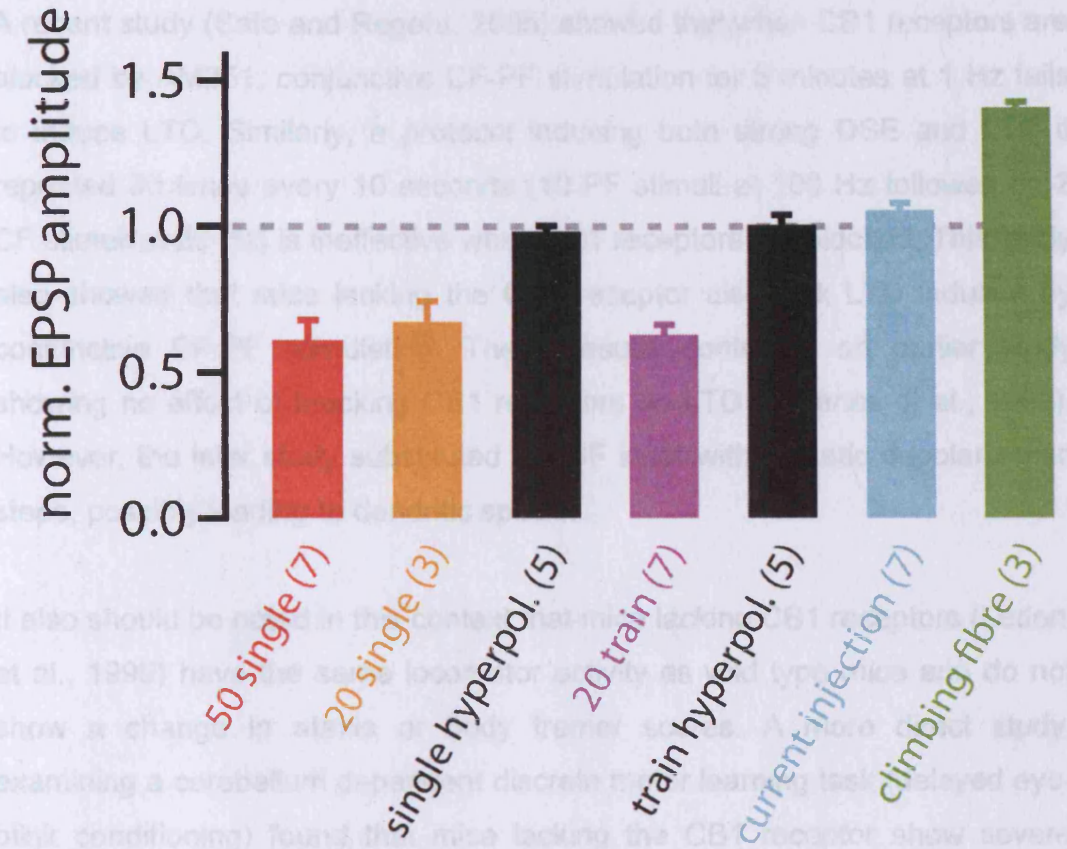

Figure 5.8 Different induction protocols triggering dendritic spikes produce different changes in synaptic strength
Summary bar graph showing all the experimentally tested dendritic spike triggering protocols. The numbers in brackets represent the number of cells for every protocol.

5.2.3 The involvement of CB1 receptors in cerebellar LTD

A recent study (Safo and Regehr, 2005) showed that when CB1 receptors are blocked by AM251, conjunctive CF-PF stimulation for 5 minutes at 1 Hz fails to induce LTD. Similarly, a protocol inducing both strong DSE and LTD if repeated 30 times every 10 seconds (10 PF stimuli at 100 Hz followed by 2 CF stimuli at 20 Hz) is ineffective when CB1 receptors are blocked. This study also showed that mice lacking the CB1 receptor also lack LTD induced by conjunctive CF-PF stimulation. These results contradict an earlier study showing no effect of blocking CB1 receptors on LTD (Levenes et al., 1998). However, the later study substituted the CF input with somatic depolarization steps, possibly leading to dendritic spikes.

It also should be noted in this context that mice lacking CB1 receptors (Ledent et al., 1999) have the same locomotor activity as wild type mice and do not show a change in ataxia or body tremor scores. A more direct study, examining a cerebellum dependent discrete motor learning task (delayed eye-blink conditioning) found that mice lacking the CB1 receptor show severe impairment in this learning paradigm (Kishimoto and Kano, 2006). Interestingly, no difference was detected between wild type and CB1 -/- animals in motor coordination using a rotarod test, the extinction of delayed eye-blink conditioning or trace eye-blink conditioning, a learning paradigm dependent on the hippocampal formation.

In Figure 5.5 I show evidence for the existence of PF triggered dendritic spikes evoked LTD in the presence of a CB1 receptor blocker. Furthermore, when CB1 receptors are blocked, a stimulus paradigm leading to no change in synaptic strength readily induces LTD, contradicting earlier findings. This later, seemingly pro-LTD effect is a direct consequence of the increase in glutamate release and consecutively higher number of dendritic spikes triggered when DSE is blocked (Figure 5.5.E). The surprising result is the existence of PF-LTD in the absence of retrograde endocannabinoid signalling (Figure 5.5.CD). This could have two explanations: first, the PF-LTD described in this chapter is mechanistically different from the CF-PF LTD.

Second, an implied anterograde messenger (NO), which may be released following CB1 activation from PF or interneuron terminals (Duguid and Sjöström, 2006), may be readily released following strong PF stimulation without the need of CB1 activation. The differential involvement of NO, CB1 and mGluR signalling in PF-LTD thus needs to be studied further to provide a better understanding of different forms of synaptic depression in the cerebellum and most crucially, their involvement in behavioural and learning paradigms.

6. Dendritic spikes control somatic output of cerebellar Purkinje cells

6.1 Introduction

Dendrites, abundant in voltage-gated ion channels, can profoundly affect the way neurons respond to synaptic input. In the previous chapters, I have focused on the effect of dendritic spikes in Purkinje cells on regulating parallel fibre input. A similarly important question is what influence dendritic spikes have on the somatic action potential initiation, thus the output of the cell.

Dendritic spikes detect synchronous input and provide a non-linear response. As they are regenerative events and this nonlinearity is positive, a reasonable null hypothesis is that they should boost the output of the neuron, i.e. the initiation of axonal sodium spikes. They have been shown to enhance the precision of axonal action potentials in hippocampal CA1 pyramidal cells (Ariav et al., 2003) as well as in cortical pyramidal cells *in vivo* (Crochet et al., 2004). By providing a strong depolarization, they can also help distal synaptic inputs - which would be severely attenuated when they reach the soma - influence spike output by themselves (Williams, 2004; Gasparini and Magee, 2006) or in concert with backpropagating action potentials (Larkum et al., 1999a). Dendritic spikes thus can boost the synaptic input reaching the soma. However, the resultant calcium entry, similarly to somatic action potentials (Cingolani et al., 2002; Womack and Khodakhah, 2002b) can also activate calcium-dependent potassium channels and contribute to the different phases of the after-hyperpolarization (AHP) following action potentials. In CA1

pyramidal cells, small conductance calcium-activated potassium (SK) channels limit the spatial extent of calcium spikes (Cai et al., 2004). In cerebellar Purkinje cells, the high-conductance calcium-activated potassium (BK) channels serve a similar function (Chapter 3). Thus dendritic spikes provide both a strong depolarization and a hyperpolarizing AHP, varying in strength, depending on cell type and ion channels expression. It is difficult to predict the balance of inward and outward currents associated with dendritic spike generation. Purkinje cells are ideal for studying the effect of dendritic spikes as the lack of backpropagating action potentials, voltage-gated sodium channels and NMDA receptors in the dendrites makes the results easier to interpret.

6.2 Results

6.2.1 Synaptically triggered dendritic spikes suppress somatic firing

In order to assess the possible effect of dendritic calcium spikes on the action potential firing of Purkinje cells, I made double somato-dendritic whole-cell patch clamp recordings from Purkinje cells in acute cerebellar slices. Purkinje cells fired action potentials spontaneously (Häusser and Clark, 1997) which backpropagated poorly into the dendritic tree (Stuart and Häusser, 1994); Figure 6.1.AB).

Using a stimulation electrode buried in the molecular layer beneath the dendritic recording electrode, I activated parallel fibers (PF) with 10 stimuli delivered at 100 Hz, similar to the sensory stimulus evoked firing pattern of granule cells *in vivo* (Chadderton et al., 2004). Excitatory postsynaptic potentials depolarized the dendrite and resulted in increasing somatic AP output, as shown by the monotonic increase in the instantaneous firing rate recorded at the soma (Figure 6.1.A) which lasted as long as the stimulus. To trigger dendritic spikes, I gradually increased the strength of the stimulus, taking advantage of the stimulation intensity dependence of dendritic spikes (Chapter 3). The relative location of the stimulation and dendritic recording electrodes together with the orientation of the parallel fibres allowed me to record as close to the synaptic input as possible, thus maximizing the chance of detecting local supralinear events. Stronger stimulation resulted in higher instantaneous somatic firing rates at the beginning of the train (Figure 6.1.BC), however, when dendritic spikes were evoked, the instantaneous firing rate dropped, despite the continuous synaptic input (Figure 6.1.BD). Interestingly, the average firing rate during dendritic spike triggering input

appeared to be independent of the stimulus strength, as the average somatic firing rate was clamped at 214 ± 8 Hz (n = 5, Figure 6.1.D). Thus, dendritic spikes appear to have an inhibitory effect on average somatic output rates.

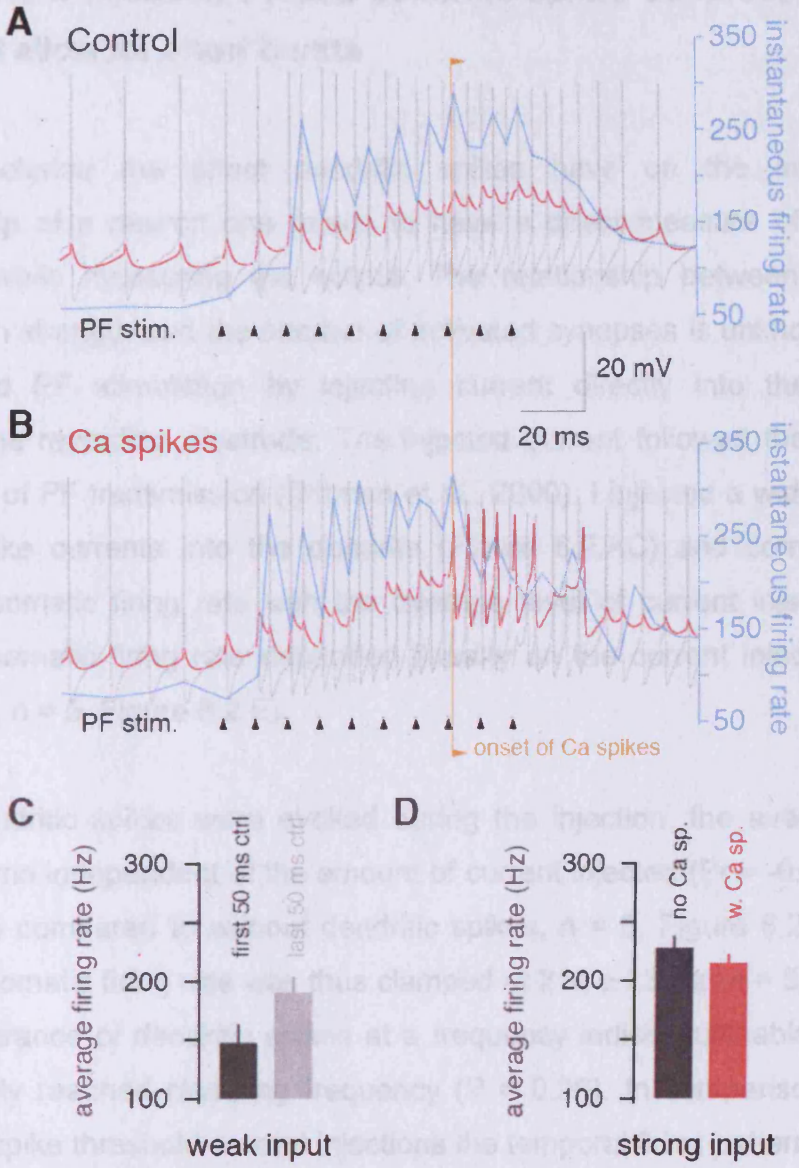

Figure 6.1 Synaptically triggered dendritic spikes suppress somatic firing.
A. Somatic (grey) and dendritic (red) voltage traces during 10 PF stimuli delivered at 100 Hz. The instantaneous somatic firing rate (blue) is increasing as long as the synaptic input is on. **B.** Same as in A except with stronger synaptic stimulus. The onset of dendritic spikes in the dendritic voltage trace (orange line) coincides with a sharp drop in the somatic instantaneous firing rate. **C.** Comparison of the average somatic firing rate during the first and last 50 ms of the stimulus when no dendritic spikes were triggered, showing a clear increase during the stimulus. **D.** Comparison of the average somatic firing rate during the whole stimulus with stimuli just below the dendritic spike threshold and well above the dendritic spike threshold. Despite the stronger stimulus resulting in dendritic spikes, the average somatic rate is unchanged.

6.2.2 Current injection evoked dendritic spikes suppress somatic firing but allow for short bursts

To characterize the effect dendritic spikes have on the input-output relationship of a neuron one needs to have a direct measure of the input strength while measuring the output. The relationship between electrical stimulation strength and the number of activated synapses is unknown, thus I substituted PF stimulation by injecting current directly into the dendrite through the recording electrode. The injected current followed the temporal dynamics of PF transmission (Dittman et al., 2000). I injected a wide range of synaptic-like currents into the dendrite (Figure 6.2.AC) and correlated the average somatic firing rate with the average level of current injection. The average somatic firing rate depended linearly on the current injection (Pr = 0.98-0.99, n = 5, Figure 6.2.E).

When dendritic spikes were evoked during the injection, the average firing rate became independent of the amount of current injected (Pr = -0.08 ± 0.18, $P < 0.005$ compared to without dendritic spikes, n = 5, Figure 6.2.CE). The average somatic firing rate was thus clamped at 214 ± 23 Hz (n = 5) following the appearance of dendritic spikes at a frequency indistinguishable from the synaptically reached clamping frequency (P = 0.98). In comparison to sub-dendritic spike threshold current injections the temporal firing pattern changed the most. Figure 6.2.B and C shows the average dendritic membrane potential in red, reflecting the input, superimposed on the somatic traces in grey, showing action potentials. The blue trace is the probability of a spike in every 1 ms time-bin. The most striking difference is a consistent pause in somatic firing following a dendritic spike. Consistently with the local nature of the spike and cable filtering, the fast rising phase of the dendritic spike does not seem to contribute much to the somatic action potential output.

To obtain a more quantitative picture of the somatic firing, I also plotted the inter-spike intervals (ISI) during the current injection for trials with and without dendritic spikes evoked (Figure 6.3.F). When no calcium spikes were evoked, the inter-spike intervals followed a unimodal distribution with a mean

corresponding to the average firing rate. However, the ISI distribution showed two distinct peaks when dendritic spikes were triggered, one corresponding to faster than average ISIs and one corresponding to short pauses in firing. These second, longer ISI values always followed dendritic calcium spikes (Figure 6.2.D) suggesting a mechanistic link between the two phenomena. I next sought to determine the underlying mechanism. The most likely candidate was the high conductance calcium-activated potassium (BK) channel as it participates in the after-hyperpolarization following somatic action potentials in Purkinje cells (Womack and Khodakhah, 2002b) as well as the AHP and spatial restriction of dendritic calcium spikes (Chapter 3).

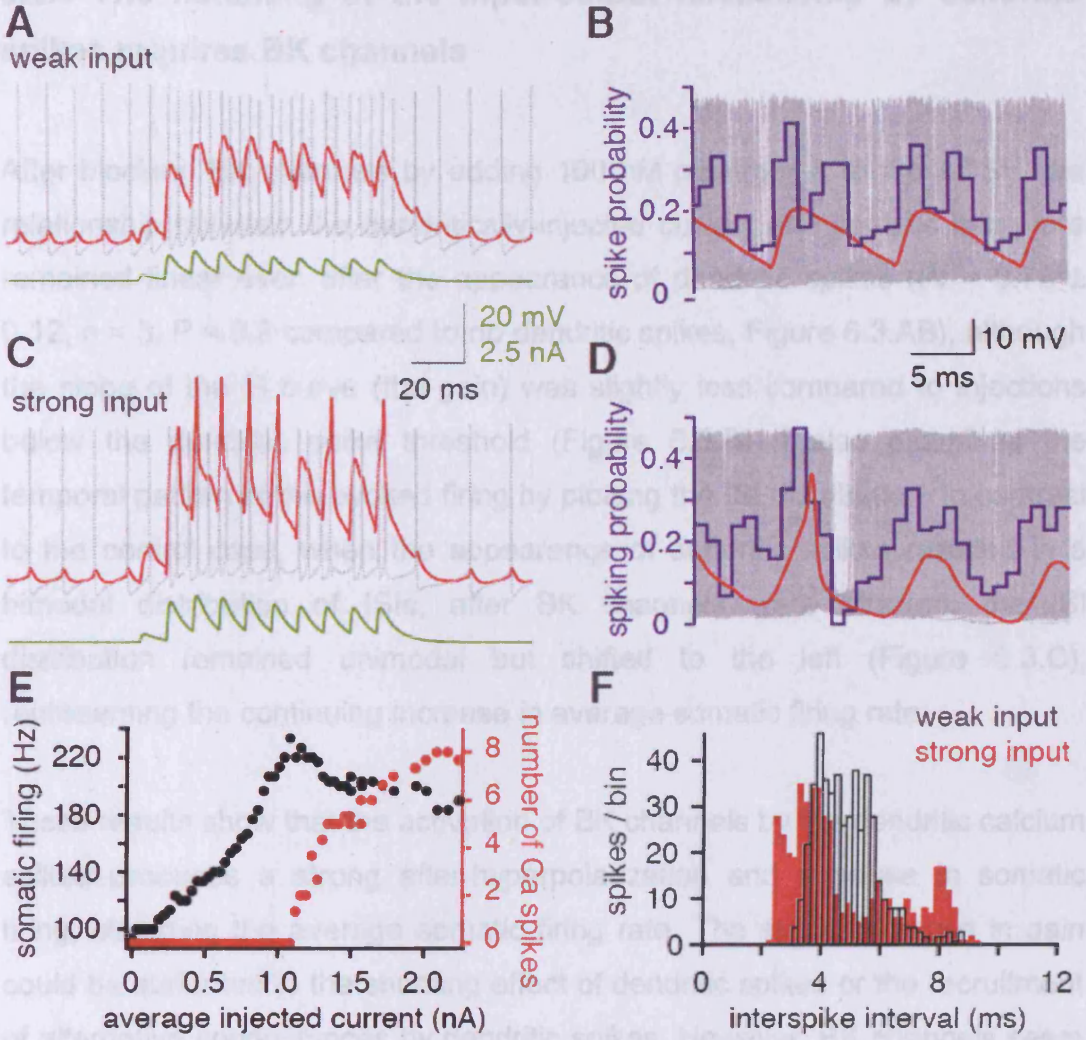

Figure 6.2 Current injection-evoked dendritic spikes suppress somatic firing

A. Somatic (grey) and dendritic (red) voltage trace during dendritic injection of synaptic-like current (green). **B.** Superimposed somatic (grey) and average dendritic (red) traces triggered by the current injection. Spike probability (blue) follows the input strength. **C.** As in A but with stronger current injection triggering dendritic spikes. **D.** Superimposed somatic (grey) and average dendritic (red) traces triggered at dendritic spikes. Spike probability (blue) is slightly enhanced by inputs triggering dendritic spikes. Note the strong inhibition of somatic firing following the dendritic spikes. **E.** Average somatic firing rate (black) and the number of dendritic spikes (red) during the current injection is plotted versus the peak of the injected current. Note the linear f/I relationship before dendritic spikes occur. In the injection range where dendritic spikes are triggered, the average somatic firing rate is independent of the input. **F.** Plot of inter-spike interval distribution with current injection just below and well above dendritic spike threshold. Note, that the distribution becomes bimodal with peaks to the right and left of the control condition when dendritic spikes are triggered.

6.2.3 The flattening of the input-output relationship by dendritic spikes requires BK channels

After blocking BK channels by adding 100 nM penitrem A to the ACSF, the relationship between the dendritically-injected current and somatic firing rate remained linear even after the appearance of dendritic spikes (Pr = 0.78 ± 0.12, n = 3, P = 0.2 compared to no dendritic spikes, Figure 6.3.AB), although the slope of the f/I curve (the gain) was slightly less compared to injections below the dendritic spike threshold (Figure 6.3.B). I also examined the temporal pattern of the evoked firing by plotting the ISI distribution. In contrast to the control case, when the appearance of dendritic spikes resulted in a bimodal distribution of ISIs, after BK channels were blocked, the ISI distribution remained unimodal but shifted to the left (Figure 6.3.C), representing the continuing increase in average somatic firing rate.

These results show that the activation of BK channels by the dendritic calcium spikes produces a strong after-hyperpolarization and a pause in somatic firing, clamping the average somatic firing rate. The slight decrease in gain could be attributed to the shunting effect of dendritic spikes or the recruitment of alternative conductances by dendritic spikes. However, BK channels seem to be the strongest contributors to the clamping effect.

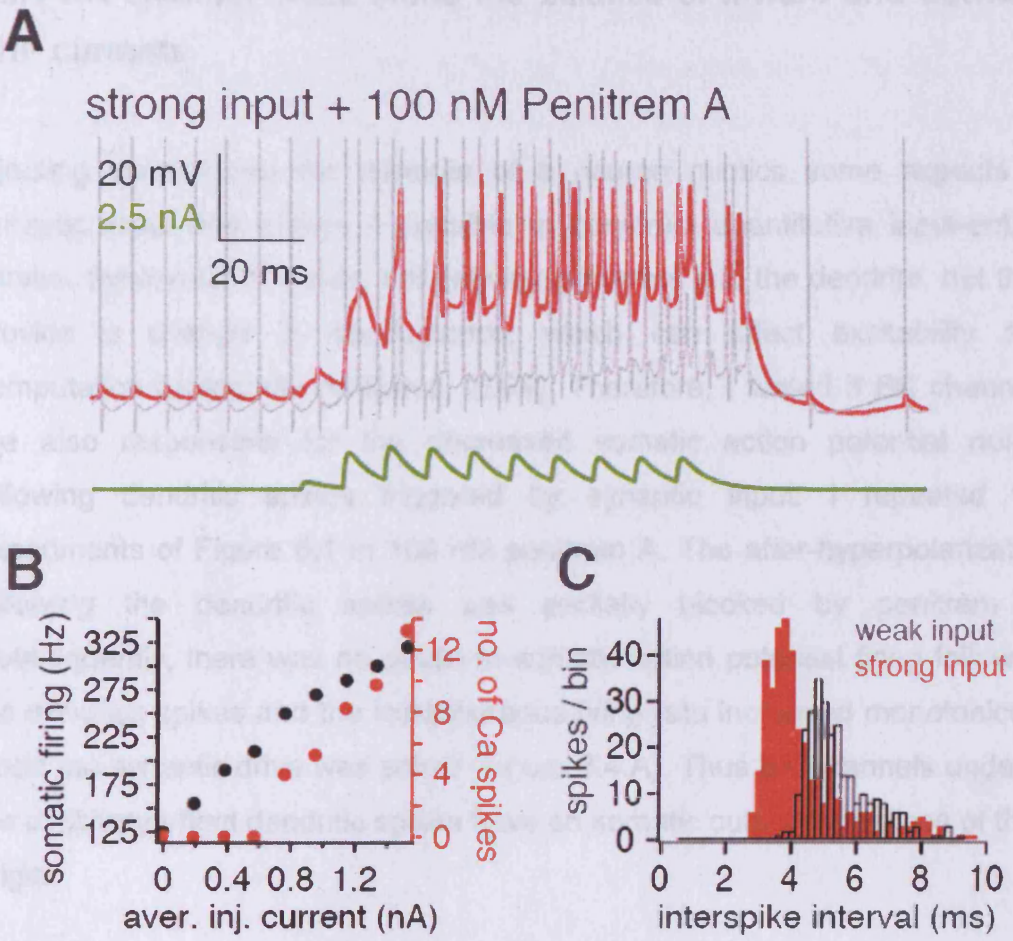

Figure 6.3 The flattening of the input-output relationship by dendritic spikes requires BK channels. A. Somatic (grey) and dendritic (red) recording during dendritic current injection (green). BK channels were blocked by 100 nM penitrem A. Note the lack of after-hyperpolarization and somatic pause following dendritic spikes in the dendritic recording. The slow AHP of somatic spikes is also reduced. **B.** Average somatic firing rate (black) and the number of dendritic spikes (red) during the current injection is plotted versus the peak of the injected current. Note that with the appearance of dendritic spikes, the somatic output continues to depend linearly on the input, although with a reduced gain. **C.** The inter-spike interval histogram is shifted to the left and remains unimodal with the appearance of dendritic spikes when BK channels are blocked.

6.2.4 BK channel block shifts the balance of inward and outward AHP currents

Injecting current into the dendrite of a neuron mimics some aspects of synaptic input and makes it possible to construct quantitative input-output curves. Synapses, however, not only inject current into the dendrite, but they provide a change in conductance, which can affect excitability and computation profoundly (Williams, 2004). Therefore, I tested if BK channels are also responsible for the decreased somatic action potential output following dendritic spikes triggered by synaptic input. I repeated the experiments of Figure 6.1 in 100 nM penitrem A. The after-hyperpolarization following the dendritic spikes was partially blocked by penitrem A. Consequently, there was no pause in somatic action potential firing following the dendritic spikes and the instantaneous firing rate increased monotonically when the synaptic drive was active (Figure 6.4.A). Thus BK channels underlie the inhibitory effect dendritic spikes have on somatic output regardless of their origin.

To understand the functional relevance of this dampening mechanism, I compared the maximal firing rates measure with and without dendritic spikes to the propagation limit of the Purkinje cell axon (Khaliq and Raman, 2005; Monsivais et al., 2005). First, I have compared the maximal sustained firing rate, measured as the average firing rate during the synaptic-like current injection (Figure 6.4.B). The maximal firing rate, both below dendritic spike threshold (225 ± 13 Hz, n = 5) and above dendritic spike threshold (214 ± 23 Hz, n = 5) fell below the axonal propagation limit (236 ± 15 Hz, Monsivais et al., 2005). However, when BK channels were blocked, the average somatic firing rate reached 293 ± 13 Hz (n = 3), which would result in non-propagated action potentials which would fail to reach the deep cerebellar nuclei. Taking into account the ability of the axon to propagate short bursts more efficiently than the sustained firing of action potentials, it becomes clear in Figure 6.4.C, that the altered temporal pattern of somatic action potentials after reaching supra-dendritic spike threshold input strength may serve a functional role. The fastest burst occurring during input below dendritic spike threshold reached

303 ± 26 Hz (n = 5), well below the axonal limit for short bursts. However, with stronger input, triggering dendritic spikes, the fastest bursts reached an instantaneous firing rate of 461 ± 36 Hz, a value comparable to the axonal propagation limit for short bursts (438 ± 37 Hz, (Monsivais et al., 2005). When BK channels were blocked, the fastest bursts reached frequencies of 669 ± 73 Hz (n = 3), resulting in the production of somatic action potentials which would never be relayed to the deep cerebellar nuclei.

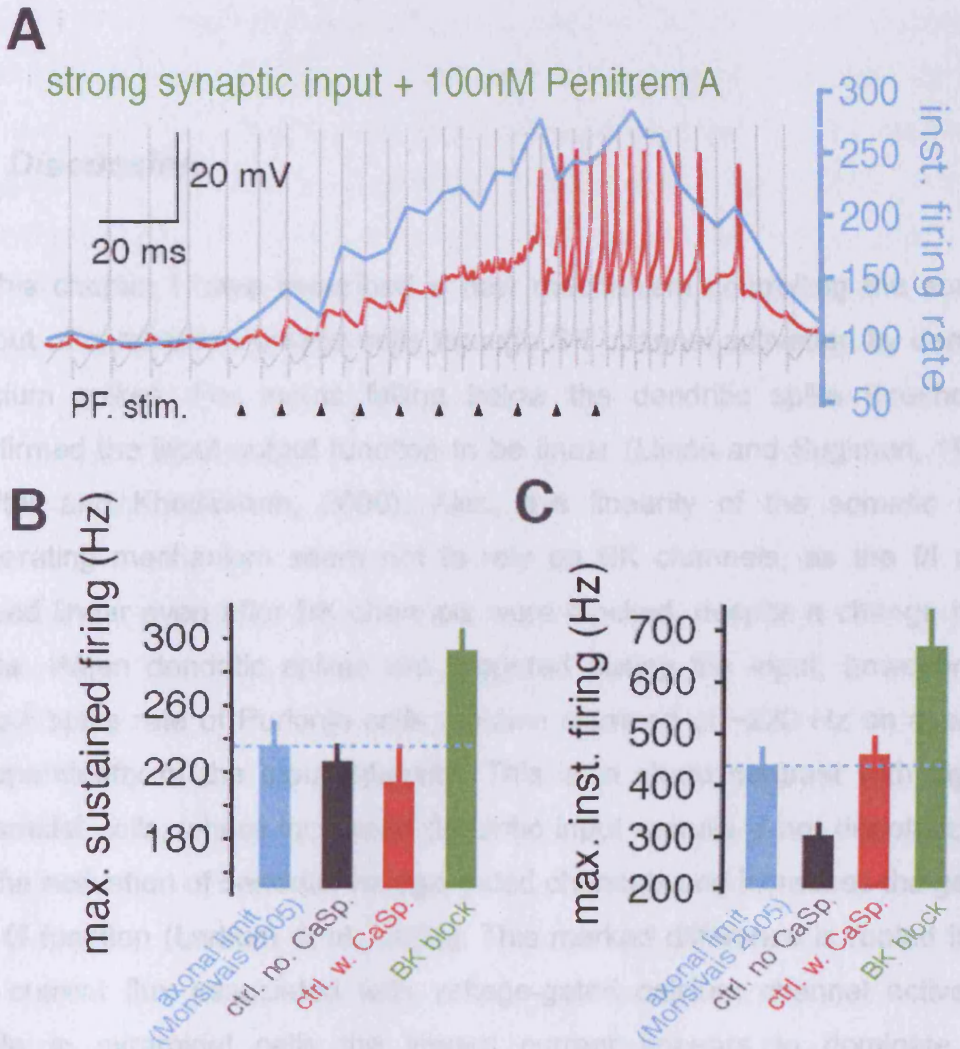

Figure 6.4 Dendritic spikes keep axonal output below the propagation limit.
A. Somatic (grey) and dendritic (red) voltage trace during synaptically triggered dendritic spikes. BK channels were blocked by 100 nM penitrem A. The instantaneous firing rate (blue) keeps increasing when the synaptic input is active despite the appearance of dendritic spikes. B. Pooled average of maximal sustained firing rates during synaptic-like current injections. C. Pooled average of the maximal instantaneous firing rates. Here again, the dendritic spike invoked and BK channel dependent dampening mechanism keeps the instantaneous firing rate below the axonal propagation limit.

6.3 Discussion

In this chapter I have described a new mechanism controlling the somatic output of cerebellar Purkinje cells through BK channel activation by dendritic calcium spikes. For inputs falling below the dendritic spike threshold, I confirmed the input-output function to be linear (Llinás and Sugimori, 1980b; Walter and Khodakhah, 2006). Also, this linearity of the somatic spike generating mechanism seem not to rely on BK channels, as the f/I curve stayed linear even after BK channels were blocked, despite a change in the slope. When dendritic spikes are triggered during the input, however, the output spike rate of Purkinje cells remains clamped at ~220 Hz on average, independently of the input intensity. This is in sharp contrast with layer 5 pyramidal cells, where increased dendritic input recruits a net depolarization by the activation of dendritic voltage-gated channels and increases the gain of the f/I function (Larkum et al., 2004). This marked difference is rooted in the net current flux associated with voltage-gated calcium channel activation. While in pyramidal cells the inward current appears to dominate, the subsequent activation of BK channels - and possibly other potassium channels (Martina et al., 2003; Khavandgar et al., 2005) - produces a net outward current in Purkinje cells (Raman and Bean, 1999) resulting in an inhibition of somatic AP firing. Future experiments are required to determine if this mechanism is unique to Purkinje cells or if is a more general feature, for example of spontaneously firing neurons.

A notable difference to *in vivo* conditions in these experiments is the lack of synaptic inhibition. $GABA_A$ receptor mediated neurotransmission was blocked to isolate the effect of excitatory drive (similar to Walter and Khodakhah, 2006). With inhibition intact, a feed-forward IPSP would normally follow every EPSP (Mittmann et al., 2005), decreasing the probability of a dendritic spike. However, as the paired-pulse facilitation of PF synapses (Dittman et al., 2000) heavily outweighs that of the interneuron synapses (Diana and Marty, 2003),

this effect should be decreased during a train. Also, the spatial distribution of feed-forward inhibition relative to excitation is not well understood (Santamaria et al., 2002) and could affect the size of functional dendritic subunits required to trigger a dendritic spike. As inhibition in itself can change the gain of neurons (Chance et al., 2002; Mitchell and Silver, 2003), it will be interesting to see how inhibition affects the f/I function of Purkinje cells below and above the dendritic spike threshold. Other possible modification of calcium and BK channels can also come from neuromodulators. *In vivo* studies using sensory activation of granule cells and consequent activation of interneurons are required to determine under what circumstances and how often this mechanism is called into action.

An extreme case of the involvement of dendritic spikes in regulating output is the so-called trimodal firing pattern described by Khodakhah and colleagues (Womack and Khodakhah, 2002a; Womack and Khodakhah, 2004), where spontaneous firing is terminated by a short burst of somatic spikes leading to a dendritic spike, resulting in a quiescent period. I do not consider this activity pattern to be a spontaneous, baseline physiological state of Purkinje cells (cf. Chapter 1.3.3). Nevertheless, exploring this phenomenon may lead us to a better understanding of what may be happening in severe cerebellar ataxias, where the calcium homeostasis or BK channel function are disturbed by genetic mutations, since overexcitable dendrites, for example caused by lack of BK channels (Sausbier et al., 2004) or mutations in P-type calcium channels (Walter et al., 2006) profoundly disrupts the function of Purkinje cells.

6.3.1 Functional considerations

Dendritic calcium spikes, when evoked by parallel fibre input as in this study, result in retrograde endocannabinoid signalling and in a reduction of the excitatory drive from parallel fibres (Chapter 4). This safety net activates in 1-2 seconds and lasts for a few tens of seconds, and thus it is fairly slow. It seems reasonable that if such a safety net exists, it should control Purkinje cell excitability on shorter timescales as well. The BK channel-dependent

clamping of somatic firing rate may serve exactly this function. Comparing the average firing rates where dendritic spikes appear and stop the further increase of output rate with the ability of Purkinje cell axons to transmit action potentials in a sustained fashion (Khaliq and Raman, 2005; Monsivais et al., 2005) shows a remarkable match (Figure 6.4.B). Similarly, the maximal firing rates in short burst associated with calcium spikes reach a maximum level comparable to the axonal transmission limit (Figure 6.4.C). However, when the BK channel dependent clamping is disabled by penitrem A, average and instantaneous somatic firing rates are able to rise well above the axonal transmission limit (Figure 6.4.BC).

Alternatively, it is possible that the mechanism enables two distinct coding regimes for Purkinje cell – deep cerebellar nuclei (DCN) information transfer. As the temporal firing pattern changes to doublets or short bursts of somatic APs followed by short quiescent periods during dendritic spiking, both the short-term dynamics of Purkinje cell synapses and excitability of DCN neurons are affected. This intriguing prediction requires further experimental testing. A recent study (Steuber et al., 2007) raised the possibility of information coding through pauses of Purkinje cell firing. As predicted by this modeling, BK channels would be ideal candidates for such a mechanism.

On a highly speculative note, one function of the mechanism described here may be in the regulation of cerebellar oscillations (Isope et al., 2002; Maex and De Schutter, 2005). Despite the lack of direct evidence for their existence under normal conditions *in vivo*, this mechanism could be a candidate to help Purkinje cells synchronize. A large population of Purkinje cells - firing at similar rates independently of minor fluctuations in their input –could be easily synchronized either by molecular layer interneurons or by recurrent inhibition through Purkinje axon collaterals (Watt et al., 2006).

7. GENERAL DISCUSSION

The basic structure of the cerebellar cortex is conserved from lower vertebrates to primates and humans. The first part of the cerebellum to evolve was, as it name suggests, the archicerebellum, comprising the flocculonodular node responsible for vestibular processing. Next was the medial zone, involved in adaptive control of somatic and autonomic reflexes and compound movements. As the cerebellum expanded laterally, the intermediate zones of the cerebellar hemispheres followed, which are responsible for fine-tuning voluntary movements in mammals. The lateral zones of the hemispheres are related to higher-order functions as they are reciprocally connected to the cerebral associative cortex. The most lateral regions are evolutionary the newest parts of the cerebellum and are likely to be related to cognitive functions like language and executive function (Gebhart et al., 2002; Exner et al., 2004). This phylogenetic developmental pattern shows up in the inputs and outputs of the cerebellar cortex as well, as the different regions receive afferent mossy fibres from different parts of the rest of the brain and Purkinje cells send their axons to different output nuclei (Voogd and Glickstein, 1998). Thus the cerebellum takes part in processing sensory input and shaping motor output, behaviour and cognition. The highly conserved structure and wiring (Figure 1.5) supports the assumption that the different parts process information in similar ways. In this work, I have presented data on dendritic spikes in Purkinje cells of the rat vermis and discussed their possible functional roles. I will now consider the relevance of these findings in a more general way by putting it into a systemic context, hopefully facilitating the formulation of future questions.

7.1 Purkinje cells in the cerebellar circuitry – beams and oscillations

This thesis has investigated the functional role of dendritic calcium spikes in cerebellar Purkinje cells. One key question, and a complex one, is to understand under what conditions in the behaving animal do dendritic spikes occur in Purkinje cells. The powerful climbing fibre excitation is known to produce global dendritic spikes in Purkinje cell dendrites both *in vitro* and *in vivo* (Eccles et al., 1964; Schmolesky et al., 2002; Loewenstein et al., 2005a). In the work presented in this thesis however, I have focused on local dendritic spikes triggered by parallel fibre input. Most of the studies on dendritic spikes were done *in vitro*, despite the very first description of dendritic spikes came from *in vivo* studies of the alligator cerebellum (Llinás et al., 1968; Llinás and Nicholson, 1971). They showed that stimulating the superficial layers of the cerebellar cortex evokes synchronous activity in a beam of parallel fibres and subsequently excites a beam of Purkinje cells. The beam hypothesis, as a key organizational principle and computational unit of the cerebellar cortex, was established in the now classic book, "The Cerebellum as a Neuronal Machine" by Eccles, Ito and Szentágothai (1967), a seminal work pioneering a scientific approach to the cerebellum, refreshingly modern in its time. The structure and wiring of the cerebellar cortex clearly supports the beam hypothesis but experimental demonstrations remain contradictory or indirect. The work of James Bower showed strong vertical organization in the activity of the cortex following somato-sensory rather than direct electrical stimulation in rats. The short-latency activation of Purkinje-cells followed the increased activity in the immediately underlying granule cell layer with millisecond delay (Bower and Woolston, 1983). However, Purkinje cells along the parallel fibres were not activated while inhibitory receptive fields of Purkinje cells were much bigger than the excitatory receptive fields. These results question whether beams occur *in vivo* and whether they could serve as an underlying mechanism for the generation of dendritic spikes. However, more recent evidence from intrinsic imaging, which reflects metabolic activity, as well as calcium imaging shows activity along the parallel fibre beams (Coutinho et al., 2004; Diez-

Garcia et al., 2005; Reinert et al., 2007), thus parallel fibres are faithfully relaying granule cell firing. The lack of electrical activation of Purkinje cells along the parallel fibre beam is possibly due to feed-forward inhibition (Mittmann et al., 2005), a notion supported by the appearance of beams of activated Purkinje cells following the blockade of $GABA_A$ receptors (Santamaria et al., 2007). It is an intriguing possibility, that under 'baseline' conditions *in vivo* the net effects of parallel fibres are to relay ionotropic inhibition through feed-forward shunting inhibition and mostly metabotropic excitation through mGluR1 receptor activation (Batchelor and Garthwaite, 1997) to Purkinje cells. Taking this idea further, feed-forward inhibition in the cerebellar cortex could be scaled by neuromodulators (McElligott et al., 1986; Kondo and Marty, 1998a; Pompeiano, 2006) or by climbing fibre activity (Ebner and Bloedel, 1984), gating the ionotropic excitation by parallel fibres of Purkinje cells. A similar type of activity scaling by neuromodulators is known in the granule cell layer, where serotoninergic regulation of Lugaro cells potentially synchronises Golgi-cell activity (Dieudonne, 2001). The overall activity of the cerebellar cortex thus is set by the balance of excitation and feed-forward inhibition and by the excitability of the different cell types. As the homeostasis and plasticity of synaptic transmission and excitability are reciprocally interlinked, it is easy to conceive that shifting this balance only slightly can result in strong activation of Purkinje cells. Endocannabinoids for example could link short-term (Chapter 4) and long-term synaptic plasticity (Chapter 5) to local excitability by acting on BK channels (Sade et al., 2006) of Purkinje cell dendritic branches. In a highly active cerebellar cortex, dendritic spikes could thus easily steal the show by regulating the input (Chapters 4 and 5) and output (Chapter 6) of Purkinje cells.

It is noteworthy to remember here the controversy surrounding oscillatory activity in the cerebellum (Isope et al., 2002), a potential mechanism underlying dendritic spike generation in Purkinje cells. One of the first ever measurements of cerebellar activity (Adrian, 1935) reported high frequency (150-250 Hz) electrical activity measured in an identical way to cortical activity. Oscillations in other brain areas went on to become well-recognized in their proposed role in temporal binding in sensory cortical areas (Engel et

al., 2001; Engel and Singer, 2001), path integration and memory formation in the hippocampus (Buzsáki, 2005) and sensory stimulus discrimination in the olfactory bulb (Schaefer et al., 2006), to name a few. The cerebellar field, however, was not involved in these developments, because the evidence for cerebellar oscillations is scarce and indirect. Correlated firing of Purkinje cells (Bell and Grimm, 1969; Ebner and Bloedel, 1981; but see Jaeger, 2003 who did not find such correlations in anaesthetised rats) could be explained by both a common input by a beam of parallel fibres (let it be either excitatory or inhibitory, resetting the firing phase) or by synchronization through network oscillation. Network oscillation would not exclude the possibility of parallel fibre beams, as the input layer of cortex is equipped with the necessary circuit elements to produce oscillations in the granule cell layer and provide synchronized input to Purkinje cells. The Lugaro-cell - Golgi cell system as well as feedback inhibition through parallel fibre excitation of Golgi cells could underlie the low frequency (8 Hz) oscillation measured by Hartmann and Bower (Hartmann and Bower, 1998) in the granule cell layer. This relatively slow oscillation however probably reflects a system-wide cerebello-olivary rhythm (Welsh et al., 1995). A recent study from awake, behaving monkeys supports the role of cerebro-cerebellar communications in modulating cerebellar field-potential oscillations in the 10-25 Hz regime (Courtemanche and Lamarre, 2005). A better candidate for the substrate of high-frequency oscillations is the possible synchronization of molecular layer interneurons through reciprocal synaptic connections (Kondo and Marty, 1998b) or through electrical coupling (Mann-Metzer and Yarom, 1999, 2000). Using these reciprocal connections, a modelling study (Maex and De Schutter, 2005) produced 10-50 Hz oscillations in the granule cell layer and 100-250 Hz oscillations in the molecular layer based on synaptic delay and kinetics (Maex and De Schutter, 2003).

Thus there is considerable evidence, that activity in the cerebellum can reach a much higher spatio-temporal synchrony (possibly under challenging situations, like during a startle response, Frings et al., 2006). An analogy would be the hippocampus, where feed-forward and feedback inhibition has an established role in network oscillations (Penttonen et al., 1998; Whittington

et al., 2000; Somogyi and Klausberger, 2005). Interestingly, hippocampal sharp waves or spindles, a highly synchronized oscillatory activity in the region of 200 Hz, are known to trigger dendritic spikes in CA1 pyramidal cells *in vivo* (Kamondi et al., 1998).

In terms of future directions, first it is essential to establish the conditions under which dendritic spikes occur in Purkinje cells in the behaving animal. Second, the role of endocannabinoids in determining the activity-dependent balance of excitation and inhibition and in altering the intrinsic excitability of Purkinje cells by modulating BK and other channels provides a particularly promising direction. Third, by targeted pharmacological or genetical modulation of dendritic spike properties much will be learnt about their role in cerebellum-dependent functions. Finally, by teasing out the molecular and cellular processes underlying cerebellar function it will become possible to cure or ameliorate pathological conditions by ways of causal treatment.

7.2 Epilogue

The ultimate goal of neuroscience is to understand how the brain works. By 'work' I mean the way the brain processes sensory input and produces motor output. Naturally, this also involves everything that happens between input and output: forming models of the world through learning and planning actions and making decisions using these models. To understand the most complex organ of mammals, all organizational levels need to be studied from molecules, through cells to brain regions and the behaviour of the animal as a whole. Different disciplines, however, use not only different experimental approaches but theoretical frameworks as well, making the synthesis of this knowledge especially difficult. Despite these communicational barriers, I believe all behaviour can be understood based on the brain's input, output and what happens in-between. This idea was already conceived by Valentino Braitenberg in the form of the Braitenberg vehicles (Braitenberg, 1984) and recent evidence showing the evolution of 'character' in computer programs using neural network based adaptations of learning agents (like bluffing poker 'bots': Hurwitz and Marwale, 2007) substantiates this view. Computational and robotics analogues can be quite revealing, but don't necessarily bring us closer to finding out how the brain works. Neuroscience research is becoming more integrative and an important task for the future is to relate the findings from reduced model systems to the behaving animal. I would like to finish this thesis by a quote from Valentino Braitenberg (noted by James Bower in *Ann N.Y, Acad. Sci.* **978**: 184-187):

"[...] We must admit we have all been beaten, [...] our pet ideas have been taken apart by people who have made beautiful experiments, and we learned something in the process. So, I think we should go back to the essentials, to build up some model of the cerebellum, [...] Why, even a child looking at the cerebellum can tell it is different from the cerebral cortex, macroscopically. But we don't know why. I am fanatically convinced, however, that the cerebellum's structure can be explained and must be explained... perhaps by thinking some more, and going back to basics, we can arrive to a beautiful synthesis."

Now back to work.

References

Abbott LF, Nelson SB (2000) Synaptic plasticity: taming the beast. Nature Neuroscience 3:1178-1183.

Adrian ED (1935) Discharge frequencies in the cerebral and cerebellar cortex. J Physiol 83:33.

Akaike N (1996) Gramicidin perforated patch recording and intracellular chloride activity in excitable cells. Prog Biophys Mol Biol 65:251-264.

Albus J (1971) A theory of cerebellar function. Math Biosci 28:167-171.

Amitai Y, Friedman A, Connors BW, Gutnick MJ (1993) Regenerative activity in apical dendrites of pyramidal cells in neocortex. Cereb Cortex 3:26-38.

Archie KA, Mel BW (2000) A model for intradendritic computation of binocular disparity. Nat Neurosci 3:54-63.

Ariav G, Polsky A, Schiller J (2003) Submillisecond precision of the input-output transformation function mediated by fast sodium dendritic spikes in basal dendrites of CA1 pyramidal neurons. J Neurosci 23:7750-7758.

Auger C, Attwell D (2000) Fast removal of synaptic glutamate by postsynaptic transporters. Neuron 28:547-558.

Batchelor AM, Garthwaite J (1997) Frequency detection and temporally dispersed synaptic signal association through a metabotropic glutamate receptor pathway. Nature 385:74-77.

Baude A, Nusser Z, Roberts JD, Mulvihill E, McIlhinney RA, Somogyi P (1993) The metabotropic glutamate receptor (mGluR1 alpha) is concentrated at perisynaptic membrane of neuronal subpopulations as detected by immunogold reaction. Neuron 11:771-787.

Beierlein M, Regehr WG (2006) Local interneurons regulate synaptic strength by retrograde release of endocannabinoids. J Neurosci 26:9935-9943.

Bekkers JM, Häusser M (2007) Targeted dendrotomy reveals active and passive contributions of the dendritic tree to synaptic integration and neuronal output. Proc Natl Acad Sci U S A in press.

Bell CC, Grimm RJ (1969) Discharge properties of Purkinje cells recorded on single and double microelectrodes. J Neurophysiol 32:1044-1055.

Bienenstock EL, Cooper LN, Munro PW (1982) Theory for the development of neuron selectivity: orientation specificity and binocular interaction in visual cortex. Journal of Neuroscience 2:32-48.

Bliss TV, Lømo T (1970) Plasticity in a monosynaptic cortical pathway. J Physiol 207:61P.

Bower JM, Woolston DC (1983) Congruence of spatial organization of tactile projections to granule cell and Purkinje cell layers of cerebellar hemispheres of the albino rat: vertical organization of cerebellar cortex. J Neurophysiol 49:745-766.

Bower JM, Beeman D (1994) The book of GENESIS: exploring realistic neural models with the GEneral NEural SImulation System. New York: Springer.

Boxall AR, Garthwaite J (1996) Long-term depression in rat cerebellum requires both NO synthase and NO-sensitive guanylyl cyclase. Eur J Neurosci 8:2209-2212.

Boxall AR, Lancaster B, Garthwaite J (1996) Tyrosine kinase is required for long-term depression in the cerebellum. Neuron 16:805-813.

Boyden ES, Raymond JL (2003) Active reversal of motor memories reveals rules governing memory encoding. Neuron 39:1031-1042.

Boyden ES, Katoh A, Raymond JL (2004) Cerebellum-dependent learning: the role of multiple plasticity mechanisms. Annu Rev Neurosci 27:581-609.

Braitenberg V (1984) Vehicles, experiments in synthetic psychology: MIT Press.

Brasnjo G, Otis TS (2004) Isolation of glutamate transport-coupled charge flux and estimation of glutamate uptake at the climbing fiber-Purkinje cell synapse. Proc Natl Acad Sci U S A 101:6273-6278.

Brenowitz SD, Regehr WG (2003) Calcium dependence of retrograde inhibition by endocannabinoids at synapses onto Purkinje cells. J Neurosci 23:6373-6384.

Brenowitz SD, Regehr WG (2005) Associative short-term synaptic plasticity mediated by endocannabinoids. Neuron 45:419-431.

Brown SP, Brenowitz SD, Regehr WG (2003) Brief presynaptic bursts evoke synapse-specific retrograde inhibition mediated by endogenous cannabinoids. Nat Neurosci 6:1048-1057.

Brown SP, Safo PK, Regehr WG (2004) Endocannabinoids inhibit transmission at granule cell to Purkinje cell synapses by modulating three types of presynaptic calcium channels. J Neurosci 24:5623-5631.

Buzsáki G (2005) Theta rhythm of navigation: link between path integration and landmark navigation, episodic and semantic memory. Hippocampus 15:827-840.

Cai X, Liang CW, Muralidharan S, Kao JP, Tang CM, Thompson SM (2004) Unique roles of SK and Kv4.2 potassium channels in dendritic integration. Neuron 44:351-364.

Casado M, Dieudonne S, Ascher P (2000) Presynaptic N-methyl-D-aspartate receptors at the parallel fiber-Purkinje cell synapse. Proc Natl Acad Sci U S A 97:11593-11597.

Casado M, Isope P, Ascher P (2002) Involvement of presynaptic N-methyl-D-aspartate receptors in cerebellar long-term depression. Neuron 33:123-130.

Cerminara NL, Rawson JA (2004) Evidence that climbing fibers control an intrinsic spike generator in cerebellar Purkinje cells. J Neurosci 24:4510-4517.

Chadderton P, Margrie TW, Häusser M (2004) Integration of quanta in cerebellar granule cells during sensory processing. Nature 428:856-860.

Chance FS, Abbott LF, Reyes AD (2002) Gain modulation from background synaptic input. Neuron 35:773-782.

Chen WR, Midtgaard J, Shepherd GM (1997) Forward and backward propagation of dendritic impulses and their synaptic control in mitral cells. Science 278:463-467.

Chevaleyre V, Castillo PE (2004) Endocannabinoid-mediated metaplasticity in the hippocampus. Neuron 43:871-881.

Christensen SR (2002) Synaptic integration and dendritic excitability in cerebellar Purkinje neurons. In: Department of Physioogy. London: University College London.

Cingolani LA, Gymnopoulos M, Boccaccio A, Stocker M, Pedarzani P (2002) Developmental regulation of small-conductance Ca2+-activated K+ channel expression and function in rat Purkinje neurons. J Neurosci 22:4456-4467.

Clark BA, Monsivais P, Branco T, London M, Häusser M (2005) The site of action potential initiation in cerebellar Purkinje neurons. Nat Neurosci 8:137-139.

Clarke AL, Petrou S, Walsh JV, Jr., Singer JJ (2002) Modulation of BK(Ca) channel activity by fatty acids: structural requirements and mechanism of action. Am J Physiol Cell Physiol 283:C1441-1453.

Coesmans M, Weber JT, De Zeeuw CI, Hansel C (2004) Bidirectional parallel fiber plasticity in the cerebellum under climbing fiber control. Neuron 44:691-700.

Connors BW, Gutnick MJ (1990) Intrinsic firing patterns of diverse neocortical neurons. Trends Neurosci 13:99-104.

Courtemanche R, Lamarre Y (2005) Local field potential oscillations in primate cerebellar cortex: synchronization with cerebral cortex during active and passive expectancy. J Neurophysiol 93:2039-2052.

Coutinho V, Mutoh H, Knöpfel T (2004) Functional topology of the mossy fibre-granule cell--Purkinje cell system revealed by imaging of intrinsic fluorescence in mouse cerebellum. Eur J Neurosci 20:740-748.

Crochet S, Fuentealba P, Timofeev I, Steriade M (2004) Selective amplification of neocortical neuronal output by fast prepotentials in vivo. Cereb Cortex 14:1110-1121.

Dan Y, Poo MM (2004) Spike timing-dependent plasticity of neural circuits. Neuron 44:23-30.

Dan Y, Poo MM (2006) Spike timing-dependent plasticity: from synapse to perception. Physiol Rev 86:1033-1048.

Daniel H, Levenes C, Crepel F (1998) Cellular mechanisms of cerebellar LTD. Trends Neurosci 21:401-407.

Davie JT, Kole MH, Letzkus JJ, Rancz EA, Spruston N, Stuart GJ, Häusser M (2006) Dendritic patch-clamp recording. Nat Protoc 1:1235-1247.

Delaney AJ, Jahr CE (2002) Kainate receptors differentially regulate release at two parallel fiber synapses. Neuron 36:475-482.

Denk W, Strickler JH, Webb WW (1990) Two-photon laser scanning fluorescence microscopy. Science 248:73-76.

Diana MA, Marty A (2003) Characterization of depolarization-induced suppression of inhibition using paired interneuron--Purkinje cell recordings. J Neurosci 23:5906-5918.

Dieudonne S (2001) Serotonergic neuromodulation in the cerebellar cortex: cellular, synaptic, and molecular basis. Neuroscientist 7:207-219.

Diez-Garcia J, Matsushita S, Mutoh H, Nakai J, Ohkura M, Yokoyama J, Dimitrov D, Knöpfel T (2005) Activation of cerebellar parallel fibers monitored in transgenic mice expressing a fluorescent Ca2+ indicator protein. Eur J Neurosci 22:627-635.

Dittman JS, Kreitzer AC, Regehr WG (2000) Interplay between facilitation, depression, and residual calcium at three presynaptic terminals. J Neurosci 20:1374-1385.

Duguid I, Sjöström PJ (2006) Novel presynaptic mechanisms for coincidence detection in synaptic plasticity. Curr Opin Neurobiol 16:312-322.

Duguid IC, Smart TG (2004) Retrograde activation of presynaptic NMDA receptors enhances GABA release at cerebellar interneuron-Purkinje cell synapses. NatNeurosci 7:525-533.

Ebner TJ, Bloedel JR (1981) Correlation between activity of Purkinje cells and its modification by natural peripheral stimuli. J Neurophysiol 45:948-961.

Ebner TJ, Bloedel JR (1984) Climbing fiber action on the responsiveness of Purkinje cells to parallel fiber inputs. Brain Res 309:182-186.

Eccles J, Llinas R, Sasaki K (1964) Excitation of Cerebellar Purkinje Cells by the Climbing Fibres. Nature 203:245-246.

Eccles JC, Ito M, Szentágothai J (1967) The Cerebellum as a Neuronal Machine: Springer-Verlag.

Edgerton JR, Reinhart PH (2003) Distinct contributions of small and large conductance Ca2+-activated K+ channels to rat Purkinje neuron function. J Physiol 548:53-69.

Endo S, Suzuki M, Sumi M, Nairn AC, Morita R, Yamakawa K, Greengard P, Ito M (1999) Molecular identification of human G-substrate, a possible downstream component of the cGMP-dependent protein kinase cascade in cerebellar Purkinje cells. Proc Natl Acad Sci U S A 96:2467-2472.

Engel AK, Singer W (2001) Temporal binding and the neural correlates of sensory awareness. Trends Cogn Sci 5:16-25.

Engel AK, Fries P, Singer W (2001) Dynamic predictions: oscillations and synchrony in top-down processing. Nat Rev Neurosci 2:704-716.

Engel J, Schultens HA, Schild D (1999) Small conductance potassium channels cause an activity-dependent spike frequency adaptation and make the transfer function of neurons logarithmic. Biophys J 76:1310-1319.

Ermentrout B (1998) Linearization of F-I curves by adaptation. Neural Comput 10:1721-1729.

Etzion Y, Grossman Y (1998) Potassium currents modulation of calcium spike firing in dendrites of cerebellar Purkinje cells. Exp Brain Res 122:283-294.

Exner C, Weniger G, Irle E (2004) Cerebellar lesions in the PICA but not SCA territory impair cognition. Neurology 63:2132-2135.

Fetz EE, Gustafsson B (1983) Relation between shapes of post-synaptic potentials and changes in firing probability of cat motoneurones. J Physiol 341:387-410.

Fierro L, Llano I (1996) High endogenous calcium buffering in Purkinje cells from rat cerebellar slices. J Physiol 496 (Pt 3):617-625.

Fisyunov A, Tsintsadze V, Min R, Burnashev N, Lozovaya N (2006) Cannabinoids modulate the P-type high-voltage-activated calcium currents in purkinje neurons. J Neurophysiol 96:1267-1277.

Freund TF, Katona I, Piomelli D (2003) Role of endogenous cannabinoids in synaptic signaling. Physiol Rev 83:1017-1066.

Frick A, Johnston D (2005) Plasticity of dendritic excitability. J Neurobiol 64:100-115.

Frick A, Magee J, Johnston D (2004) LTP is accompanied by an enhanced local excitability of pyramidal neuron dendrites. Nat Neurosci 7:126-135.

Frings M, Awad N, Jentzen W, Dimitrova A, Kolb FP, Diener HC, Timmann D, Maschke M (2006) Involvement of the human cerebellum in short-term and long-term habituation of the acoustic startle response: a serial PET study. Clin Neurophysiol 117:1290-1300.

Gao W, Dunbar RL, Chen G, Reinert KC, Oberdick J, Ebner TJ (2003) Optical imaging of long-term depression in the mouse cerebellar cortex in vivo. J Neurosci 23:1859-1866.

Garthwaite J, Charles SL, Chess-Williams R (1988) Endothelium-derived relaxing factor release on activation of NMDA receptors suggests role as intercellular messenger in the brain. Nature 336:385-388.

Gasparini S, Magee JC (2002) Phosphorylation-dependent differences in the activation properties of distal and proximal dendritic Na+ channels in rat CA1 hippocampal neurons. J Physiol 541:665-672.

Gasparini S, Magee JC (2006) State-dependent dendritic computation in hippocampal CA1 pyramidal neurons. J Neurosci 26:2088-2100.

Gasparini S, Migliore M, Magee JC (2004) On the initiation and propagation of dendritic spikes in CA1 pyramidal neurons. J Neurosci 24:11046-11056.

Gatley SJ, Gifford AN, Volkow ND, Lan R, Makriyannis A (1996) 123I-labeled AM251: a radioiodinated ligand which binds in vivo to mouse brain cannabinoid CB1 receptors. Eur J Pharmacol 307:331-338.

Gebhart AL, Petersen SE, Thach WT (2002) Role of the posterolateral cerebellum in language. Ann N Y Acad Sci 978:318-333.

Goldberg J, Holthoff K, Yuste R (2002) A problem with Hebb and local spikes. Trends Neurosci 25:433.

Goldberg JH, Yuste R (2005) Space matters: local and global dendritic Ca^{2+} compartmentalization in cortical interneurons. Trends Neurosci 28:158-167.

Goldberg JH, Tamas G, Yuste R (2003a) Ca^{2+} imaging of mouse neocortical interneurone dendrites: Ia-type K^{+} channels control action potential backpropagation. J Physiol 551:49-65.

Goldberg JH, Tamas G, Aronov D, Yuste R (2003b) Calcium microdomains in aspiny dendrites. Neuron 40:807-821.

Golding NL, Spruston N (1998) Dendritic sodium spikes are variable triggers of axonal action potentials in hippocampal CA1 pyramidal neurons. Neuron 21:1189-1200.

Golding NL, Staff NP, Spruston N (2002) Dendritic spikes as a mechanism for cooperative long-term potentiation. Nature 418:326-331.

Golding NL, Jung HY, Mickus T, Spruston N (1999) Dendritic calcium spike initiation and repolarization are controlled by distinct potassium channel subtypes in CA1 pyramidal neurons. J Neurosci 19:8789-8798.

Guan S, Ma S, Zhu Y, Wang J (2006) The postnatal development of refractory periods and threshold potentials at cerebellar Purkinje neurons. Brain Res 1097:59-64.

Gundappa-Sulur G, De Schutter E, Bower JM (1999) Ascending granule cell axon: an important component of cerebellar cortical circuitry. J Comp Neurol 408:580-596.

Gutkin BS, Ermentrout GB, Reyes AD (2005) Phase-response curves give the responses of neurons to transient inputs. J Neurophysiol 94:1623-1635.

Hájos N, Mann E, Freund TF, Paulsen O (2004) Increased oxygen supply enables cholinergically-induced network oscillations in submerged hippocampal slices. In: FENS Abstr. 2, A009.13.

Hamill OP, Marty A, Neher E, Sakmann B, Sigworth FJ (1981) Improved patch-clamp techniques for high-resolution current recording from cells and cell-free membrane patches. Pflugers Arch 391:85-100.

Hartell NA (1996) Strong activation of parallel fibers produces localized calcium transients and a form of LTD that spreads to distant synapses. Neuron 16:601-610.

Hartmann MJ, Bower JM (1998) Oscillatory activity in the cerebellar hemispheres of unrestrained rats. J Neurophysiol 80:1598-1604.

Hashimotodani Y, Ohno-Shosaku T, Tsubokawa H, Ogata H, Emoto K, Maejima T, Araishi K, Shin HS, Kano M (2005) Phospholipase Cbeta serves as a coincidence detector through its Ca2+ dependency for triggering retrograde endocannabinoid signal. Neuron 45:257-268.

Häusser M, Clark BA (1997) Tonic synaptic inhibition modulates neuronal output pattern and spatiotemporal synaptic integration. Neuron 19:665-678.

Häusser M, Roth A (1997) Dendritic and somatic glutamate receptor channels in rat cerebellar Purkinje cells. J Physiol 501 (Pt 1):77-95.

Häusser M, Mel B (2003) Dendrites: bug or feature? Curr Opin Neurobiol 13:372-383.

Häusser M, Spruston N, Stuart GJ (2000) Diversity and dynamics of dendritic signaling. Science 290:739-744.

Hebb DO (1949) The organization of behavior. In. New York: Wiley.

Heckman CJ, Lee RH, Brownstone RM (2003) Hyperexcitable dendrites in motoneurons and their neuromodulatory control during motor behavior. Trends Neurosci 26:688-695.

Helmchen F, Svoboda K, Denk W, Tank DW (1999) In vivo dendritic calcium dynamics in deep-layer cortical pyramidal neurons. Nature Neuroscience 2:989-996.

Hines ML, Carnevale NT (1997) The NEURON simulation environment. Neural Comput 9:1179-1209.

Holthoff K, Kovalchuk Y, Konnerth A (2006) Dendritic spikes and activity-dependent synaptic plasticity. Cell Tissue Res 326:369-377.

Holthoff K, Kovalchuk Y, Yuste R, Konnerth A (2004) Single-shock LTD by local dendritic spikes in pyramidal neurons of mouse visual cortex. J Physiol 560:27-36.

Hopper RA, Garthwaite J (2006) Tonic and phasic nitric oxide signals in hippocampal long-term potentiation. J Neurosci 26:11513-11521.

Hurwitz E, Marwale T (2007) Learning to Bluff. In: http://www.arxiv.org/abs/0705.0693.

Isope P, Barbour B (2002) Properties of unitary granule cell-->Purkinje cell synapses in adult rat cerebellar slices. J Neurosci 22:9668-9678.

Isope P, Dieudonne S, Barbour B (2002) Temporal organization of activity in the cerebellar cortex: a manifesto for synchrony. Ann N Y Acad Sci 978:164-174.

Ito M (2002) The molecular organization of cerebellar long-term depression. Nat Rev Neurosci 3:896-902.

Ito M, Kano M (1982) Long-lasting depression of parallel fiber-Purkinje cell transmission induced by conjunctive stimulation of parallel fibers and climbing fibers in the cerebellar cortex. NeurosciLett 33:253-258.

Izhikevich EM (2007) Dynamical Systems in Neuroscience: The Geometry of Excitability and Bursting. In, pp 443-505. Cambridge, MA: MIT Press.

Jacoby S, Sims RE, Hartell NA (2001) Nitric oxide is required for the induction and heterosynaptic spread of long-term potentiation in rat cerebellar slices. J Physiol 535:825-839.

Jaeger D (2003) No parallel fiber volleys in the cerebellar cortex: evidence from cross-correlation analysis between Purkinje cells in a computer model and in recordings from anesthetized rats. J Comput Neurosci 14:311-327.

Jaffe DB, Carnevale NT (1999) Passive normalization of synaptic integration influenced by dendritic architecture. J Neurophysiol 82:3268-3285.

Jarsky T, Roxin A, Kath WL, Spruston N (2005) Conditional dendritic spike propagation following distal synaptic activation of hippocampal CA1 pyramidal neurons. Nat Neurosci 8:1667-1676.

Kamondi A, Acsády L, Buzsáki G (1998) Dendritic spikes are enhanced by cooperative network activity in the intact hippocampus. Journal of Neuroscience 18:3919-3928.

Kampa BM, Letzkus JJ, Stuart GJ (2006) Requirement of dendritic calcium spikes for induction of spike-timing-dependent synaptic plasticity. J Physiol 574:283-290.

Kerr JN, Greenberg D, Helmchen F (2005) Imaging input and output of neocortical networks in vivo. Proc Natl Acad Sci U S A 102:14063-14068.

Khaliq ZM, Raman IM (2005) Axonal propagation of simple and complex spikes in cerebellar Purkinje neurons. J Neurosci 25:454-463.

Khavandgar S, Walter JT, Sageser K, Khodakhah K (2005) Kv1 channels selectively prevent dendritic hyperexcitability in rat Purkinje cells. J Physiol 569:545-557.

Kishimoto Y, Kano M (2006) Endogenous cannabinoid signaling through the CB1 receptor is essential for cerebellum-dependent discrete motor learning. J Neurosci 26:8829-8837.

Knaus HG, Schwarzer C, Koch RO, Eberhart A, Kaczorowski GJ, Glossmann H, Wunder F, Pongs O, Garcia ML, Sperk G (1996) Distribution of high-conductance Ca(2+)-activated K+ channels in rat brain: targeting to axons and nerve terminals. J Neurosci 16:955-963.

Knaus HG, McManus OB, Lee SH, Schmalhofer WA, Garcia-Calvo M, Helms LM, Sanchez M, Giangiacomo K, Reuben JP, Smith AB, 3rd, et al. (1994) Tremorgenic indole alkaloids potently inhibit smooth muscle high-conductance calcium-activated potassium channels. Biochemistry 33:5819-5828.

Knöpfel T, Grandes P (2002) Metabotropic glutamate receptors in the cerebellum with a focus on their function in Purkinje cells. Cerebellum 1:19-26.

Koekkoek SK, Hulscher HC, Dortland BR, Hensbroek RA, Elgersma Y, Ruigrok TJ, De Zeeuw CI (2003) Cerebellar LTD and learning-dependent timing of conditioned eyelid responses. Science 301:1736-1739.

Kondo S, Marty A (1998a) Differential effects of noradrenaline on evoked, spontaneous and miniature IPSCs in rat cerebellar stellate cells. J Physiol 509 (Pt 1):233-243.

Kondo S, Marty A (1998b) Synaptic currents at individual connections among stellate cells in rat cerebellar slices. J Physiol 509 (Pt 1):221-232.

Konnerth A, Dreessen J, Augustine GJ (1992) Brief dendritic calcium signals initiate long-lasting synaptic depression in cerebellar Purkinje cells. Proc Natl Acad Sci U S A 89:7051-7055.

Kreitzer AC, Regehr WG (2001) Retrograde inhibition of presynaptic calcium influx by endogenous cannabinoids at excitatory synapses onto Purkinje cells. Neuron 29:717-727.

Kreitzer AC, Malenka RC (2007) Endocannabinoid-mediated rescue of striatal LTD and motor deficits in Parkinson's disease models. Nature 445:643-647.

Lang EJ, Sugihara I, Welsh JP, Llinás R (1999) Patterns of spontaneous purkinje cell complex spike activity in the awake rat. J Neurosci 19:2728-2739.

Larkum ME, Zhu JJ (2002) Signaling of layer 1 and whisker-evoked Ca^{2+} and Na^{+} action potentials in distal and terminal dendrites of rat neocortical pyramidal neurons in vitro and in vivo. J Neurosci 22:6991-7005.

Larkum ME, Zhu JJ, Sakmann B (1999a) A new cellular mechanism for coupling inputs arriving at different cortical layers. Nature 398:338-341.

Larkum ME, Kaiser KMM, Sakmann B (1999b) Calcium electrogenesis in distal apical dendrites of layer 5 pyramidal cells at a critical frequency of back-propagating action potentials. Proc Natl Acad Sci U S A 96:14600-14604.

Larkum ME, Zhu JJ, Sakmann B (2001) Dendritic mechanisms underlying the coupling of the dendritic with the axonal action potential initiation zone of adult rat layer 5 pyramidal neurons. J Physiol 533:447-466.

Larkum ME, Senn W, Lüscher HR (2004) Top-down dendritic input increases the gain of layer 5 pyramidal neurons. Cereb Cortex 14:1059-1070.

Launey T, Endo S, Sakai R, Harano J, Ito M (2004) Protein phosphatase 2A inhibition induces cerebellar long-term depression and declustering of synaptic AMPA receptor. Proc Natl Acad Sci U S A 101:676-681.

Ledent C, Valverde O, Cossu G, Petitet F, Aubert JF, Beslot F, Bohme GA, Imperato A, Pedrazzini T, Roques BP, Vassart G, Fratta W, Parmentier M (1999) Unresponsiveness to cannabinoids and reduced addictive effects of opiates in CB1 receptor knockout mice. Science 283:401-404.

Leitges M, Kovac J, Plomann M, Linden DJ (2004) A unique PDZ ligand in PKCalpha confers induction of cerebellar long-term synaptic depression. Neuron 44:585-594.

Lev-Ram V, Wong ST, Storm DR, Tsien RY (2002) A new form of cerebellar long-term potentiation is postsynaptic and depends on nitric oxide but not cAMP. Proc Natl Acad Sci U S A 99:8389-8393.

Lev-Ram V, Mehta SB, Kleinfeld D, Tsien RY (2003) Reversing cerebellar long-term depression. Proc Natl Acad Sci U S A 100:15989-15993.

Lev-Ram V, Makings LR, Keitz PF, Kao JP, Tsien RY (1995) Long-term depression in cerebellar Purkinje neurons results from coincidence of nitric oxide and depolarization-induced Ca2+ transients. Neuron 15:407-415.

Lev-Ram V, Nebyelul Z, Ellisman MH, Huang PL, Tsien RY (1997a) Absence of cerebellar long-term depression in mice lacking neuronal nitric oxide synthase. Learn Mem 4:169-177.

Lev-Ram V, Jiang T, Wood J, Lawrence DS, Tsien RY (1997b) Synergies and coincidence requirements between NO, cGMP, and Ca2+ in the induction of cerebellar long-term depression. Neuron 18:1025-1038.

Levenes C, Daniel H, Soubrie P, Crepel F (1998) Cannabinoids decrease excitatory synaptic transmission and impair long-term depression in rat cerebellar Purkinje cells. J Physiol 510 (Pt 3):867-879.

Li C, Lu J, Wu C, Duan S, Poo M (2004) Bidirectional modification of presynaptic neuronal excitability accompanying spike timing-dependent synaptic plasticity. Neuron 41:257-268.

Li SJ, Wang Y, Strahlendorf HK, Strahlendorf JC (1993) Serotonin alters an inwardly rectifying current (I_h) in rat cerebellar Purkinje cells under voltage clamp. Brain Res 617:87-95.

Linden DJ, Connor JA (1991) Participation of postsynaptic PKC in cerebellar long-term depression in culture. Science 254:1656-1659.

Linden DJ, Ahn S (1999) Activation of presynaptic cAMP-dependent protein kinase is required for induction of cerebellar long-term potentiation. J Neurosci 19:10221-10227.

Litschig S, Gasparini F, Rueegg D, Stoehr N, Flor PJ, Vranesic I, Prezeau L, Pin JP, Thomsen C, Kuhn R (1999) CPCCOEt, a noncompetitive metabotropic glutamate receptor 1 antagonist, inhibits receptor signaling without affecting glutamate binding. Mol Pharmacol 55:453-461.

Llano I, Leresche N, Marty A (1991) Calcium entry increases the sensitivity of cerebellar Purkinje cells to applied GABA and decreases inhibitory synaptic currents. Neuron 6:565-574.

Llinas R, Sugimori M (1980a) Electrophysiological properties of in vitro Purkinje cell somata in mammalian cerebellar slices. J Physiol 305:171-195.

Llinas R, Sugimori M (1980b) Electrophysiological properties of in vitro Purkinje cell dendrites in mammalian cerebellar slices. J Physiol 305:197-213.

Llinás R, Nicholson C (1971) Electrophysiological properties of dendrites and somata in alligator Purkinje cells. J Neurophysiol 34:532-551.

Llinás R, Sugimori M (1980a) Electrophysiological properties of in vitro Purkinje cell dendrites in mammalian cerebellar slices. J Physiol 305:197-213.

Llinás R, Sugimori M (1980b) Electrophysiological properties of in vitro Purkinje cell somata in mammalian cerebellar slices. J Physiol 305:171-195.

Llinás R, Nicholson C, Freeman JA, Hillman DE (1968) Dendritic spikes and their inhibition in alligator Purkinje cells. Science 160:1132-1135.

Loewenstein Y, Mahon S, Chadderton P, Kitamura K, Sompolinsky H, Yarom Y, Hausser M (2005a) Bistability of cerebellar Purkinje cells modulated by sensory stimulation. Nat Neurosci 8:202-211.

Loewenstein Y, Mahon S, Chadderton P, Kitamura K, Sompolinsky H, Yarom Y, Häusser M (2005b) Bistability of cerebellar Purkinje cells modulated by sensory stimulation. Nat Neurosci 8:202-211.

London M, Häusser M (2005) Dendritic computation. Annu Rev Neurosci 28:503-532.

Losonczy A, Magee JC (2006) Integrative properties of radial oblique dendrites in hippocampal CA1 pyramidal neurons. Neuron 50:291-307.

Ludwig M, Pittman QJ (2003) Talking back: dendritic neurotransmitter release. Trends Neurosci 26:255-261.

Maejima T, Ohno-Shosaku T, Kano M (2001a) Endogenous cannabinoid as a retrograde messenger from depolarized postsynaptic neurons to presynaptic terminals. Neurosci Res 40:205-210.

Maejima T, Hashimoto K, Yoshida T, Aiba A, Kano M (2001b) Presynaptic inhibition caused by retrograde signal from metabotropic glutamate to cannabinoid receptors. Neuron 31:463-475.

Maex R, De Schutter E (2003) Resonant synchronization in heterogeneous networks of inhibitory neurons. J Neurosci 23:10503-10514.

Maex R, De Schutter E (2005) Oscillations in the cerebellar cortex: a prediction of their frequency bands. Prog Brain Res 148:181-188.

Magee JC, Johnston D (2005) Plasticity of dendritic function. Curr Opin Neurobiol 15:334-342.

Mann-Metzer P, Yarom Y (1999) Electrotonic coupling interacts with intrinsic properties to generate synchronized activity in cerebellar networks of inhibitory interneurons. J Neurosci 19:3298-3306.

Mann-Metzer P, Yarom Y (2000) Electrotonic coupling synchronizes interneuron activity in the cerebellar cortex. Prog Brain Res 124:115-122.

Marcaggi P, Attwell D (2005) Endocannabinoid signaling depends on the spatial pattern of synapse activation. Nat Neurosci 8:776-781.

Marder E, Abbott LF, Turrigiano GG, Liu Z, Golowasch J (1996) Memory from the dynamics of intrinsic membrane currents. Proc Natl Acad Sci U S A 93:13481-13486.

Marr D (1969) A theory of cerebellar cortex. J Physiol 202:437-470.

Martina M, Vida I, Jonas P (2000) Distal initiation and active propagation of action potentials in interneuron dendrites. Science 287:295-300.

Martina M, Yao GL, Bean BP (2003) Properties and functional role of voltage-dependent potassium channels in dendrites of rat cerebellar Purkinje neurons. J Neurosci 23:5698-5707.

Matsuda S, Launey T, Mikawa S, Hirai H (2000) Disruption of AMPA receptor GluR2 clusters following long-term depression induction in cerebellar Purkinje neurons. Embo J 19:2765-2774.

McElligott JG, Ebner TJ, Bloedel JR (1986) Reduction of cerebellar norepinephrine alters climbing fiber enhancement of mossy fiber input to the Purkinje cell. Brain Res 397:245-252.

Medina JF, Nores WL, Ohyama T, Mauk MD (2000) Mechanisms of cerebellar learning suggested by eyelid conditioning. Curr Opin Neurobiol 10:717-724.

Mehaffey WH, Doiron B, Maler L, Turner RW (2005) Deterministic multiplicative gain control with active dendrites. J Neurosci 25:9968-9977.

Mehta MR (2004) Cooperative LTP can map memory sequences on dendritic branches. Trends Neurosci 27:69-72.

Mel BW (1993) Synaptic integration in an excitable dendritic tree. J Neurophysiol 70:1086-1101.

Mel BW (1994) Information processing in dendritic trees. Neural Computation 6:1031-1085.

Migliore M, Shepherd GM (2002) Emerging rules for the distributions of active dendritic conductances. Nat Rev Neurosci 3:362-370.

Mitchell SJ, Silver RA (2003) Shunting inhibition modulates neuronal gain during synaptic excitation. Neuron 38:433-445.

Mittmann W, Häusser M (2007) Linking synaptic plasticity and spike output at excitatory and inhibitory synapses onto cerebellar Purkinje cells. J Neurosci 27:5559-5570.

Mittmann W, Koch U, Häusser M (2005) Feed-forward inhibition shapes the spike output of cerebellar Purkinje cells. J Physiol 563:369-378.

Miyakawa H, Lev-Ram V, Lasser-Ross N, Ross WN (1992) Calcium transients evoked by climbing fiber and parallel fiber synaptic inputs in guinea pig cerebellar Purkinje neurons. J Neurophysiol 68:1178-1189.

Monsivais P, Clark BA, Roth A, Häusser M (2005) Determinants of action potential propagation in cerebellar Purkinje cell axons. J Neurosci 25:464-472.

Mugnaini E, Dino MR, Jaarsma D (1997) The unipolar brush cells of the mammalian cerebellum and cochlear nucleus: cytology and microcircuitry. Prog Brain Res 114:131-150.

Murphy GJ, Darcy DP, Isaacson JS (2005) Intraglomerular inhibition: signaling mechanisms of an olfactory microcircuit. Nat Neurosci 8:354-364.

Nevian T, Larkum ME, Polsky A, Schiller J (2007) Properties of basal dendrites of layer 5 pyramidal neurons: a direct patch-clamp recording study. Nat Neurosci 10:206-214.

Nitz D, Tononi G (2002) Tonic rhythmic activity of rat cerebellar neurons. Exp Brain Res 146:265-270.

Nolte J (1999) The Human Brain: an introduction to its functional anatomy. St. Louis: Mosby Inc.

Oancea E, Meyer T (1998) Protein kinase C as a molecular machine for decoding calcium and diacylglycerol signals. Cell 95:307-318.

Ohno-Shosaku T, Tsubokawa H, Mizushima I, Yoneda N, Zimmer A, Kano M (2002) Presynaptic cannabinoid sensitivity is a major determinant of depolarization-induced retrograde suppression at hippocampal synapses. J Neurosci 22:3864-3872.

Otis TS, Kavanaugh MP, Jahr CE (1997) Postsynaptic glutamate transport at the climbing fiber-Purkinje cell synapse. Science 277:1515-1518.

Oviedo H, Reyes AD (2002) Boosting of neuronal firing evoked with asynchronous and synchronous inputs to the dendrite. Nat Neurosci 5:261-266.

Oviedo H, Reyes AD (2005) Variation of input-output properties along the somatodendritic axis of pyramidal neurons. J Neurosci 25:4985-4995.

Palay SL, Chan-Palay V (1974) Cerebellar cortex: cytology and organization. Berlin: Springer-Verlag.

Penttonen M, Kamondi A, Acsády L, Buzsáki G (1998) Gamma frequency oscillation in the hippocampus of the rat: intracellular analysis in vivo. European Journal of Neuroscience 10:718-728.

Piomelli D (2003) The molecular logic of endocannabinoid signalling. Nat Rev Neurosci 4:873-884.

Poirazi P, Brannon T, Mel BW (2003) Pyramidal neuron as two-layer neural network. Neuron 37:989-999.

Pompeiano O (2006) The vestibulo-ocular and the vestibulospinal reflexes: noradrenergic influences on the plastic changes which affect the cerebellar cortex during vestibular adaptation. Arch Ital Biol 144:197-253.

Prescott SA, De Koninck Y (2003) Gain control of firing rate by shunting inhibition: roles of synaptic noise and dendritic saturation. Proc Natl Acad Sci U S A 100:2076-2081.

Qiu DL, Knöpfel T (2007) An NMDA receptor/nitric oxide cascade in presynaptic parallel fiber-Purkinje neuron long-term potentiation. J Neurosci 27:3408-3415.

Raastad M, Shepherd GM (2003) Single-axon action potentials in the rat hippocampal cortex. J Physiol 548:745-752.

Raffaelli G, Saviane C, Mohajerani MH, Pedarzani P, Cherubini E (2004) BK potassium channels control transmitter release at CA3-CA3 synapses in the rat hippocampus. J Physiol 557:147-157.

Rall W (1959) Branching dendritic trees and motoneuron membrane resistivity. Experimental Neurology 1:491-527.

Rall W (1964) Theoretical significance of dendritic trees for neuronal input-output relations. In: Neural theory and modeling (Reiss R, ed), pp 73-97: Stanford University Press.

Rall W (1969) Time constants and electrotonic length of membrane cylinders and neurons. Biophys J 9:1483-1508.

Raman IM, Bean BP (1997) Resurgent sodium current and action potential formation in dissociated cerebellar Purkinje neurons. J Neurosci 17:4517-4526.

Raman IM, Bean BP (1999) Ionic currents underlying spontaneous action potentials in isolated cerebellar Purkinje neurons. J Neurosci 19:1663-1674.

Ramón y Cajal S (1911) Histologie du Système Nerveux de l'Homme et des Vertebrés. Paris: Malone.

Reichelt W, Knöpfel T (2002) Glutamate uptake controls expression of a slow postsynaptic current mediated by mGluRs in cerebellar Purkinje cells. J Neurophysiol 87:1974-1980.

Reinert KC, Gao W, Chen G, Ebner TJ (2007) Flavoprotein autofluorescence imaging in the cerebellar cortex in vivo. J Neurosci Res.

Ross WN, Werman R (1987) Mapping calcium transients in the dendrites of Purkinje cells from the guinea-pig cerebellum in vitro. J Physiol 389:319-336.

Ross WN, Nakamura T, Watanabe S, Larkum M, Lasser-Ross N (2005) Synaptically activated ca2+ release from internal stores in CNS neurons. Cell Mol Neurobiol 25:283-295.

Roth A, Häusser M (2001) Compartmental models of rat cerebellar Purkinje cells based on simultaneous somatic and dendritic patch-clamp recordings. J Physiol 535:445-472.

Ruiz-Stewart I, Tiyyagura SR, Lin JE, Kazerounian S, Pitari GM, Schulz S, Martin E, Murad F, Waldman SA (2004) Guanylyl cyclase is an ATP sensor coupling nitric oxide signaling to cell metabolism. Proc Natl Acad Sci U S A 101:37-42.

Sacchetti B, Scelfo B, Tempia F, Strata P (2004) Long-term synaptic changes induced in the cerebellar cortex by fear conditioning. Neuron 42:973-982.

Sade H, Muraki K, Ohya S, Hatano N, Imaizumi Y (2006) Activation of large-conductance, Ca^{2+}-activated K^{+} channels by cannabinoids. Am J Physiol Cell Physiol 290:C77-C86.

Safo PK, Regehr WG (2005) Endocannabinoids control the induction of cerebellar LTD. Neuron 48:647-659.

Sakurai M (1990) Calcium is an intracellular mediator of the climbing fiber in induction of cerebellar long-term depression. Proc Natl Acad Sci U S A 87:3383-3385.

Salin PA, Malenka RC, Nicoll RA (1996) Cyclic AMP mediates a presynaptic form of LTP at cerebellar parallel fiber synapses. Neuron 16:797-803.

Santamaria F, Tripp PG, Bower JM (2007) Feedforward inhibition controls the spread of granule cell-induced Purkinje cell activity in the cerebellar cortex. J Neurophysiol 97:248-263.

Santamaria F, Jaeger D, De Schutter E, Bower JM (2002) Modulatory effects of parallel fiber and molecular layer interneuron synaptic activity on purkinje cell responses to ascending segment input: a modeling study. J Comput Neurosci 13:217-235.

Satake S, Song SY, Cao Q, Satoh H, Rusakov DA, Yanagawa Y, Ling EA, Imoto K, Konishi S (2006) Characterization of AMPA receptors targeted by the climbing fiber transmitter mediating presynaptic inhibition of GABAergic transmission at cerebellar interneuron-Purkinje cell synapses. J Neurosci 26:2278-2289.

Sausbier M, Hu H, Arntz C, Feil S, Kamm S, Adelsberger H, Sausbier U, Sailer CA, Feil R, Hofmann F, Korth M, Shipston MJ, Knaus HG, Wolfer DP, Pedroarena CM, Storm JF, Ruth P (2004) Cerebellar ataxia and Purkinje cell dysfunction caused by Ca2+-activated K+ channel deficiency. Proc Natl Acad Sci U S A 101:9474-9478.

Schaefer AT, Angelo K, Spors H, Margrie TW (2006) Neuronal oscillations enhance stimulus discrimination by ensuring action potential precision. PLoS Biol 4:e163.

Schiller J, Schiller Y, Stuart G, Sakmann B (1997) Calcium action potentials restricted to distal apical dendrites of rat neocortical pyramidal neurons. J Physiol 505:605-616.

Schiller J, Major G, Koester HJ, Schiller Y (2000) NMDA spikes in basal dendrites of cortical pyramidal neurons. Nature 404:285-289.

Schmolesky MT, Weber JT, De Zeeuw CI, Hansel C (2002) The making of a complex spike: ionic composition and plasticity. Ann N Y Acad Sci 978:359-390.

Schulz DJ, Goaillard JM, Marder E (2006) Variable channel expression in identified single and electrically coupled neurons in different animals. Nat Neurosci 9:356-362.

Schweighofer N, Doya K, Kuroda S (2004) Cerebellar aminergic neuromodulation: towards a functional understanding. Brain Res Brain Res Rev 44:103-116.

Schwindt PC, Crill WE (1995) Amplification of synaptic current by persistent sodium conductance in apical dendrite of neocortical neurons. J Neurophysiol 74:2220-2224.

Segev I, Burke RE (1998) Compartmental models of complex neurons. In: Methods in neuronal modeling: from ions to networks (Koch C, Segev I, eds), pp 93-136: MIT Press.

Segev I, London M (1999) A theoretical view of passive and active dendrites. In: Dendrites (Stuart G, Spruston N, Häusser M, eds). Oxford: Oxford University Press.

Segev I, Rinzel J, Shepherd GM (1995) The Theoretical Foundation of Dendritic Function. Cambridge, MA: MIT Press.

Shin JH, Linden DJ (2005) An NMDA receptor/nitric oxide cascade is involved in cerebellar LTD but is not localized to the parallel fiber terminal. J Neurophysiol 94:4281-4289.

Sims RE, Hartell NA (2005) Differences in transmission properties and susceptibility to long-term depression reveal functional specialization of ascending axon and parallel fiber synapses to Purkinje cells. J Neurosci 25:3246-3257.

Sims RE, Hartell NA (2006) Differential susceptibility to synaptic plasticity reveals a functional specialization of ascending axon and parallel fiber synapses to cerebellar Purkinje cells. J Neurosci 26:5153-5159.

Sjöström PJ, Turrigiano GG, Nelson SB (2001) Rate, timing, and cooperativity jointly determine cortical synaptic plasticity. Neuron 32:1149-1164.

Sjöström PJ, Turrigiano GG, Nelson SB (2003) Neocortical LTD via coincident activation of presynaptic NMDA and cannabinoid receptors. Neuron 39:641-654.

Sjöström PJ, Turrigiano GG, Nelson SB (2004) Endocannabinoid-dependent neocortical layer-5 LTD in the absence of postsynaptic spiking. J Neurophysiol 92:3338-3343.

Sjöström PJ, Rancz EA, Roth A, Häusser M (In press) Dendritic excitability and synaptic plasticity. Physiol Rev.

Smith SL, Otis TS (2003) Persistent changes in spontaneous firing of Purkinje neurons triggered by the nitric oxide signaling cascade. J Neurosci 23:367-372.

Somogyi P, Klausberger T (2005) Defined types of cortical interneurone structure space and spike timing in the hippocampus. J Physiol 562:9-26.

Southam E, Morris R, Garthwaite J (1992) Sources and targets of nitric oxide in rat cerebellum. Neurosci Lett 137:241-244.

Steuber V, Mittmann W, Hoebeek FE, Silver RA, De Zeeuw CI, Häusser M, De Schutter E (2007) Cerebellar LTD and pattern recognition by Purkinje cells. Neuron 54:121-136.

Stuart G, Häusser M (1994) Initiation and spread of sodium action potentials in cerebellar Purkinje cells. Neuron 13:703-712.

Stuart G, Spruston N (1998) Determinants of voltage attenuation in neocortical pyramidal neuron dendrites. J Neurosci 18:3501-3510.

Stuart G, Schiller J, Sakmann B (1997) Action potential initiation and propagation in rat neocortical pyramidal neurons. Journal of Physiology 505 (Pt 3):617-632.

Stuart GJ, Häusser M (2001) Dendritic coincidence detection of EPSPs and action potentials. Nature Neuroscience 4:63-71.

Stuart GJ, Dodt HU, Sakmann B (1993) Patch-clamp recordings from the soma and dendrites of neurons in brain slices using infrared video microscopy. Pflügers Arch 423:511-518.

Svoboda K, Helmchen F, Denk W, Tank DW (1999) Spread of dendritic excitation in layer 2/3 pyramidal neurons in rat barrel cortex in vivo. Nature Neuroscience 2:65-73.

Tateno T, Harsch A, Robinson HP (2004) Threshold firing frequency-current relationships of neurons in rat somatosensory cortex: type 1 and type 2 dynamics. J Neurophysiol 92:2283-2294.

Tempia F, Alojado ME, Strata P, Knöpfel T (2001) Characterization of the mGluR(1)-mediated electrical and calcium signaling in Purkinje cells of mouse cerebellar slices. J Neurophysiol 86:1389-1397.

Ueno S, Bracamontes J, Zorumski C, Weiss DS, Steinbach JH (1997) Bicuculline and gabazine are allosteric inhibitors of channel opening of the GABAA receptor. J Neurosci 17:625-634.

Urban NN, Castro JB (2005) Tuft calcium spikes in accessory olfactory bulb mitral cells. J Neurosci 25:5024-5028.

Usowicz MM, Sugimori M, Cherksey B, Llinás R (1992) P-type calcium channels in the somata and dendrites of adult cerebellar Purkinje cells. Neuron 9:1185-1199.

Vetter P, Roth A, Häusser M (2001) Propagation of action potentials in dendrites depends on dendritic morphology. J Neurophysiol 85:926-937.

Voogd J, Glickstein M (1998) The anatomy of the cerebellum. Trends Neurosci 21:370-375.

Vos BP, Maex R, Volny-Luraghi A, De Schutter E (1999) Parallel fibers synchronize spontaneous activity in cerebellar Golgi cells. J Neurosci 19:RC6.

Wadiche JI, Jahr CE (2005) Patterned expression of Purkinje cell glutamate transporters controls synaptic plasticity. Nat Neurosci 8:1329-1334.

Walter JT, Khodakhah K (2006) The linear computational algorithm of cerebellar Purkinje cells. J Neurosci 26:12861-12872.

Walter JT, Alvina K, Womack MD, Chevez C, Khodakhah K (2006) Decreases in the precision of Purkinje cell pacemaking cause cerebellar dysfunction and ataxia. Nat Neurosci 9:389-397.

Wang SS, Denk W, Häusser M (2000) Coincidence detection in single dendritic spines mediated by calcium release. Nature Neuroscience 3:1266-1273.

Wang YT, Linden DJ (2000) Expression of cerebellar long-term depression requires postsynaptic clathrin-mediated endocytosis. Neuron 25:635-647.

Watanabe S, Takagi H, Miyasho T, Inoue M, Kirino Y, Kudo Y, Miyakawa H (1998) Differential roles of two types of voltage-gated Ca2+ channels in the dendrites of rat cerebellar Purkinje neurons. Brain Res 791:43-55.

Waters J, Larkum M, Sakmann B, Helmchen F (2003) Supralinear Ca^{2+} influx into dendritic tufts of layer 2/3 neocortical pyramidal neurons in vitro and in vivo. J Neurosci 23:8558-8567.

Watkins JC, Evans RH (1981) Excitatory amino acid transmitters. Annu Rev Pharmacol Toxicol 21:165-204.

Watt AJ, Sjöström PJ, Mori M, Ramakrishnan L, Häusser M (2006) Functional synaptic connections between mouse cerebellar Purkinje cells C108. In: The Physiological Society Main Meeting.

Welsh JP, Lang EJ, Suglhara I, Llinás R (1995) Dynamic organization of motor control within the olivocerebellar system. Nature 374:453-457.

Whittington MA, Traub RD, Kopell N, Ermentrout B, Buhl EH (2000) Inhibition-based rhythms: experimental and mathematical observations on network dynamics. Int J Psychophysiol 38:315-336.

Widmer HA, Rowe IC, Shipston MJ (2003) Conditional protein phosphorylation regulates BK channel activity in rat cerebellar Purkinje neurons. J Physiol 552:379-391.

Williams SR (2004) Spatial compartmentalization and functional impact of conductance in pyramidal neurons. Nat Neurosci 7:961-967.

Williams SR, Stuart GJ (2002) Dependence of EPSP efficacy on synapse location in neocortical pyramidal neurons. Science 295:1907-1910.

Williams SR, Stuart GJ (2003) Voltage- and site-dependent control of the somatic impact of dendritic IPSPs. J Neurosci 23:7358-7367.

Williams SR, Christensen SR, Stuart GJ, Häusser M (2002) Membrane potential bistability is controlled by the hyperpolarization-activated current I(H) in rat cerebellar Purkinje neurons in vitro. J Physiol 539:469-483.

Womack M, Khodakhah K (2002a) Active contribution of dendrites to the tonic and trimodal patterns of activity in cerebellar Purkinje neurons. J Neurosci 22:10603-10612.

Womack MD, Khodakhah K (2002b) Characterization of large conductance Ca2+-activated K+ channels in cerebellar Purkinje neurons. Eur J Neurosci 16:1214-1222.

Womack MD, Khodakhah K (2003) Somatic and dendritic small-conductance calcium-activated potassium channels regulate the output of cerebellar purkinje neurons. J Neurosci 23:2600-2607.

Womack MD, Khodakhah K (2004) Dendritic control of spontaneous bursting in cerebellar Purkinje cells. J Neurosci 24:3511-3521.

Wong RK, Prince DA, Basbaum AI (1979) Intradendritic recordings from hippocampal neurons. Proc Natl Acad Sci U S A 76:986-990.

Yasuda R, Nimchinsky EA, Scheuss V, Pologruto TA, Oertner TG, Sabatini BL, Svoboda K (2004) Imaging calcium concentration dynamics in small neuronal compartments. Sci STKE 2004:pl5.

Yeckel MF, Berger TW (1990) Feedforward excitation of the hippocampus by afferents from the entorhinal cortex: redefinition of the role of the trisynaptic pathway. Proc Natl Acad Sci U S A 87:5832-5836.

Yuste R, Denk W (1995) Dendritic spines as basic functional units of neuronal integration. Nature 375:682-684.

Yuste R, Gutnick MJ, Saar D, Delaney KR, Tank DW (1994) Ca^{2+} accumulations in dendrites of neocortical pyramidal neurons: an apical band and evidence for two functional compartments. Neuron 13:23-43.

Zhu L, Scelfo B, Tempia F, Sacchetti B, Strata P (2006) Membrane excitability and fear conditioning in cerebellar Purkinje cell. Neuroscience 140:801-810.

Zucker RS, Regehr WG (2002) Short-term synaptic plasticity. Annu Rev Physiol 64:355-405.